



Norwegian University of
Science and Technology

Optimisation of a New Energy System in Longyearbyen based on LNG and Solar Energy

Applying Mixed Integer Linear Programming
and a Rolling Horizon Heuristic

Petter Hovden

Marine Technology

Submission date: June 2018

Supervisor: Ekaterina Kim, IMT

Co-supervisor: Inge Norstad, SINTEF OCEAN
Harald Ellingsen, UNIS
Harald Vartdal, Seatres AS

Norwegian University of Science and Technology
Department of Marine Technology

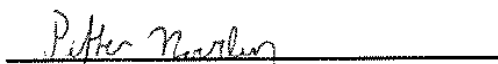
Preface

This Master's thesis is the concluding part of my Master of Science in Marine Technology with a degree specialisation in Marine system design and logistics at the Norwegian University of Science and Technology (NTNU), spring 2018. The thesis is a continuation of my project thesis, done in the fall semester 2017.

I would like to thank my supervisor Associate Professor Ekaterina Kim at NTNU, and my co-supervisor, Research Scientist Inge Norstad at SINTEF Ocean, for their valuable guidance throughout this semester. In addition, I would like to thank Managing Director at the University Centre in Svalbard, Harald Ellingsen, for the local contribution during my stays in Longyearbyen.

A special thanks to Harald Vartdal, Per-Christian Endsjø and LMG Marin for giving me this interesting and relevant assignment, as well as financial support to go to Longyearbyen. I have enjoyed working with this thesis and cooperating with you, and I am grateful for the possibilities this thesis has given me.

Trondheim, June 8, 2018

A handwritten signature in black ink, appearing to read "Petter Hovden", is written over a solid black horizontal line.

Petter Hovden

Executive summary

Longyearbyen is an isolated, Arctic settlement, where the energy situation is facing changes in near future. Today's energy system in Longyearbyen is a stand-alone system, consisting of a coal power plant as primary power producer and a diesel reserve system as a backup. In addition, the energy system offers fuel supply to the marine traffic in Longyearbyen, mainly Marine Gas Oil (MGO). The Ministry of Petroleum and Energy is currently assessing the possibilities for new energy carriers in Longyearbyen, and the general focus is that the new system should be more environmentally friendly than today's system.

LMG Marin is a company that is currently designing a solution applicable to the changes Longyearbyen is facing, and has given the inspiration for the problem description in this thesis. The energy carriers in the new energy system in Longyearbyen is Liquefied Natural Gas (LNG) and solar energy, and the system design is shown in Figure E1 below. The aim of this thesis has been to create an optimisation model intended to minimize the total lifetime costs over a 30-year period for the new energy system in Longyearbyen.

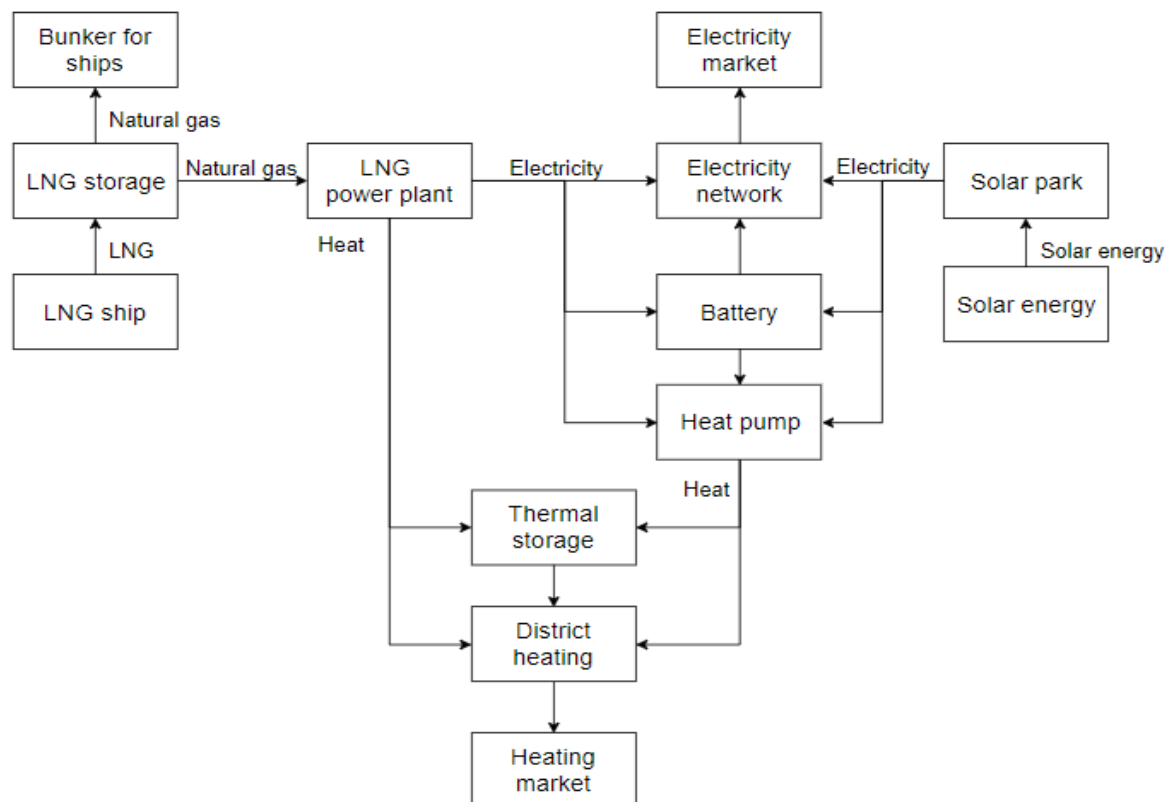


Figure E1: Flowchart of the new energy system in Longyearbyen based on LNG and solar energy modelled in this thesis.

The optimisation model in this thesis has been formulated by applying Mixed Integer Linear Programming, and implemented in the linear solver FICO® Xpress. A Rolling Horizon Heuristic algorithm was created to reduce the computational time of the model to an applicable level. The optimisation model was successfully validated in cooperation with the industry partners, and concluded to reflect the energy system realistically.

An economic and environmental study were conducted to see the cost and emission effects of different system designs. The results were based on future energy demand predictions in Longyearbyen. The predictions assumed an electricity demand reduction of 25% due to the removal of the coal power plant, and a reduction of the heat demand with 40% due to energy efficiency actions. The LNG ship bunkering demand corresponded to 80% of today's MGO demand, and the solar irradiance level was assumed to remain at today's level. Four different energy system designs were investigated, directly based on Figure E1, and were:

- With LNG storage and LNG power plant
- With LNG storage, LNG power plant, battery, thermal storage and heat pump
- With LNG storage, LNG power plant, battery, thermal storage, heat pump and solar park
- With LNG storage, LNG power plant, 50 MWh battery, thermal storage, heat pump and solar park

The economic study concluded that it is advantageous to invest in a battery, thermal storage and heat pump to enhance the efficiency of the system, because it potentially can reduce the total lifetime costs of the new energy system with almost 50 million USD compared with the system with only the power plant for power production. If installing the solar park in addition to that system, it is possible to reduce the total lifetime costs with another 24 million USD. Table E1 below shows the recommended system design to achieve the minimum total lifetime costs of the new energy system in Longyearbyen based on the model results. Notice that the ship arrivals are not fully loaded.

Yearly ship arrivals	4 ships à 5 000 m ³
LNG storage [m³]	5 132
Gas engines à 3500 KW in the power plant [-]	3
Yearly LNG consumption in the power plant [m³]	9 913
Thermal storage (atmospheric freshwater tank) [m³]	2 000
Battery [KWh]	5 549
Heat pump heat output [KW]	12 820
Solar park [solar panels à 300 W]	55 833

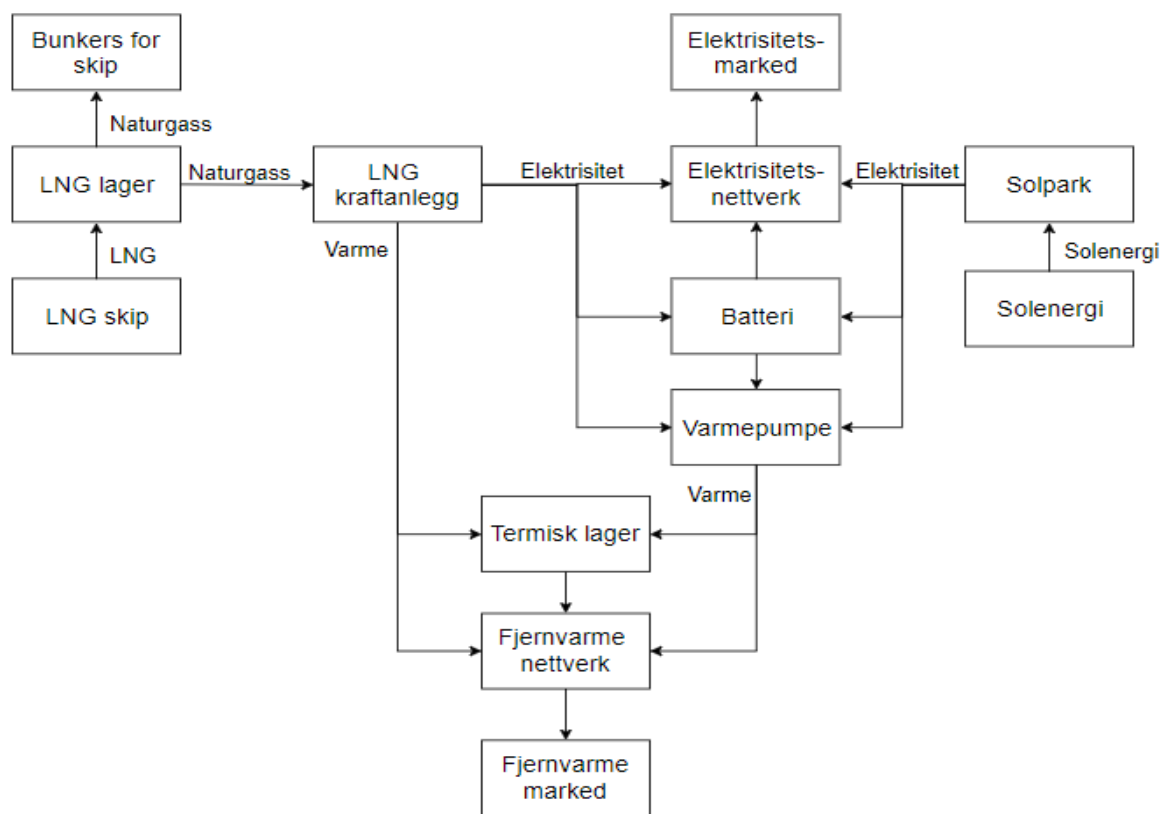
Table E1: Final dimensions for the recommended design of the new energy system in Longyearbyen.

An environmental study was conducted analysing the same four system designs as mentioned above. The conclusion was that by changing the power production from coal to LNG and the marine fuel from MGO to LNG, it is possible to reduce the CO₂ emission with at least 60%. In addition, by implementing energy efficiency-enhancing components, such as a battery, thermal storage, and heat pump, in addition to the solar park, the CO₂ emissions can be further reduced by around 36% compared with the LNG power plant alone. Notice that this is also the most cost-effective design. Installing a battery of 50 MWh will reduce the emissions with another 6%, but it will be 23 million USD costlier than the most cost-effective design given in Table E1 above.

Sammendrag

Longyearbyen er et isolert, Arktisk samfunn, der dagens energisituasjon står ovenfor endring i nær fremtid. Dagens energisystem i Longyearbyen er et frittstående system uten kobling mot andre kilder. Det er bygd opp av et kullkraftverk som primær kraftprodusent, og et dieselanlegg som reserve. I tillegg tilbyr systemet bunkers til skip, i hovedsak Marinegassolje (MGO). Olje og Energi Departementet ser for øyeblikket på mulighetene for nye energibærere i Longyearbyen, der det generelle fokuset er at det nye systemet skal være mer miljøvennlig enn dagens system.

LMG Marin er et selskap som for øyeblikket designer en løsning som er anvendelig for endringene Longyearbyen står ovenfor, og har gitt inspirasjon til denne oppgaven. Energibærerne som er tiltenkt det nye energisystemet i Longyearbyen er flytende naturgass (LNG) og solenergi. Systemets design er vist i Figur E1 under. Målet med denne oppgaven har vært å lage en optimeringsmodell med hensikt å minimere de totale levetidskostnadene for et nytt energisystem i Longyearbyen over en 30-års periode.



Figur E1: Flytskjema av det nye energisystemet i Longyearbyen basert på LNG og solenergi, modellert i denne oppgaven.

Optimeringsmodellen i denne oppgaven har blitt formulert ved å anvende blandet, lineær heltallsprogrammering, og implementert i det lineære løsningsprogrammet FICO® Xpress. En Rullerende Horisont Heuristikk algoritme har blitt laget for å redusere modellens løsnings tid til et anvendelig nivå. Modellen har blitt validert i samarbeid med industripartnerne av oppgaven, og det er konkludert at modellen reflekterer energisystemet på en realistisk måte.

En økonomi- og utslippsstudie har blitt utført for å se hvordan kostnader og utslipp er påvirket av ulike system design. Disse studiene har basert resultatene på en fremtidig prediksjon av energiforbruket i Longyearbyen. Prediksjonen tilsvarer at elektrisitetsforbruket blir redusert med 25% ettersom kullkraftverket forsvinner, og at varmekraftforbruket blir redusert med 40% på grunn av iverksatte energieffektiviseringstiltak. Videre har det blitt antatt at 80% av dagens MGO forbruk til skip går over på LNG, og dagens solinnstråling til Longyearbyen holder seg. Fire ulike design har blitt undersøkt, direkte basert på Figur E1, og er:

- Med LNG lager og LNG kraftanlegg
- Med LNG lager, LNG kraftanlegg, batteri, termisk lager og varmpumpe
- Med LNG lager, LNG kraftanlegg, batteri, termisk lager, varmpumpe og solpark
- Med LNG lager, LNG kraftanlegg, 50 MWt batteri, termisk lager, varmpumpe og solpark

Den økonomiske studien konkluderte med at det vil lønne seg å investere i et batteri, termisk lager og varmpumpe for å øke effektiviteten av systemet. Dette fordi det potensielt kan redusere de totale levekostnadene til systemet med 50 millioner USD sammenlignet med et system med bare et LNG kraftanlegg. Hvis en i tillegg investerer i en solpark, kan de total levekostnadene bli redusert ytterligere med 24 millioner USD. Tabell E1 viser det anbefalte systemet som, basert på modellresultatene, vil gi de laveste totale levekostnadene for et nytt energisystem i Longyearbyen basert på LNG og solenergi. Legg merke til at skipene som anløper ikke er fullt lastet.

Årlige skipsanløp	4 skip à 5 000 m ³
LNG lager [m³]	5 132
Gassmotorer à 3500 KW i kraftanlegget [-]	3
Årlig LNG forbruk i kraftanlegget [m³]	9 913
Termisk lager (atmosfærisk ferskvannstank) [m³]	2 000
Batteri [KWt]	5 549
Varmeeffekt varmpumpe [KW]	12 820
Solpark [solcellepaneler à 300 W]	55 833

Tabell E1: Endelige dimensjoner for det anbefalte designet av et nytt energisystem i Longyearbyen.

Utslippsstudien ble utført med de samme systemdesignene som nevnt ovenfor, og det ble konkludert med at uansett hvilket nytt design som tas i bruk, vil CO₂ utslippene knyttet til kraftproduksjon bli redusert med minst 60% sammenlignet mot dagens kullkraftverk. Dersom batteri, termisk lager, varmpumpe og en solpark er en del av designet, kan utslippene bli redusert med ytterligere 36% sammenlignet med LNG kraftanlegget alene. Legg merke til at dette også er den mest kostnadseffektive løsningen. Ved å installere et batteri på 50 MWt kan utslippene sammenlignet med det mest kostnadseffektive systemet bli redusert med ytterligere 6%, men dette vil øke de totale levekostnadene med 23 millioner USD.

Table of Contents

Preface	i
Executive summary	iii
Sammendrag	v
Table of Contents	vii
List of Tables	xi
List of Figures	xiii
Abbreviations	xvii
1. Introduction	1
2. Current and future energy situation in Longyearbyen	5
2.1 Today's energy situation in Longyearbyen	5
2.1.1 The electricity and heat production in Longyearbyen.....	6
2.1.2 The ship bunkering demand	9
2.1.3 Solar irradiance	11
2.1.4 Summary of the energy demands in Longyearbyen	12
2.2 An introduction to the new energy system in Longyearbyen.....	12
2.3 Technical description of the new energy system in Longyearbyen	13
2.3.1 Supply.....	14
2.3.2 LNG Storage	15
2.3.3 LNG power plant	16
2.3.4 Solar panels.....	16
2.3.5 Battery.....	17
2.3.6 Heat pump	17
2.3.7 Thermal storage	18
2.3.8 Reserve power system	18
2.3.9 Electricity and district heating network.....	18
2.3.10 Market demand	18
2.3.11 Energy management system	19
3. Problem description	21
3.1 Problem scope.....	21
3.2 The New Energy System in Longyearbyen problem aim and objective.....	22
4. Literature review	23
4.1 Optimisation and Mixed Integer Programming	23

4.2	Stand-alone energy system	24
4.3	Solution methods	25
4.3.1	Exact methods.....	25
4.3.2	Rolling Horizon Heuristic.....	26
4.4	Sensitivity analysis.....	28
5.	Model Formulation.....	31
5.1	Modelling choices and model assumptions.....	31
5.1.1	Overall assumptions.....	31
5.1.2	Ship supply	32
5.1.3	LNG storage.....	32
5.1.4	LNG power plant	32
5.1.5	Solar park	33
5.1.6	Battery.....	33
5.1.7	Heat pump	33
5.1.8	Thermal storage	33
5.1.9	Electricity and heating network.....	34
5.1.10	Demand.....	34
5.2	Definition of sets, indices, parameters, and variables.....	34
5.3	Mathematical model	38
5.3.1	Objective function.....	38
5.3.2	Constraints	38
	LNG supply constraints	38
	LNG storage constraints.....	39
	LNG power plant constraints	39
	Solar park constraints	41
	Battery constraints.....	41
	Heat pump constraints	42
	Thermal Storage constraints.....	42
	District heating constraints.....	43
	Electricity network constraints	43
	Non-negativity constraints.....	44
6.	Solution method.....	45
6.1	Data pre-processing	45

6.2	Rolling Horizon Heuristic method	45
7.	Computational study	47
7.1	Implementation.....	47
7.2	Data provided by the industry	47
	Overall data	47
	LNG ships	48
	LNG Storage	48
	LNG power plant.....	48
	Solar park.....	49
	Battery	49
	Heat pump	50
	Thermal Storage	50
	The solar irradiance and the energy demands.....	50
7.3	Technical study.....	51
7.3.1	Verification of the Rolling Horizon Heuristic	52
7.3.2	Stopping criteria analysis using the RHH method	53
7.3.3	Analysis of the starting and ending storage conditions using the RHH method 55	
7.3.4	Analysis of the model starting month using the RHH method	56
7.3.5	Analysis of the model simulation length	56
7.3.6	Quantitative validation	57
7.4	Economic study	61
7.4.1	Future scenarios and full factorial design.....	61
7.4.2	Sensitivity analysis	63
	Ship arrivals.....	63
	LNG Storage	65
	Gas engines	66
	Solar park	66
	Battery.....	68
	Heat pump	70
	Thermal storage	71
	Objective value	71
	Sensitivity analysis summary	72
7.4.3	Space limitations LNG storage	73

7.4.4	Changing safety level for different seasons.....	75
7.4.5	Waste limit analysis	77
7.4.6	Comparison of different NESL designs.....	80
7.4.7	Summary and final cost recommendation of the NESL based on LNG and/or solar energy	82
7.5	Environmental study	84
7.6	Validity of the results	89
7.6.1	Model quality	89
7.6.2	Input data quality.....	91
8.	Concluding remarks	93
9.	Further work	97
	References	99
	Appendix.....	I
	A. Table containing all the information about the ship supply.....	I
	B. Results obtained from the sensitivity analysis.....	II
	C. Formulas for a three-factor ANOVA test	IV

List of Tables

Table 1: Annual coal and diesel consumption in Energiverket, 2016(Hegle, 2018)	9
Table 2: Indices.	34
Table 3: Sets.	34
Table 4: Parameters	35
Table 5: Variables.....	36
Table 6: The overall input data in the model(Vartdal, 2018).	48
Table 7: The input data in the model related to the LNG ships(Vartdal, 2018).	48
Table 8: The input data in the model related to the LNG storage(Vartdal, 2018).	48
Table 9: The input data in the model related to the LNG power plant(Vartdal, 2018).....	49
Table 10: Input data in the model related to the solar park(Melaa, 2018).....	49
Table 11: Input data in the model related to the battery. Data has been collected by Melaa(2018) and Vartdal (2018).....	49
Table 12: Input data in the model related to the heat pump(Vartdal, 2018).	50
Table 13: Input data in the model related to the thermal storage(Dahlberg, 2018).	50
Table 14: Result of the computational time and minimum total cost found for the exact method and the RHH method. Optimality gap is the difference between the best solution found and the best possible solution that still can be found for the exact method.....	52
Table 15: Computational time difference and total cost deviation between exact method and RHH method.....	53
Table 16: Resulting computational time and minimum total cost deviation with different stopping criterion percentage. The stopping criterion is a value that determines when the found solution is assumed accurate enough, and the calculations can proceed. The deviation is against the total cost found for the model run with 0% stopping criteria. .54	
Table 17: Total cost of the system and deviation when running the model with different model lengths. A longer model length means that the time horizon is adjusted, so that the operational time is 30 years for all model lengths.	57
Table 18: The decision variables obtained from the validation run.	60
Table 19: The factors and events that have been used to create the full factorial design.	62
Table 20: The schedule routines that are present in the model results in the sensitivity analysis.....	63
Table 21: Maximum LNG storage capacity restriction implemented in the model and resulting optimal LNG storage capacity for the respective restriction.	73

Table 22: The new and old safety limits for stored LNG in the storage. The new limit is based on actual monthly LNG consumption in the power plant for the respective season.	75
Table 23: Resulting decision variables associated with the new and old safety limits from the model results.	76
Table 24: Cost associated with the new and old safety limits.....	77
Table 25: Resulting decision variables associated with and without the waste from the model results.	79
Table 26: The cost deviations between the result with and without the waste- Negative deviation means that the result with waste is more expensive.....	79
Table 27: Resulting decision variables associated with the different NESL designs.	80
Table 28: The recommended decision variables for the NESL to achieve the minimum total cost for scenario 15.....	83
Table 29: Yearly costs associated with the recommended NESL design for scenario 15.....	83
Table 30: The emission difference between the NESL with LNG storage, LNG power plant, battery, thermal storage, heat pump and solar park and today’s coal power plant, and yearly emission costs related to different carbon prices.	88
Table 31: The final system dimensions for the recommended design of the new energy system in Longyearbyen.	95

List of Figures

Figure 1: Location of Svalbard(Google sites, 2018).	1
Figure 2: Flowchart of today's energy system in Longyearbyen	6
Figure 3: Historical yearly electricity production in Longyearbyen 2010-2016(Hovden, 2017).	6
Figure 4: Hourly electricity production in Longyearbyen 2017(Hegle, 2018). Hour 1 is the first hour in 2017, the last hour is the last hour in 2017.	7
Figure 5: Hourly electricity production in Longyearbyen week 8, 2017(Hegle, 2018). Hour 1 is the first hour in week 8, the last hour is the last hour in week 8.....	7
Figure 6: Main electricity consumers in Longyearbyen 2017(Hegle, 2018).	8
Figure 7: Hourly heating production Longyearbyen 2017(Hegle, 2018). Hour 1 is the first hour 22 nd of January, the last hour is the last hour of the 31 st of July.	8
Figure 8: Hourly heat production in Longyearbyen week 8, 2017(Hegle, 2018). Hour 1 is the first hour in week 8, the last hour is the last hour in week 8.	9
Figure 9: Yearly calls for local ships in Longyearbyen 2011-2017(Hovden, 2017)	10
Figure 10: Estimated monthly marine MGO consumption in Longyearbyen, 2016(Jakobsen, 2017).	10
Figure 11: Received Global Horizontal Irradiance in Longyearbyen, 1990(Thorud, 2018).	11
Figure 12: Illustrative picture of how the solar park outside of Longyearbyen may look like(Melaa, 2018).	12
Figure 13: Illustrative picture of how the GraviFloat in Longyearbyen may look like(Vartdal, 2018).	12
Figure 14: Overall flowchart of the New Energy System in Longyearbyen	13
Figure 15: Flowchart of the solar energy supply to the system.	14
Figure 16: Flowchart of the LNG supply to the system.	15
Figure 17: Flowchart of the diesel supply to the system.....	15
Figure 18: Flowchart of the LNG distribution from the LNG storage.	15
Figure 19: Flowchart of the electricity and heat distribution from the LNG power plant.	16
Figure 20: Flowchart of the electricity distribution from the solar park.	17
Figure 21: Flowchart of the electricity distribution in the battery.	17
Figure 22: Flowchart of the electricity and heat distribution into and out of the heat pump.	17
Figure 23: Flowchart of the heat distribution in the thermal storage.	18

Figure 24: Flowchart of the energy distribution in the reserve power system.....	18
Figure 25: Flowchart of the NESL that will be modelled in this thesis.	21
Figure 26: Illustration of the forward RHH(Dimitriadis et al., 1997).	27
Figure 27: Illustration of the backward RHH(Dimitriadis et al., 1997).	27
Figure 28: Illustration of RHH with overlap(Marquand et al., 2015).....	28
Figure 29: Illustration of a full factorial design with a factor A with two levels, and a factor B with three levels. That makes a total of 6 different scenarios.	29
Figure 30 Sailing route from Rotterdam to Longyearbyen(Searoutes.com)	32
Figure 31: Hourly heat production in Longyearbyen 2017 completed by linear regression. The obtained heat production data contained missing data. Linear regression based on temperature has been used to estimate the missing values.	51
Figure 32: A graphical presentation of how the stopping criterion affects the computational time and total cost deviation from 0% stopping criteria using the RHH method.	54
Figure 33: A graphical presentation of how the computational time and total cost is affected by different starting and endings storage levels using the RHH method.....	55
Figure 34: A graphical presentation of how the computational time and total cost is affected by different model starting months using the RHH method. The four starting months are January, April, July, and October.	56
Figure 35: A graphical presentation of how the computational time is affected by the model length simulated.	57
Figure 36: A graphical presentation of the monthly LNG consumption for the studied NESL in this section.	58
Figure 37: A graphical presentation of the monthly distribution of produced electricity for the NESL.	59
Figure 38: A graphical presentation of the monthly heat distribution from the LNG power plant and from the heat pump.	59
Figure 39: A graphical presentation of the monthly storage level in the LNG storage.	60
Figure 40: Pareto chart of the ship schedules indicating what factors are significantly affecting the ship scheduling.	64
Figure 41: Histogram showing the frequency of the occurring schedule types in the sensitivity analysis.....	64
Figure 42: Pareto chart of the LNG storage showing what factors are significantly affecting the capacity of the LNG storage.	65

Figure 43: Main effects plot of the LNG storage showing how the levels of the factors are affecting the capacity of the LNG storage.	66
Figure 44: Main effects plot of the gas engines showing how the levels of the factors are affecting the number of gas engines in the LNG power plant.....	66
Figure 45: Pareto chart of the number of solar panels in the solar park showing what factors are significantly affecting the number of solar panels.	67
Figure 46: Main effects plot of the solar panels showing how the levels of the factors are affecting the number of solar panels in the solar park.	67
Figure 47: Interaction plot of the number of solar panels showing how different levels of two factors are affecting the number of solar panels. It is the interaction plot at the bottom left corner that has a significant effect on the solar park size.	68
Figure 48: Pareto chart of the battery showing what factors are significantly affecting the capacity of the battery.....	69
Figure 49: Main effects plot of the battery showing how the levels of the factors are affecting the battery capacity.....	69
Figure 50: Pareto chart of the heat pump showing what factors are significantly affecting the capacity of the heat pump.....	70
Figure 51: Main effects plot of the heat pump showing how the levels of the factors are affecting the battery capacity.....	70
Figure 52: Pareto chart of the objective value showing what factors are significantly affecting the objective value, i.e. total cost of the NESL when operating in 30 years....	71
Figure 53: Main effects plot of the objective value showing how the levels of the factors are affecting the objective value, i.e. total cost of the NESL, when operating for 30 years. 72	
Figure 54: A graphical presentation of how the total cost and the investment cost are affected by upper LNG storage capacity restrictions. Further relaxation of the maximum LNG storage capacity will result in the same numbers as are present for the upper two LNG storage capacity restrictions in the figure because that provides the minimum total cost of the model.	74
Figure 55: A graphical presentation of the monthly LNG storage levels when having the new and old safety limits.....	76
Figure 56: A graphical presentation of the monthly electricity production in the power plant with and without waste of renewable energy.....	78
Figure 57: A graphical presentation of the monthly electricity production in the solar park with and without waste of renewable energy. The electricity production that lies above the waste line indicates wasted solar energy due to overproduction.	78

Figure 58: The resulting costs associated with and without the waste obtained from the model results.	79
Figure 59: The resulting costs associated with the four different NESL designs investigated.	82
Figure 60: Monthly LNG consumption of the NESL containing a LNG storage and LNG power plant.	84
Figure 61: Monthly LNG consumption of the NESL containing an LNG storage, LNG power plant, battery, thermal storage and heat pump. The LNG saving potential due to the battery, thermal storage, and heat pump is indicated versus the previous design.....	85
Figure 62: Monthly LNG consumption of the NESL containing an LNG storage, LNG power plant, battery, thermal storage, heat pump and solar park. The LNG saving potential due to the solar park is indicated versus the previous design without the solar park. ..	86
Figure 63: Monthly LNG consumption of the NESL containing an LNG storage, LNG power plant, 50 MWh battery, thermal storage, heat pump and solar park. The LNG saving potential due to the battery is indicated versus the previous design.....	86
Figure 64: Yearly CO ₂ emissions for the different NESL designs related to power production, and today's coal power plant.	87
Figure 65: Yearly CO ₂ emissions from marine traffic comparing today's level with a fuel type change from MGO to LNG.	89

Abbreviations

B&B	-	Branch-and-bound
CHP	-	Combined Heat and Power
EMS	-	Energy Management System
GHI	-	Global Horizontal Irradiance
LNG	-	Liquified Natural Gas
NESL	-	New Energy System in Longyearbyen
MIP	-	Mixed Integer Programming
MPE	-	Ministry of Petroleum and Energy
MGO	-	Marine Gas Oil
NCA	-	Norwegian Coastal Administration
RHH	-	Rolling Horizon Heuristic

1. Introduction

Longyearbyen is an isolated, Arctic settlement located at latitude 78.13°N at the Svalbard archipelago, Figure 1. It is the northernmost settlement in the world with more than 2000 inhabitants, and Longyearbyen is an independent community with its own power production, and educational, health, law enforcement agency and other services. It was established as a coal community in 1906, which has been the main industry in terms of revenue until today (Visit Svalbard, 2018). However, with a more challenging coal market the recent years, the industry has reduced significantly in extent and Longyearbyen's energy situation is facing changes in near future. That is mainly related to increased ship activity (Kystverket, 2016), as well as a push towards a new, more environmentally friendly power production instead of coal (Ellingsen, 2017).



Figure 1: Location of Svalbard (Google sites, 2018).

Longyearbyen's power distribution can be described as a standalone, off-grid power system due to its isolated location. It consists of an electricity network and a district heating network. No other power producer can support if a failure occurs to the power delivery. Resultantly, reliability is crucial for the settlement, as the surrounding environment is cold and inhospitable, and the inhabitants must evacuate the settlement if they do not have the required energy. The power production today is controlled by Energiverket, and it is running on coal. A diesel reserve power system can support if the energy delivery is not satisfactory. More focus and attention on the environmental impacts of coal production has in the later years pushed towards a new, more environmentally friendly power production. The Ministry of Petroleum and Energy (MPE) are currently assessing the possibilities for new energy carriers in Longyearbyen. The final report is expected to be published in summer 2018 (Hegle, 2018).

The Norwegian Coastal Administration (NCA) published a study in November 2016 of the port structure in Longyearbyen, concluding that the quay capacity has been reached. The total ship traffic between 2005 and 2015 has increased by 37%, making today's port no longer feasible. This is mainly affecting local traffic which are tendering passengers ashore. NCA recommended building a new quay for local ships after the study (Kystverket, 2016). An increasing fuel demand is a result of the rapidly changing ship traffic. Ships bunkering in Longyearbyen today are mainly refuelling Marine Gas Oil (MGO) (Jakobsen, 2017). However, with the predicted growth and the environmental focus, it is likely that a considerable

amount of the new ships will sail on Liquefied Natural Gas(LNG)(Ingero, 2017) as LNG is known to be the best fossil fuel when it comes to reducing air-polluting emissions(WPCI, 2018).

LMG Marin is a company that among other things is currently designing a solution for the changes Longyearbyen is facing. The company has a vision to solve both the increased ship traffic as well as the new energy carriers by a combined solution called GraviFloat.

GraviFloat is a new quay design that will aim to increase the quay availability to a satisfactory level, have an integrated power plant installed and be the fuel storage for both the power plant and the ships. As the environmental focus is vital for this case, LMG Marin will try to utilize the ship fuel switch, and run the power plant, on LNG. Additionally, LMG Marin will combine the power production with a renewable source, solar energy. Their vision is that during the summer when there is daylight 24 hours a day, the electricity and heat production from fossil fuels in Longyearbyen will be close to none. (Vartdal, 2018).

Optimisation, or operations research, is the science of achieving optimal or near-optimal solutions to complex decision-making problems. The application aims to optimise the whole problem by formulating a mathematical model, and not only sub-problems of the main problem. Problems are formulated by mathematical equations and programmed into the computer. During the later years, the application has grown exponentially as more computational power allows to solve bigger problems. Optimisation is intended as a support in decision-making, investigating possible options and determining the best(Hillier & Lieberman, 2015).

This study will focus on LMG Marin's energy visions for Longyearbyen and apply mathematical optimisation to create a model that can discover the most cost-effective design for a New Energy System in Longyearbyen(NESL) based on LNG and/or solar energy. The main objectives of this thesis are:

- Formulate a valid and time-efficient optimisation model that can be used as a decision support tool for designing and analysing the effects of a NESL based on LNG and/or solar energy.
- Evaluate the economic effects of four different energy system designs, based on LNG and/or solar energy. Recommend the most cost-effective design.
- Evaluate the environmental effects of the same four system designs in terms of CO₂ emissions.

The contributions of this thesis are:

- An investigation of the electricity and heat production and demand in Longyearbyen today, and future predictions.
- A survey of the ship traffic and fuel consumption in Longyearbyen today, and future predictions

- Determination and a clear description of a new energy system design that can be implemented for a cost- and environmental-effective energy utilisation in Longyearbyen based on LNG and/or solar energy
- Creation of a valid mathematical optimisation model that realistically reflects the NESL.
- Description and validation of a heuristic algorithm used to reduce the solving time of the model significantly, and to an applicable level.
- A sensitivity analysis of the NESL to obtain an understanding of how uncertainty affects the NESL design.
- Economic evaluation of four different system designs based on LNG and/or solar energy, and a recommendation of the most cost-effective solution.
- Environmental evaluation of four different system designs based on LNG and/or solar energy.

This thesis has the following structure: Chapter 2 provides a description of the energy situation in Longyearbyen today, and an explanation of the visioned NESL based on LNG and/or solar energy. The problem description outlining the NESL problem is provided in Chapter 3. Chapter 4 presents a review of the literature study that has been done to accomplish this thesis. In Chapter 5, the mathematical optimisation model is presented together with modelling choices and assumptions. The solution methods used to solve the NESL model are described in Chapter 6. Chapter 7 presents the implementation of the NESL and a computational study of the model. Concluding remarks on the main objectives of this thesis are presented in Chapter 8, before thoughts on further work are described in Chapter 9.

2. Current and future energy situation in Longyearbyen

This chapter outlines a short description of the energy system and the energy situation in Longyearbyen today, and an overview and a detailed technical explanation of the design of the NESL based on LNG and solar energy. A thorough understanding of the problem is necessary to realise the structure and complexity of the created model and results this thesis provides.

The following information in this chapter has been obtained by expert interviews. Experts locally in Longyearbyen have been interviewed to gain knowledge about Longyearbyen and the history, today's energy production and demands, and likely future events affecting the energy demand. In addition, experts working with energy systems have been interviewed, and been an important factor in the determination of the NESL design that will be presented in this chapter.

Section 2.1 provides information of Longyearbyen's energy situation today. Section 2.2 introduces the NESL design, and section 2.3 describes the NESL design in detail.

2.1 Today's energy situation in Longyearbyen

The power production in Longyearbyen is a standalone system, and thus, needs to be self-sufficient and reliable. The power network in Longyearbyen consists of an electrical network and a district heating network. By having a district heating network, it is possible to achieve a higher thermal efficiency, thus a more efficient system (Bøckman, 2017). All required electricity and heat are produced by Energiverket, which is operating a coal power plant with two gas engines. One of the gas engines produces electricity only, while the other one produces both electricity and heat. If a failure occurs to one of the gas engines, diesel generators and heating installations will be started to produce the necessary energy (Hegle, 2018). The coal used in the power plant is mined locally in Gruve 7 right outside of Longyearbyen. It is metallurgical coal, i.e. high-quality coal (Rønning, 2017).

Energiverket has been ordered by the Norwegian government to operate the coal power plant to 2038. A replacement to another energy carrier may happen sooner, and is currently being assessed by the Ministry of Petroleum and Energy (MPE). The MPE's study will evaluate all realistic energy carriers, and hybrid solutions among them. Hydrogen, LNG, Solar, wind and thermal sources are the most mentioned solutions today. One of the aims of the new solution is that it is more environmentally friendly than today's system (Hegle, 2018). This thesis has contributed to the study with initial information about an LNG based energy system, and a hybrid system with LNG and solar energy.

LNS Spitsbergen is the distributor of diesel in Longyearbyen. They store diesel for the reserve generators and heating installations, and they offer ship bunker possibilities at Gammelkaia. As the quay capacity has been reached, the availability is limited. The main fuel for ships is MGO, i.e. diesel. LNS Spitsbergen is the main distributor of fuels in

Longyearbyen, and they refuel their storages by ship supplies two to three times a year (Jakobsen, 2017).

Figure 2 below illustrates today's energy system and flows.

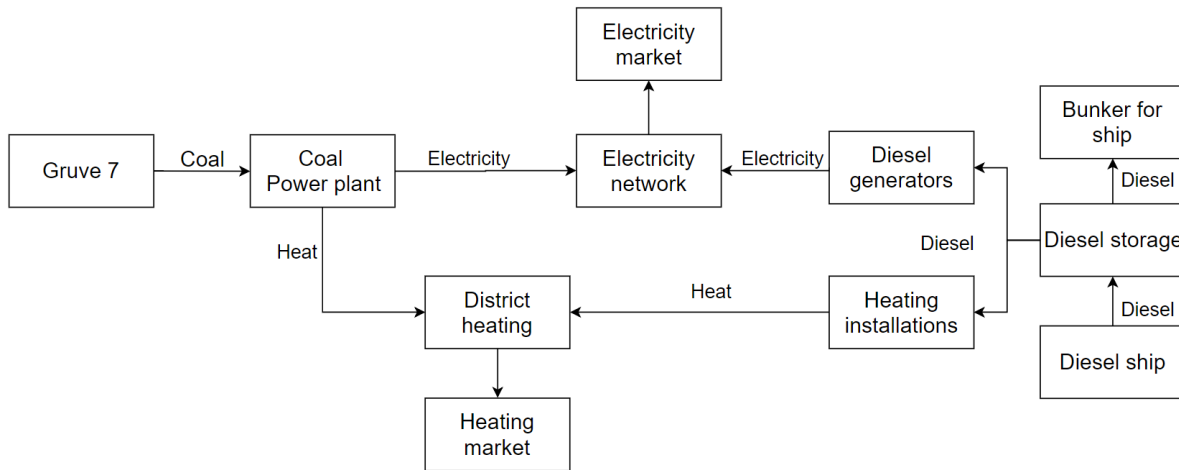


Figure 2: Flowchart of today's energy system in Longyearbyen

To obtain an understanding of the energy demands faced by the energy system, today's heat and electricity production, as well as the ship bunkering consumption are explained further. Also, the solar irradiance levels at Svalbard will be explained, to outline the potential and frame that lies in solar power production at Svalbard.

2.1.1 The electricity and heat production in Longyearbyen

Figure 3 shows that the annual heat and electricity production has been fairly constant during the last years, and is based on the statistical data reported in *Hovden (2017)*. The heat demand is dependent on outside temperature, resulting in the yearly variations. Notice that data for 2017 are not included, because the report was published at the end of 2017.

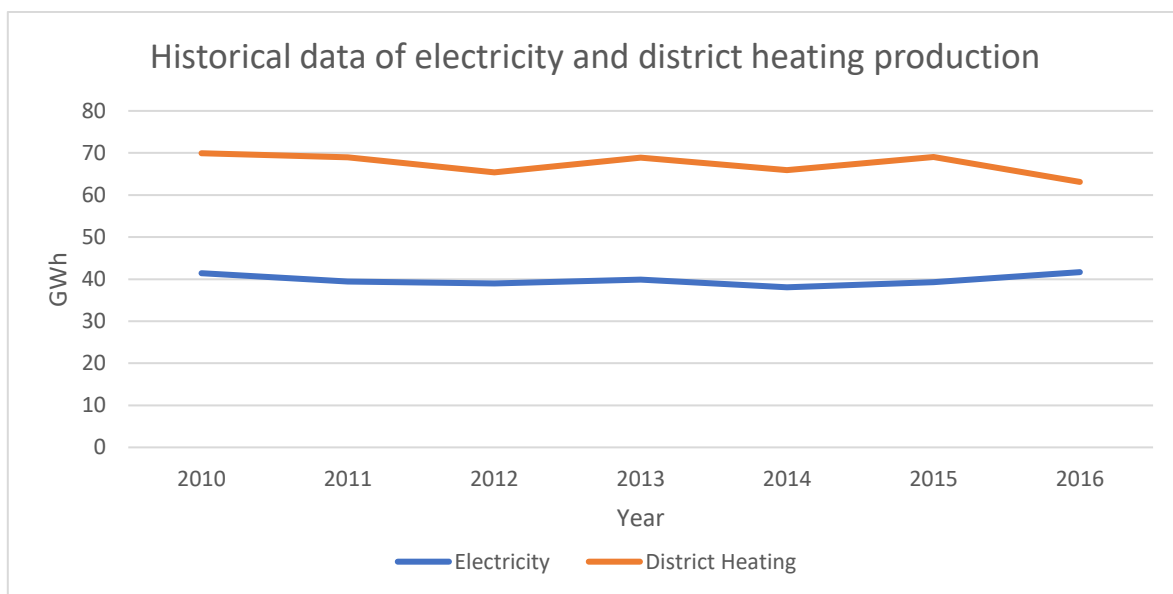


Figure 3: Historical yearly electricity production in Longyearbyen 2010-2016 (Hovden, 2017).

Looking at the hourly electricity production, it can be seen that it varies significantly with the hours, Figure 4(Hegle, 2018). The electricity production seems to be temperature dependent as the production is reduced during warmer hours. Notice that electricity is not used for heating in Longyearbyen, meaning that the electricity production variations are smaller than similar locations with equal temperature variations, e.g. the Norwegian mainland where electricity is used for heating(Hegle, 2018). The demand seems to vary significantly with weekday and time of the day.

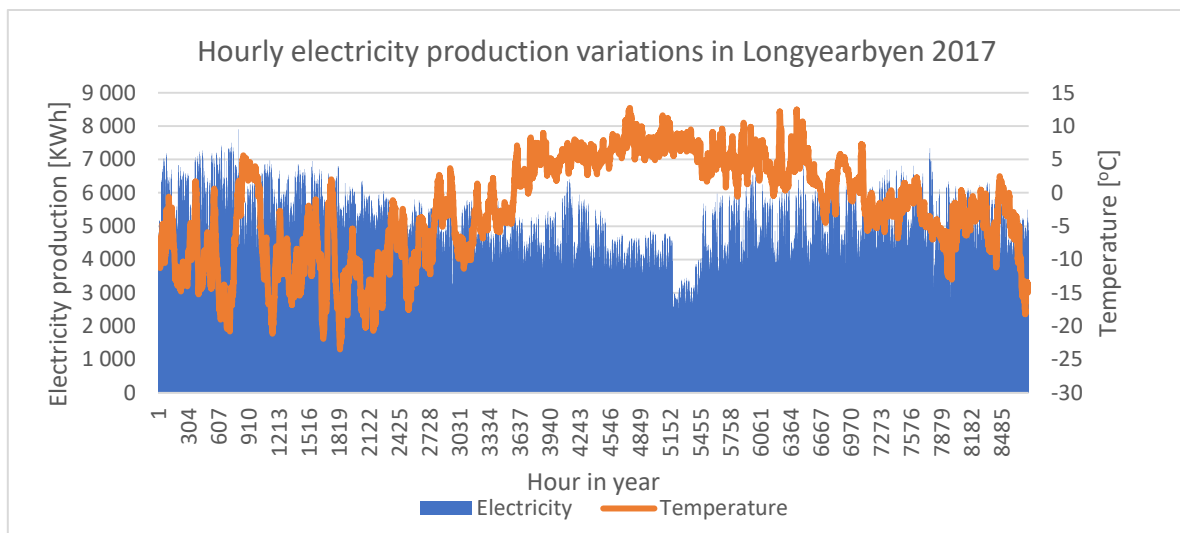


Figure 4: Hourly electricity production in Longyearbyen 2017(Hegle, 2018). Hour 1 is the first hour in 2017, the last hour is the last hour in 2017.

Figure 5 illustrates the electricity production for a normal week during winter(Hegle, 2018). It is a close up of Figure 3 for week 8. The hourly electricity variations are shown closer. Notice that the production decreases during night-time, and is less during the weekend. The hourly variations are significant, which needs to be accounted for in the design of the NESL. This trend is repeating and happens because of more activity during the daytime.

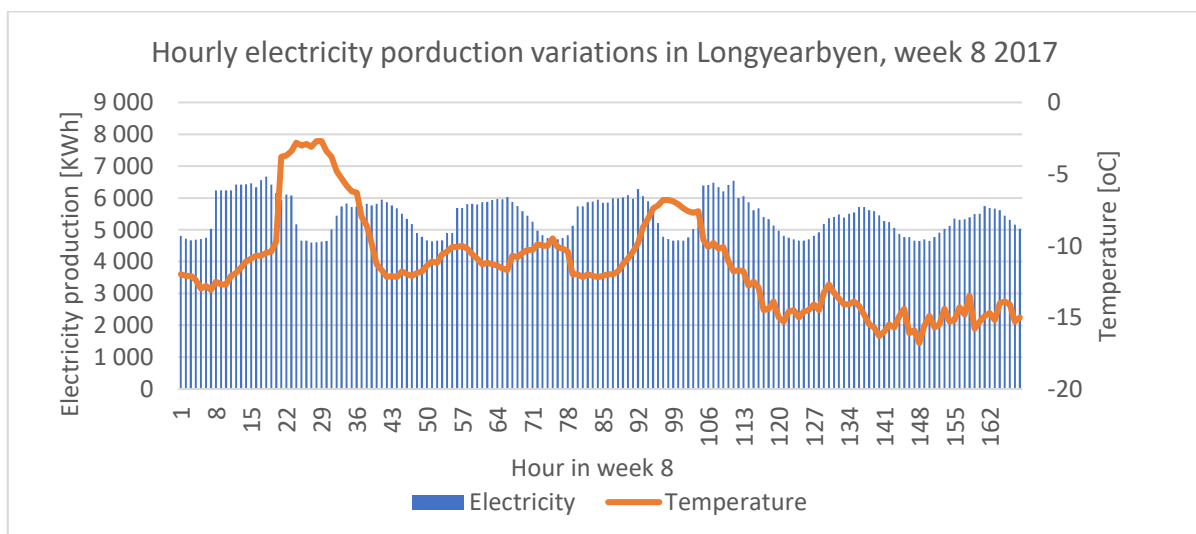


Figure 5: Hourly electricity production in Longyearbyen week 8, 2017(Hegle, 2018). Hour 1 is the first hour in week 8, the last hour is the last hour in week 8.

Below is an illustration of the main electricity consumers in Longyearbyen, Figure 6(Hegle, 2018). Notice that around 25% of the electricity consumption is related to mining in Gruve 7 and energy production in Energiverket's coal power plant today. That will be important to account for in the design of a new energy system, as the coal power plant no longer will exist.

Main electricity consumers in Longyearbyen

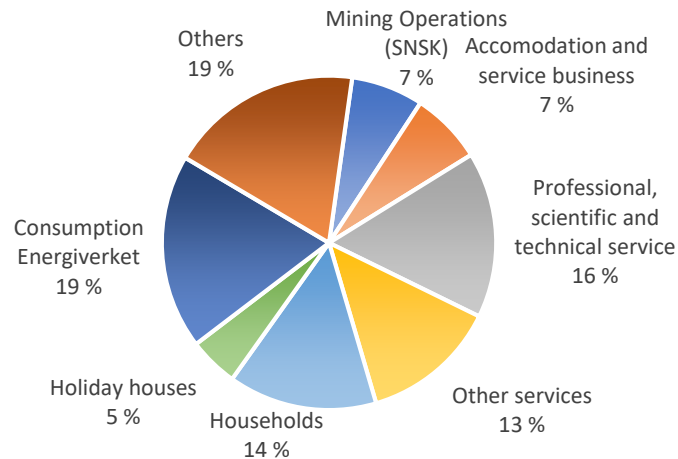


Figure 6: Main electricity consumers in Longyearbyen 2017(Hegle, 2018).

The heat production in 2017 is presented in Figure 7. As seen, it drops to below half the magnitude during summer. To thoroughly account for this will be important for the final NESL design. There are some gaps in the graph due to errors in the measuring instruments. In addition, this was the only available heat data and is why the timeline is much shorter than a whole year(Hegle, 2018). Notice that the magnitude of the heat demand is significantly higher than the electricity demand in Longyearbyen, especially during winter.

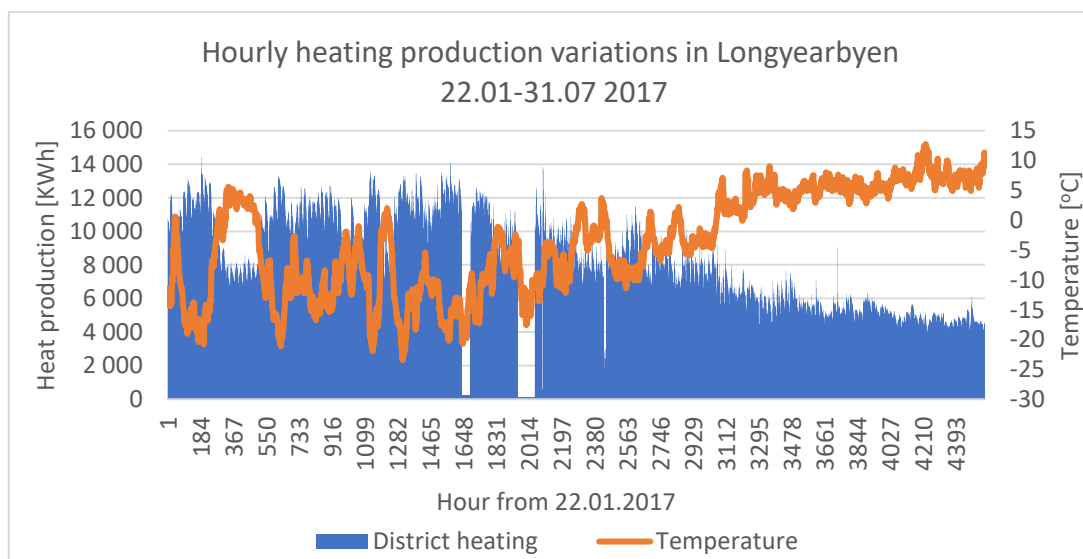


Figure 7: Hourly heating production Longyearbyen 2017(Hegle, 2018). Hour 1 is the first hour 22nd of January, the last hour is the last hour of the 31st of July.

Figure 8 illustrates the heat production for a normal week during winter (Hegle, 2018), and is a scale-up of Figure 7. Notice that the scales are different to the previous figure for electricity production in week 8, Figure 5, because the heat demand is significantly higher. The heat production also depends on the hour, due to more activity during the daytime, and will be important to account for in the design of the NESL.

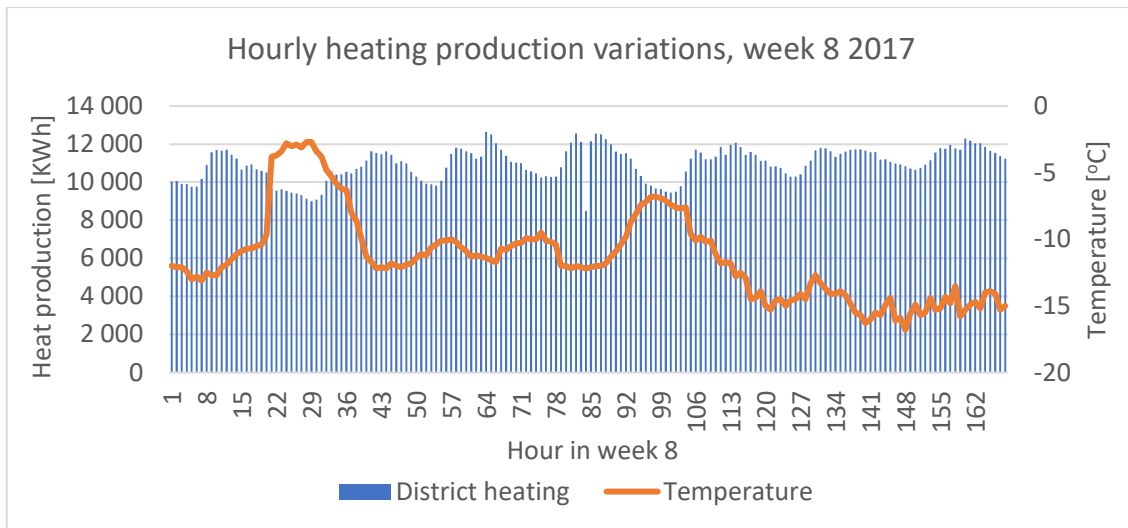


Figure 8: Hourly heat production in Longyearbyen week 8, 2017 (Hegle, 2018). Hour 1 is the first hour in week 8, the last hour is the last hour in week 8.

Table 1 shows the coal and diesel consumption in Energiverket in 2016. The fuel consumption is only related to electricity and heat production to Longyearbyen.

Table 1: Annual coal and diesel consumption in Energiverket, 2016 (Hegle, 2018)

Coal [ton]	27 467
Diesel [m³]	1 139

2.1.2 The ship bunkering demand

The ship traffic in Longyearbyen is categorised into overseas cruise ships, local ships, and vessels shorter than 40 meters. Local ships consist of expedition and day trip cruises. Based on the information and statistical data collected by Hovden (2017), the local ship traffic is the main consumer of marine fuel in Longyearbyen. That is because overseas cruise ships have the possibility to bunker elsewhere, where the prices are more competitive. Local ships, on the other hand, must bunker in Longyearbyen and are consuming considerably more than the last ship segment, vessels shorter than 40 meters (Hovden, 2017). Local ships are the segment that is most likely to switch to LNG-propulsion because of the vessel size. New ships are currently being built supporting LNG-propulsion (Kornfeldt, 2017). The annual calls of local traffic from the last year is given in Figure 9, illustrating the increasing ship traffic in Longyearbyen (Hovden, 2017).

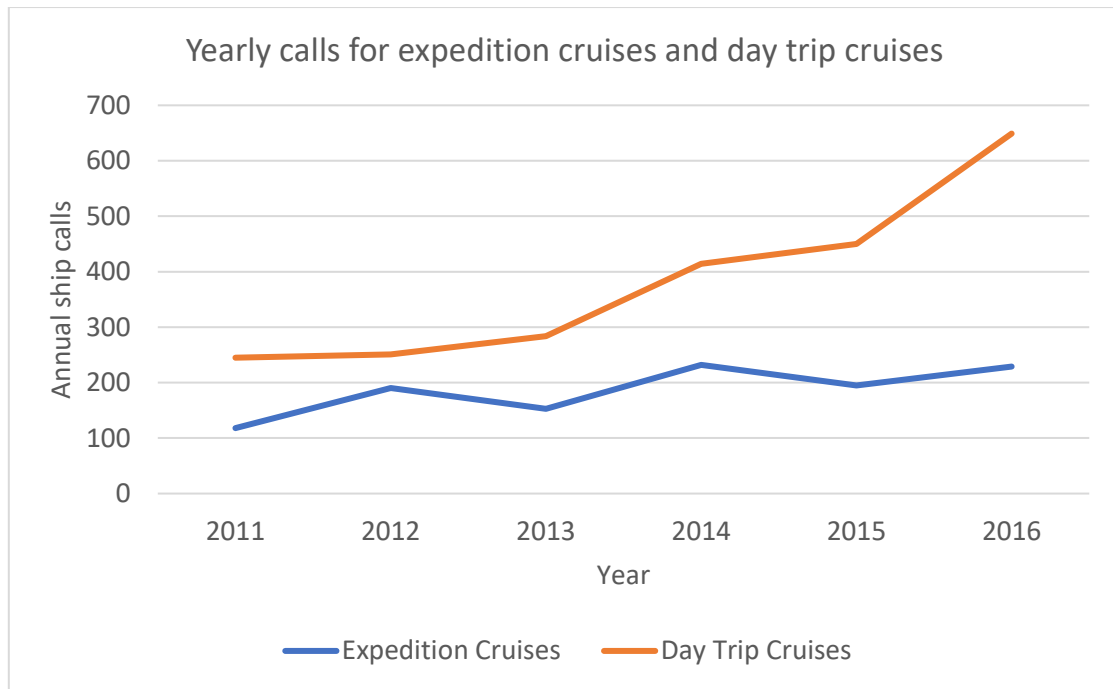


Figure 9: Yearly calls for local ships in Longyearbyen 2011-2017(Hovden, 2017)

The author has not been successful in collecting the exact monthly data for the marine consumption of MGO from LNS Spitsbergen. However, Figure 10 shows an estimate of the MGO consumption to marine traffic in Longyearbyen in 2016. The estimate is created in cooperation with LNS Spitsbergen, and the sum of the monthly consumption corresponds to the actual annual marine consumption in 2016 which has been monitored(Jakobsen, 2017). The marine traffic is season based in Longyearbyen, resulting in the consumption profile below. That is because of potential ice conditions around Svalbard before May, and little traffic in October due to few daylight hours.

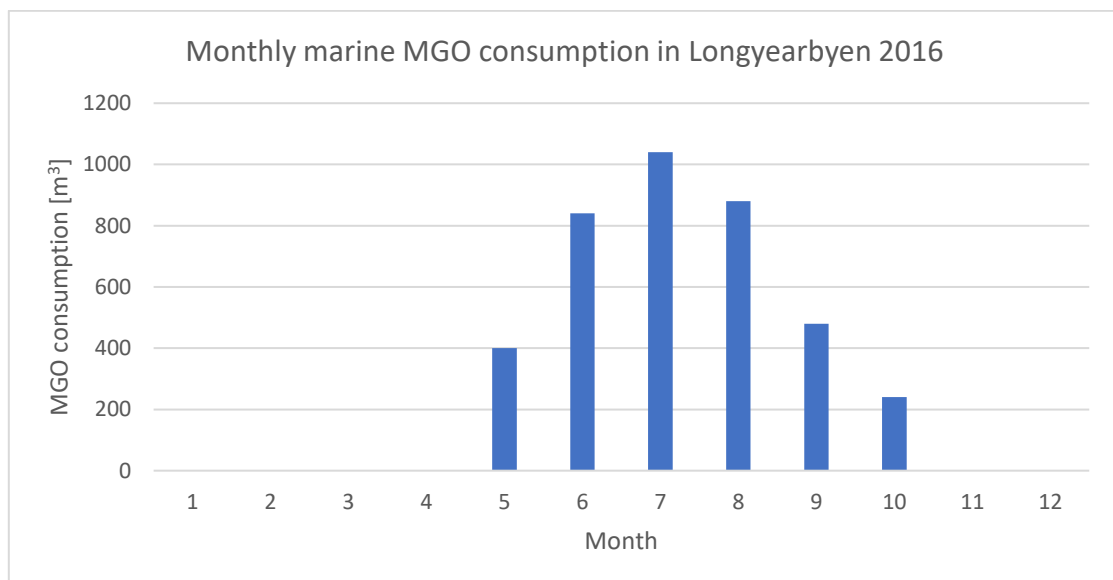


Figure 10: Estimated monthly marine MGO consumption in Longyearbyen, 2016(Jakobsen, 2017).

The overseas cruise ships and expedition cruises are polluting when they are ashore as the generators aboard the ships have to operate. There are ongoing discussions today about installing shore power in Longyearbyen Port, to reduce the emissions while the ships are ashore(Kornfeldt, 2017). This will influence the electricity demand considerably during the cruise season.

2.1.3 Solar irradiance

Solar radiation in Longyearbyen is very different from other places on the earth. Longyearbyen’s location results in midnight sun during the summer months, and polar night during the winter. In addition, the climate in Longyearbyen is commonly characterised as an Arctic desert(Sysselmannen, 2018). That results in good opportunities for utilizing solar irradiance during summertime, where electricity potentially can be produced 24 hours a day(Vartdal, 2018).

Global Horizontal Irradiance (GHI) is a common term for solar energy that can be converted into electricity in solar panels. The GHI varies with cloud presence and daylight, resulting in fluctuating electricity production. Figure 11 shows the received GHI for Longyearbyen in 1990, which accounts for clouds and sun angle variations(Thorud, 2018). Up to date information about solar irradiance in Longyearbyen is expensive, and has not been affordable in this thesis. However, this data is assumed to give a good indication of the irradiance level today.

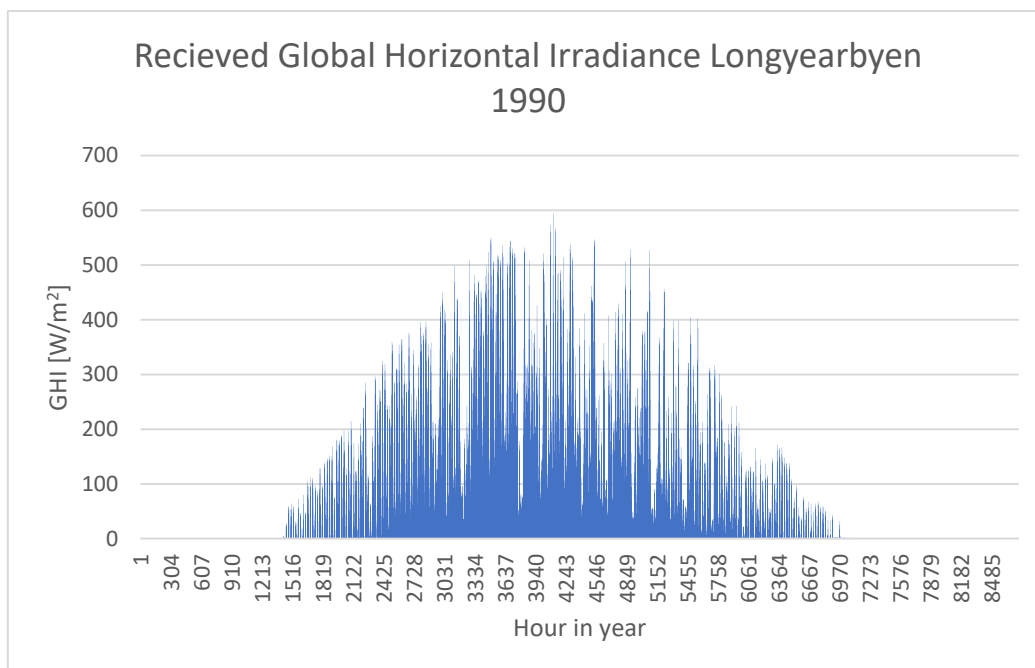


Figure 11: Received Global Horizontal Irradiance in Longyearbyen, 1990(Thorud, 2018).

Due to global change, scientists are predicting that the solar GHI at Svalbard will be reduced in the future as a result of more clouds. A reduction of up to 15% is mentioned(Endsjø, 2018).

2.1.4 Summary of the energy demands in Longyearbyen

This sub-section sums up the energy demands in Longyearbyen:

- The electricity demand today varies with time of the day, and to some extent with the outside temperature. 25% of today's demand is related to the power production itself. In addition, installation of shore power is currently being discussed and may affect the future electricity demand in Longyearbyen considerably.
- The heat demand varies with the season due to temperature effects, and the demand is more than twice the magnitude at winter compared with the summer.
- The ship bunkering demand is season based, varying with the marine traffic activity. The peak is during summer when the sea is ice-free and there is midnight sun.
- The solar irradiance is strongest during the summer when there is midnight sun. During winter, there is no solar irradiance.

2.2 An introduction to the new energy system in Longyearbyen

LMG Marin's visions for the NESL is a hybrid solution combining solar energy and LNG for power production. In addition, it is desirable to switch the marine fuel from MGO to LNG as it is less polluting. There will, thus, be built an LNG storage which will supply both the ships and the power plant with LNG. The objective of this energy solution is to achieve a much more environmentally friendly and reliable energy system in Longyearbyen than today. Figure 12, and Figure 13 below, give an illustration of LMG Marin's visions, where the solar park is installed outside of Longyearbyen, and the LNG storage and the power plant is installed in the GraviFloat. The system will be designed for a 30-year lifetime(Vartdal, 2018).

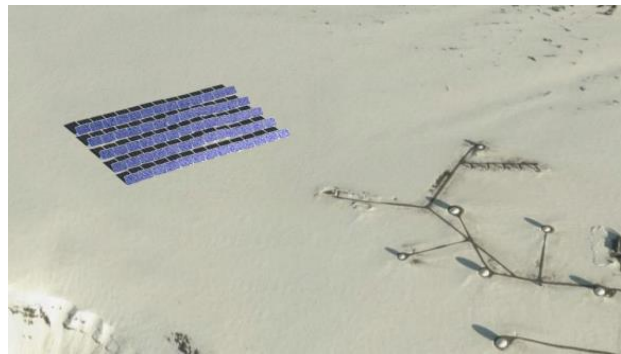


Figure 12: Illustrative picture of how the solar park outside of Longyearbyen may look like(Melaa, 2018).



Figure 13: Illustrative picture of how the GraviFloat in Longyearbyen may look like(Vartdal, 2018).

The solar park can potentially produce solar electricity 24 hours a day during summer. Due to Longyearbyen's location far north, the sun angle is low. That means that the GHI in Longyearbyen is weaker than further south. However, snow reflection and the low temperatures at Svalbard improves the received GHI and the efficiency of the panels, which makes Longyearbyen a good location for a solar park. The local climate is, in addition, defined as a desert, which means that the cloud conditions are good for solar energy (Melaa, 2018).

The LNG power plant will work as a back-up for the solar park during summer when the production drops. That can be due to a cloud cover on the sky, or if the demand increases and additional production is needed. The power plant will supplement the solar park during the transition seasons, which are the spring and autumn, to ensure the demands to be satisfied. During polar nights, when there is no daylight, the power plant will operate alone (Vartdal, 2018). The LNG power plant will be the heart of the NESL, providing reliability to the system as it can operate year-round as long as there is sufficient LNG available.

The LNG storage will supply the power plant with the required gas, as well as being the bunkering station for ships running on LNG. There is no market for LNG in Longyearbyen today, but it is believed to become a considerable market for new ships and increased ship activity when there are facilities supporting it (Vartdal, 2018).

2.3 Technical description of the new energy system in Longyearbyen

This section outlines what made the foundation for the design of the NESL, and a detailed description of the different processes in the system. Figure 14 shows the complete flowchart of the NESL design that will be studied for this thesis.

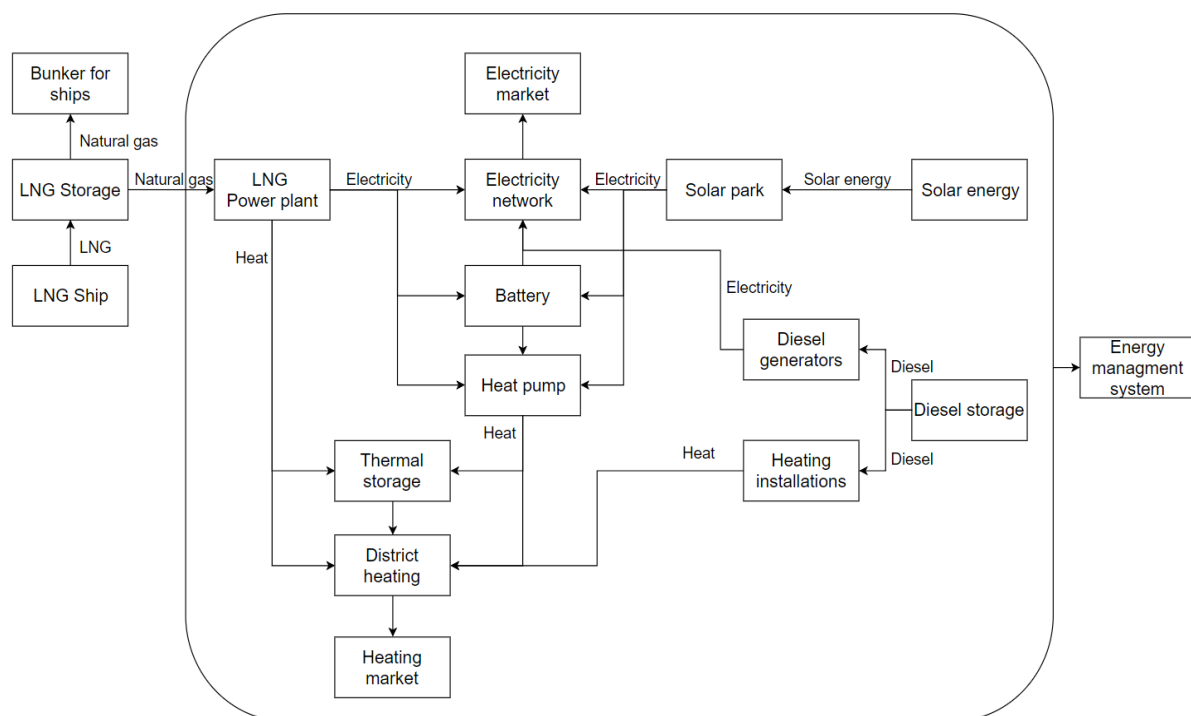


Figure 14: Overall flowchart of the New Energy System in Longyearbyen

Bjørn Thorud (2018) at MultiConsult has given the inspiration for this solution, implementing energy storages and converters to improve efficiency and potentially reduce costs. The energy storages will consist of a battery for electricity storage, and a thermal storage for heat. Energy storages are typically used for shaving peak demands in the production profile, which can reduce the required power output of the power plant for peak hours. In Longyearbyen, there are significant peaks as seen in Section 2.1, making energy storages applicable. The converter in the system is a heat pump, which can convert excess electricity into heat. It is especially useful when the heat demand in a system is much bigger than the electricity demand, which is the case for Longyearbyen during winter. In addition, the heat pump makes it possible to produce heat energy with solar panels during summer, when it is advantageous to reduce the operating hours of the LNG power plant. The intention of implementing the energy storages and the converter is to improve production efficiency, shave peak loads, that potentially will reduce the investment and operational costs. An Energy Management System (EMS) is a control system that will manage the energy flows of the NESL as efficient as possible, evaluating the weather and demand forecasts for optimum production (Thorud, 2018). This system has been presented for the politicians in Longyearbyen, Longyearbyen Lokaltstyre, and it was confirmed that they are currently also looking at the advantages of implementing energy storages and a heat pump to the energy system in Longyearbyen(Dyrstad, 2018).

A thorough explanation of each component in the system will follow.

2.3.1 Supply

Three energy sources lie the foundation of this NESL. Solar radiation and LNG will be the main drivers, and diesel will be the reserve if break-down happens(Vartdal, 2018).

The amount of solar energy received in the solar park will depend on solar irradiance, cloud layer, the angle on the solar panels, reflection, and obstacles. Cloud layers can reduce the production by up to 90%. The angle the solar panels are directed towards the sun will affect the efficiency of the panels, resulting in changing production during the day for a fixed panel orientation. Snow reflection will increase the radiation, hence the production of the panels, and obstacles will result in shade(Melaa, 2018). Figure 11 in section 2.1.3 showed the received solar energy when all these factors are accounted for. Figure 15 shows the flow of the solar energy supply to the NESL.

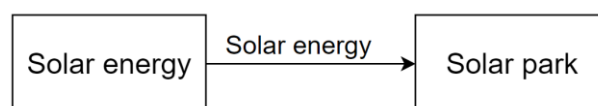


Figure 15: Flowchart of the solar energy supply to the system.

The LNG supply will consist of ships sailing from Rotterdam to Longyearbyen and back. The port has been selected because other ports that are closer does not offer LNG for so small ship capacities applicable to supply Longyearbyen(Vartdal, 2018). As Longyearbyen is in the Arctic, ships sailing there during winter may be subject to heavy ice conditions and

challenges. Since 2011 however, it has not been any ice into Longyearbyen port(National Snow & Ice Data Center, 2017), and the average local temperature is increasing due to global change(Hovden, 2017). The supply rate and the supply volume of the ship deliveries are two of the decision variables in this system. There will be losses associated with regasification during transportation due to the low temperature storing of LNG(Vartdal, 2018). The flow is shown in Figure 16 below.

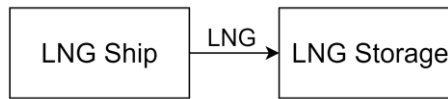


Figure 16: Flowchart of the LNG supply to the system.

The diesel is today distributed by LNS Spitsbergen(Jakobsen, 2017), and procurement of diesel will therefore not be considered in this energy system. When the main system, i.e. the LNG power plant and the solar park, cannot produce the required energy, the diesel reserve system will be started and diesel will be consumed from the storage, Figure 17(Vartdal, 2018).

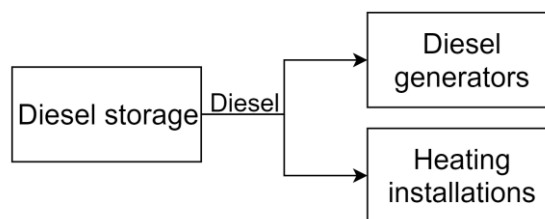


Figure 17: Flowchart of the diesel supply to the system.

2.3.2 LNG Storage

All LNG that is shipped to Longyearbyen is intended to be stored in the GraviFloat. The total capacity of the storage is one of the final decision variables. Investment costs associated with the storage are mainly related to steel and insulation. Losses due to regasification of the LNG will occur in the storage(Vartdal, 2018). The LNG-flow in and out of the storage is illustrated in Figure 18 below. The storage is required to have a safety level of LNG at any time corresponding to 30 days of power production(Dyrstad, 2018).

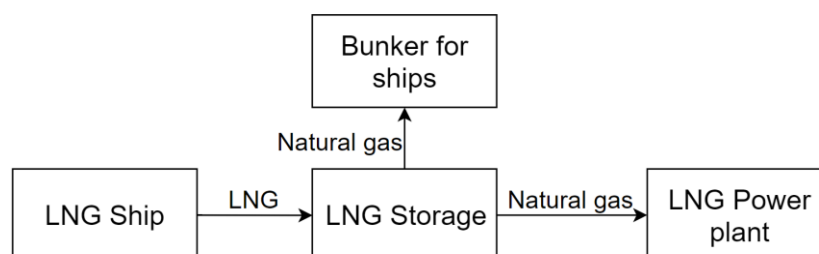


Figure 18: Flowchart of the LNG distribution from the LNG storage.

2.3.3 LNG power plant

The LNG power plant will be the converter of natural gas to electricity and heat. It will be located at the GraviFloat and consist of a set of gas engines that will produce the required energy. All gas engines are combined heat and power(CHP) engines, which produces equally much heat and electricity(Vartdal, 2018). Today's coal power plant is a CHP utilising the district heating network(Hegle, 2018), and CHP will be applicable for the new system as it increases the thermal efficiency of the production considerably(EPA, 2018). The flow of the electricity and the heat is as shown below, Figure 19.

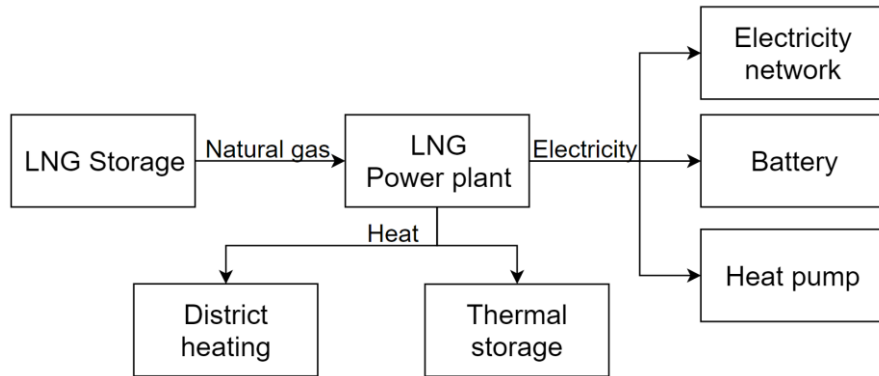


Figure 19: Flowchart of the electricity and heat distribution from the LNG power plant.

Both the LNG storage and the power plant will be located at GraviFloat, thus are the transportation losses of natural gas small. The efficiency of the gas engines will depend on the workload, where a load between 70% and 100% is ideal. Gas engines must operate above a 30% workload. The main expenses associated with the power plant are the investment costs of the gas engines and the operating costs associated with LNG consumption, crew, and maintenance. It will for maintenance reasons be advantageous to have similar gas engines, both for engine knowledge and for spare parts. For this system, gas engines with an output effect of 3500 KW will be used(Vartdal, 2018). The number of gas engines in the LNG power plant, and the yearly LNG consumption in the power plant, will be two of the decision variables in the model.

2.3.4 Solar panels

The solar panels convert solar energy into electricity. Factors affecting the production efficiency are the received solar irradiance, ambient temperature and the age of the panels. All panels will have fixed orientation for cost reason, i.e. not able to reorientate(Melaa, 2018). The main cost related to the solar park is the investment costs, as production is based on solar energy which is free of charge(Vartdal, 2018). The location of the solar park is still unknown, but there will not be any space limitations because of a lot of available space around Longyearbyen(Melaa, 2018). The number of panels is a decision variable. Figure 20 shows the incoming and outgoing energy flows of the solar park.

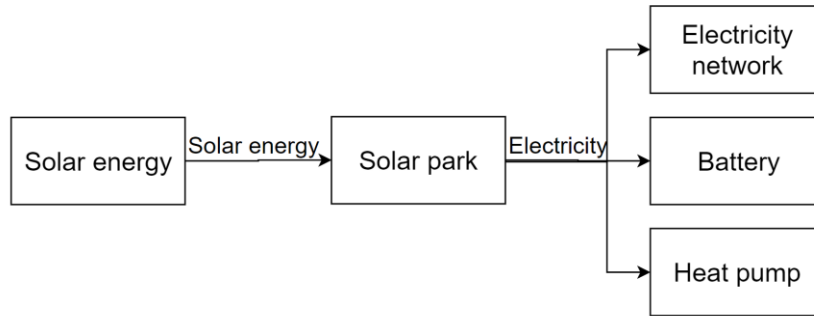


Figure 20: Flowchart of the electricity distribution from the solar park.

2.3.5 Battery

The battery will serve as the electrical storage for this system, and will be located in the GraviFloat. Overcharging and undercharging the battery reduces the capacity and lifetime dramatically and should be avoided. Age will also reduce the capacity of the battery. Storing electricity in the battery will be subject to losses which must be accounted for (Vartdal, 2018). The capacity of the battery will be a decision variable. Figure 21 shows the incoming and outgoing flow of the battery.

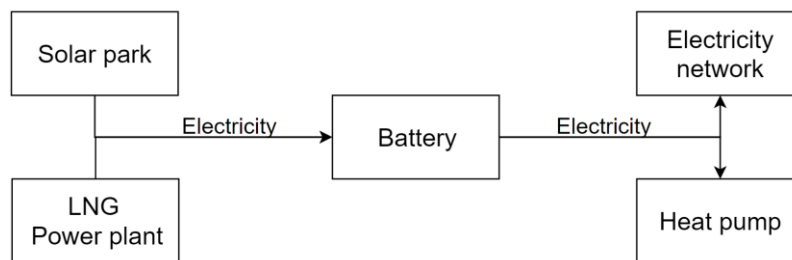


Figure 21: Flowchart of the electricity distribution in the battery.

2.3.6 Heat pump

The heat pump will convert electricity into heat in this system, and will be located in the GraviFloat. Heat pumps are known for its good efficiency, able to produce three to four times more heat out than the electricity in (NOVAP, 2018). The main cost related to the heat pump is the investment cost. Figure 22 shows the flows in and out of the heat pump. The heat pump capacity will be a decision variable.

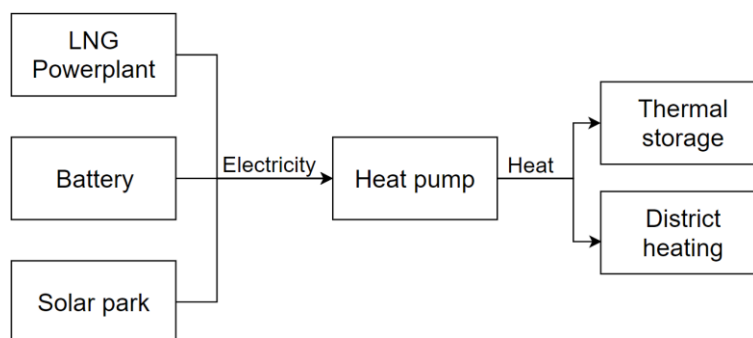


Figure 22: Flowchart of the electricity and heat distribution into and out of the heat pump.

2.3.7 Thermal storage

The thermal storage will store the heat in this system, and will be located in the GraviFloat. It will consist of a hydrostatic fresh water tank, insulated to reduce heat losses. Heat losses in the tank need to be considered, and ageing does not affect the tank. The tank will be cylindrical(Dahlberg, 2018). All excess heat can be stored in the tank by heat exchanger transferring the energy to the thermal storage, Figure 23. The main expense for the storage is related to investment, with negligible operating and maintenance costs(Vartdal, 2018). The decision variable will be the total size of the thermal storage.

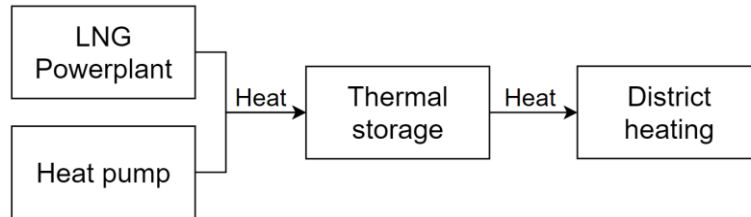


Figure 23: Flowchart of the heat distribution in the thermal storage.

2.3.8 Reserve power system

The reserve power system will consist of diesel generators producing electricity, and heating installations producing heat. They will work as the redundancy in the NESL. The reserve power system is combusting diesel, and are already existing in today's energy system, i.e. no investments are necessary. In principle will the reserve power system only run when the primary system, i.e. the LNG power plant, and the solar park, is not capable of producing the required amount of energy. That will be due to maintenance or break down as the primary system will be designed to handle all demand variations itself. Figure 24 shows the incoming and outgoing flows related to the reserve power system.

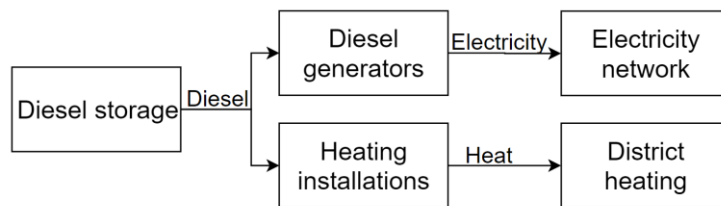


Figure 24: Flowchart of the energy distribution in the reserve power system.

2.3.9 Electricity and district heating network

Longyearbyen has existing infrastructure for both the electricity and district heating network(Bøckman, 2017). The NESL will use the same infrastructure, thus, there will not be any investment costs associated with the electricity and district heating networks.

2.3.10 Market demand

The frame of the NESL is the electricity and heat demand in Longyearbyen, as well as the natural gas demand to ships. Today's demands were given in Section 2.1, and will create the foundation for the future predicted demands that this system will be designed for. This subsection will explain the challenges that are present in predicting the future demands.

The electricity demand is to some extent dependent on the temperature, shown in sub-section 2.1.1. As the future temperature is impossible to foresee, that will make the predictions harder to make. Today, around 25% of the electricity consumption is related to the electricity production itself. Resultantly, a transition to the new energy system will influence the electricity demand, and needs to be accounted for. Additionally, shore power may be implemented in Longyearbyen port to reduce the environmental footprint from ships. This will affect the electricity demand during the cruise season(Dyrstad, 2018).

Temperature variations influence the heat demand significantly, as seen in sub-section 2.1.1. The heat production can periodically be twice as much during winter compared with the summer. Longyearbyen is a community with a high heat consumption, and it is said to be 3-4 times the consumption at Norwegian mainland when temperature effects are corrected for(Vartdal, 2018). The heat future in Longyearbyen is uncertain, where a number of energy efficiency actions are mentioned to reduce the consumption and waste. More focus has been directed towards the energy policy today. At Svalbard, heat energy is not charged based on consumption, but on the size of the apartment or building. It is believed that implementing a system where you are charged for the consumption will reduce the heat demand significantly. In addition, new houses with better insulation are being built, which requires less heat(Bøckman, 2017).

The LNG ship bunker market in Longyearbyen is not existing today. Future predictions are uncertain, and it is like the chicken or the egg dilemma. No ships will use LNG if there are no facilities supporting it. However, when already having an LNG storage at the port, it can be combined as a bunkering station for ships. It is believed that a considerable share of new ships will sail on LNG around Svalbard due to the environmental focus. LNG is a more expensive fuel than Heavy Fuel Oil and MGO, but further political restrictions may be made to reduce the emissions, thus making LNG the only allowable fuel type around Svalbard(Vartdal, 2018).

2.3.11 Energy management system

The Energy Management System (EMS) is a control system that is designed to manage the energy production and energy flows in an energy system to maximize the performance. An efficient system results in high energy utilization and low fuel costs. The EMS controls the system based on weather forecasts and predicted future heat and electricity demands.

3. Problem description

This chapter contains the problem description of the NESL presented in Chapter 2. The purpose of this thesis is to create an optimisation model that can minimize the investment, fuel and transportation costs associated with the NESL, ensuring the energy demands in Longyearbyen to be satisfied. Section 3.1 describes the problem scope that will be modelled. Section 3.2 explains the decision variables that affect the costs of the NESL, and a clear description of the main objectives of this thesis.

3.1 Problem scope

The intention with the NESL is to provide Longyearbyen with the necessary energy. The reserve system today will only produce energy when the new system is incapable to deliver the energy due to breakdowns or maintenance. It is therefore determined that the reserve system shall not be a part of the model as the intention is to design the NESL to satisfy the energy demands alone.

The EMS system is a crucial part of every efficient energy system. The optimisation model in this thesis will work as the EMS as it will control the production and flows of all energy the best way possible. The model will, therefore, work as the EMS mentioned in section 2.3.11. Figure 25 shows the flowchart of the NESL that will be modelled in this thesis.

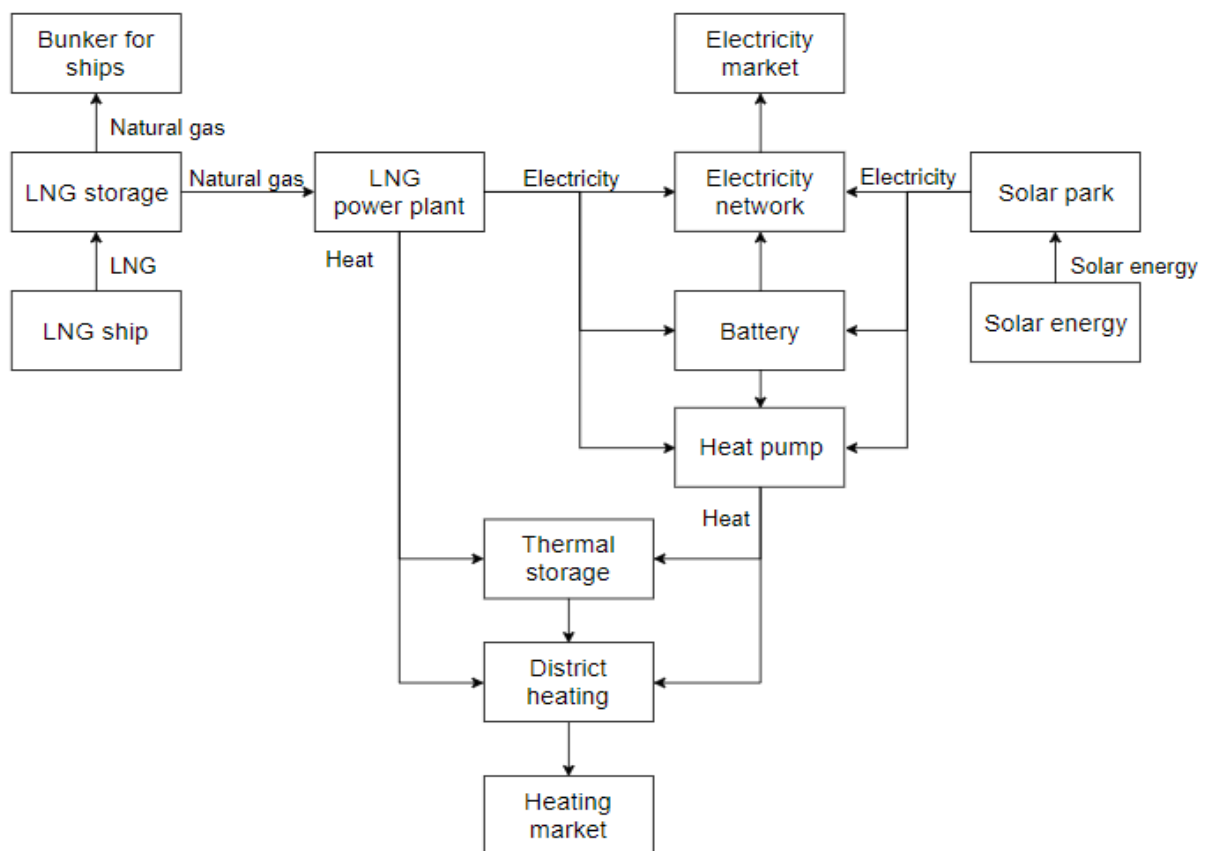


Figure 25: Flowchart of the NESL that will be modelled in this thesis.

3.2 The New Energy System in Longyearbyen problem aim and objective

The NESL problem aims to design an energy system in Longyearbyen that will provide the demanded energy at a minimum of total lifetime costs. Solar irradiance and LNG are the fundamental energy sources for the problem, as mentioned in Chapter 2. The following are the decision variables introduced in section 2.3, which sums up the total lifetime costs associated with the NESL problem:

- Total lifetime cost
 - o Investment cost
 - Capacity of the LNG-Storage [m³]
 - Power output of the LNG-power plant [number of engines à 3500 KW]
 - Number of solar panels in the solar park including private panels [panels]
 - Capacity of the battery package [KWh]
 - Capacity of the heat pump, electricity input [KW]
 - Capacity of the thermal storage tank [m³]
 - o LNG consumption cost
 - Lifetime LNG consumption in the power plant [m³]
 - o Transportation cost
 - Lifetime supply rate and volume of LNG transported by ships [number of ship calls of different sizes]

The following are the main objectives this thesis addresses:

- Formulate a valid and time-efficient optimisation model that can be used as a decision support tool for designing and analysing the effects of a NESL based on LNG and/or solar energy.
- Evaluate the economic effects of different energy system designs, all directly based on Figure 25 above, and recommend the most cost-effective design. Four different designs will be evaluated, and are:
 - o NESL containing an LNG storage and LNG power plant
 - o NESL containing an LNG storage, LNG power plant, battery, thermal storage and heat pump
 - o NESL containing an LNG storage, LNG power plant, battery, thermal storage, heat pump and solar park
 - o NESL containing an LNG storage, LNG power plant, a battery capacity of 50MWh, thermal storage, heat pump and solar park
- Evaluate the environmental effects of the different system designs above in terms of CO₂ emissions.

4. Literature review

This chapter presents a review of the literature relevant to formulate, solve and analyse the NESL model. To the author's knowledge, the energy system presented in this thesis has not been formulated and studied elsewhere. This chapter has, therefore, expanded to relevant optimisation literature covering sub-systems of the NESL.

Section 4.1 presents what optimisation is, in terms of scientific approach, and Mixed Integer Programming(MIP), which is the modelling method used in this thesis. Section 4.2 investigates different sub-systems of the NESL. Different solution methods are presented in Section 4.3, focusing on exact methods, and a heuristic approach to reduce the solving time. Section 4.4 describes how to perform a sensitivity analysis that can be statistically valid, which aims to improve the understanding of the system.

4.1 Optimisation and Mixed Integer Programming

Optimisation, or operations research, is the science of achieving optimal or near-optimal solutions to complex decision-making problems. It is executed by formulating mathematical equations that reflect the whole problem, called constraints, and solving an objective function to minimize or maximise certain decision variables, typically based on cost or profit. The beginning of the scientific approach has generally been attributed to the British military during the Second World war. At that time, they gathered scientists to allocated limited resources the best possible way. Resultantly, operations research played a vital role in winning the air battle of Britain as they discovered a better way of locating the radars to increase the area of coverage. Today, operations research is applied to, for instance, logistics, process and supply chain management to obtain an optimal setup(Hillier & Lieberman, 2015).

There are many subcategories within operations research such as queuing theory, inventory theory, simulation and linear programming to mention a few(Hillier & Lieberman, 2015). This thesis will apply linear programming, with a Mixed Integer programming (MIP) problem.

Linear MIP problems are problems that consist of a mix of continuous and integer variables, formulated by linear equations. A linear equation consists only of one variable per term. The integer variables are important to determine some variables that do not make sense being a continuous number, which for instance can be the number of factories to build. Integer variables are much harder to solve, and by including it, the problem becomes more complex(Kaufmann & Henry-Labordère, 1977).

4.2 Stand-alone energy system

Energy systems that are not connected to other energy distribution networks are called stand-alone systems. This is the case for Longyearbyen as it is an isolated island, and the whole system depends on being self-sufficient(Thorud, 2018). To the author's knowledge, the model created in this thesis is the first containing all the following for a stand-alone energy system:

- CHP power plant
- Hybrid power system with a power plant and a solar park
- LNG storage supplied by ships

The literature review has focused on covering the modelling aspects of the above-mentioned points. No similar energy systems have been found, and the review will, therefore, focus on sub-systems of the NESL.

CHP production is known for a very good total system efficiency compared with only electricity production. For Longyearbyen that already has a district heating network integrated, this is the preferred option(Bøckman, 2017). *Gopalakrishnan (2014)* looked at how a MIP model improved the power system efficiency with 6%, reduced costs with 11% and emission by 14% for the University of Massachusetts' CHP system. An important part of the study was to model the process down to an hourly timestep, to account for demand variations that affected the system. That could, for instance, be changing weather conditions or time-of-day factors(*Gopalakrishnan, 2014*).

Hybrid power systems with energy storages are common today. A study done by *Ani (2016)* showed that a combination of Solar panels and diesel generators resulted in nearly three times the capital cost compared with diesel generators alone. However, looking at the lifetime costs of the system, it was less than one-half of the diesel generators alone(*Ani, 2016*).

Omu et al. (2013) successfully created a MIP model for a combined CHP and hybrid power system. The system was not a stand-alone system, as it was connected to the national electricity grid. Wind turbines, solar panels, and CHP power plant were implemented to deliver the required electricity and heat(*Omu et al., 2013*).

Energy storage is good for peak shaving, and can potentially reduce the costs of the system considerably(Thorud, 2018). A study executed by *Lu et al. (2014)* looked into the interaction between energy capacity and costs. Batteries are expensive energy storages, and an optimal combination between capacity and peak shaving can reduce costs. The created model was a MIP(*Lu et al., 2014*).

(*Pazouki, 2014*) modelled a MIP of an energy hub containing CHP, gas storage and electricity and thermal storages. This was not a stand-alone system as it was connected to both the electricity grid and gas network. The study showed that storages reduced the costs significantly, and how a gas storage can be implemented in a MIP model.

4.3 Solution methods

The solution time for a MIP problem is directly linked to the complexity of the model. The more variables a problem contains, primarily integer variables, the more computational effort is required (Lenstra & Rinnooy Kan, 1979). The model in this thesis is complex, containing a great number of binary and integer variables. The solution method will, therefore, be important for the application of the model.

This section will present the two common solution methods solving optimisation problems, i.e. exact methods and heuristic methods. There are different heuristic methods available, but this literature review will only focus on the heuristic which has been applied in this thesis. The exact method guarantees to find the optimal solution of the model, while the heuristic method does not. The advantage of the heuristic approach is that for large problems, the solution time can be reduced dramatically and to an applicable level which is not the case for the exact method (Rothlauf, 2011). For most applications, the most important thing is not to find optimality, but a solution close to optimality within an acceptable time. The quality of the heuristic can be measured by comparing the computational time and result with an exact solution for a simplification of the same problem, e.g. run a simulation for 3 months instead of 12 and see how it affects the result (Pérez et al., 2004).

4.3.1 Exact methods

An exact solution method solves a problem to optimality, but may be very time-consuming. This section will present the most widely used exact method in commercial software's today, called the branch-and-bound (B&B) method (Clausen, 1999). This method has been used in this thesis.

The B&B method was first introduced in 1960, during a time where a lot of research was done to solve integer problems more efficiently (Land & Doig, 1960). The algorithm is numerical, and breaks down the full problem into sub-problems, making them easier to solve. By adding additional constraints, the variables will be restricted to take integer solutions, which is called branching. Sub-problems that will not strengthen the optimal solution are removed, called bounding, which may reduce the computational time significantly (Hillier & Lieberman, 2015).

Which sub-problem to solve next, branching, is of big importance for the total computational time of the model. In a study performed by (Linderoth & Savelsbergh, 1999), different search strategies were evaluated to discover a superior strategy. However, the conclusion was that no strategy outperforms the others, and that the best choice is dependent on the MIP problems individually.

4.3.2 Rolling Horizon Heuristic

A heuristic is a method to obtain a feasible and satisfactory solution to a problem that is impractical to solve with exact methods. The intention with the heuristic is to reduce the number of calculations to be executed, so that a good solution is found quickly. A good heuristic will ideally remove the bad options, and leave only a limited number of good options. The remaining options will then be much easier to solve. The downside is of course that heuristics do not know what options are good or bad, and it may, therefore, remove some good options, even the optimal one (Pearl, 1984). As problems are different, there is a broad range of different heuristics that are used for MIP.

The Rolling Horizon Heuristic (RHH) is a heuristic that is very efficient for models with decision-making issues in different periods. Some of these models are long-termed, i.e. decisions made in the first period affect the results for a long time. Other models are short-termed, where a decision made in the first month only affects the second month, or none (Sethi & Sorger, 1991). The heuristic is widely used in manufacturing scheduling, where uncertainty and planning of existing resource distribution are important (Rakke et al., 2010). The model in this thesis will consist of many periods, where decisions effects are in the short-term category. The main objective is to determine the ideal dimensions of the different components in the system, rather than how to use them. However, an optimal resource distribution will discover the most efficient system, which again will solve the main objective. The decision was, therefore, to apply a RHH for this model.

The RHH is an algorithm constructed to simplify the domain of the problem, concentrating on the current period. That is done by relaxing the problem removing the integer constraints for the future periods, and keep the integer restrictions for the current period. Previous periods, called frozen periods, that has already been solved, will have their integer variables fixed. The frozen and future periods have by that become easy to solve as the integer variables has been reduced, and the current period can be solved with the B&B method to optimality. The computational time will then drop significantly (Dimitriadis et al., 1997). By including all periods, it is ensured that the model considers the time horizon, and is less exposed to end-effects which would have been the case solving one period at a time independently. End-effects are unfavourable storage levels that occurs at the end of the run with respect to future operation (Grinold, 1983), e.g. storage level is empty and you are forced to re-supply even though that is more expensive than doing in one month earlier. The RHH presented is known as the forward RHH, and is the most common. Figure 26 illustrates the method.

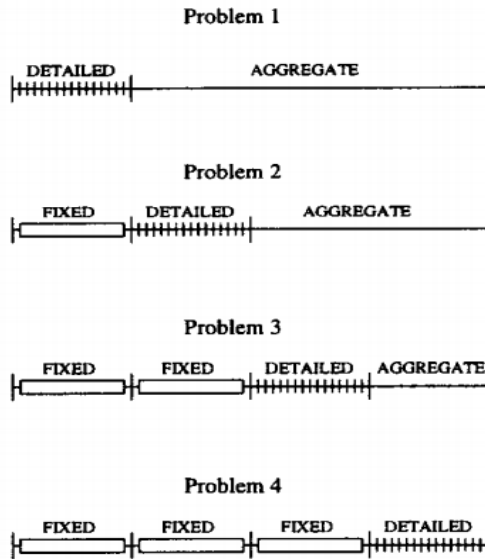


Figure 26: Illustration of the forward RHH(Dimitriadis et al., 1997).

An extension to the forward RHH, is the backward RHH, Figure 27. It was performed and compared with the forward RHH in a study done by *Dimitriadis et al. (1997)*. In the study, the backward RHH proved to be the best heuristic, resulting in better objective solution and less computational time. Further, it was concluded that the backward RHH fits better to models where the most important periods are late in the horizon(Dimitriadis et al., 1997).

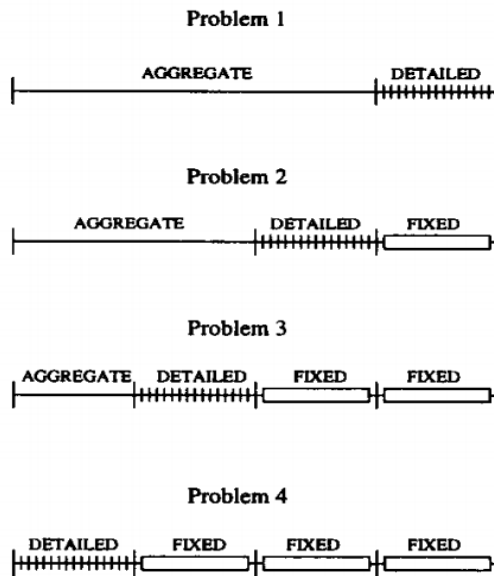


Figure 27: Illustration of the backward RHH(Dimitriadis et al., 1997).

Another extension, Figure 28, is the RHH with overlap, solving only sub-problems of the model at a time. The heuristic reduces the size of the total problem, thus the computational time. However, it is more exposed to end-effects, as this occurs for every period. The

overlapping, i.e. moving backwards to a point within the previous run, is thus effective to avoid unrealistic storage behaviours that can arise due to the end effects(Schreck, 2016).

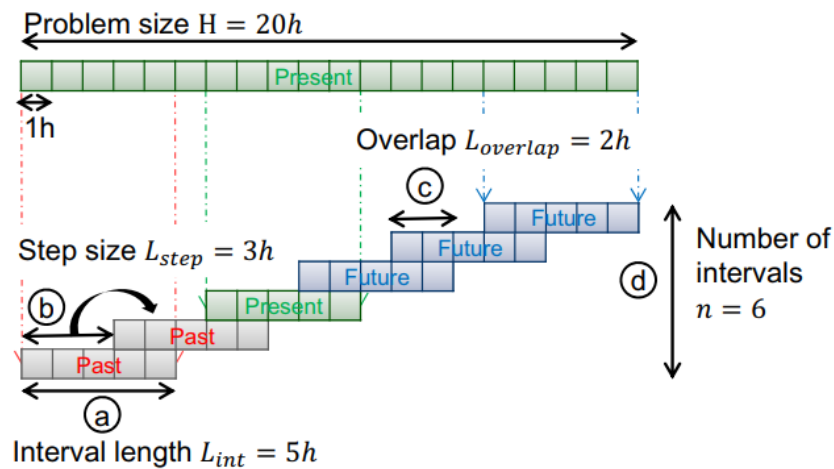


Figure 28: Illustration of RHH with overlap(Marquand et al., 2015).

4.4 Sensitivity analysis

Sensitivity analysis is often executed to MIP problems when some of the input data is uncertain, and it is desirable to see how the model output is affected by input variations. The variations could be due to dynamic factors such as price and demand variations. A sensitivity analysis will help to understand the system response, and may improve the robustness of the final design(Thie & Keough, 2008). Applying a sensitivity analysis in this thesis is applicable because the future is uncertain, and by gaining a thorough understanding of the system response, a better decision of the final design can be made.

This thesis will focus on applying a full factorial design to discover the sensitivity of the system. A factorial design is a type of experiment that can study the effects several factors can have on the response. It is executed by varying the input levels of the factors, and run a simulation for each scenario. For instance, a design with a factor A with two levels, and a factor B with three levels, will look like Figure 29. It will in total make up 6 different scenarios, where each individual combination is present. Full factorial design means that all scenarios are simulated(MiniTab, 2018).

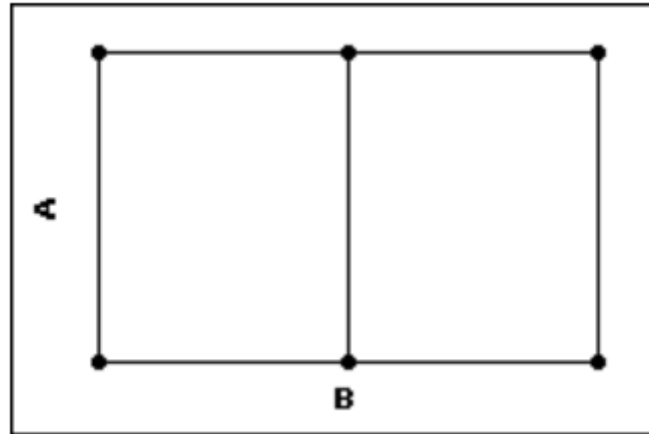


Figure 29: Illustration of a full factorial design with a factor A with two levels, and a factor B with three levels. That makes a total of 6 different scenarios.

Analysis Of Variance(ANOVA) is a widely used statistical method to discover systematic patterns between different effects. The test method can tell whether the effects are statistically significant or not(Sahai & Ageel, 2000). The ANOVA calculations will in this thesis be executed by MiniTab 18, where the results from the full factorial experiment are the input to MiniTab 18. The equations that are used by MiniTab 18 are attached in Appendix C for your convenience. MiniTab 18 provides a pareto chart, main effects plot and interaction plots when running the ANOVA test. The pareto chart illustrates what factors that statistically follows different trends, and the main effect and interaction plots illustrate how they follow the trends(MiniTab, 2018).

5. Model Formulation

This chapter presents the mathematical optimisation model of the NESL problem. The chapter starts with presenting the modelling choices and assumptions that have been done to formulate the model mathematically, Section 5.1. Each system component has been described in its own sub-section to enhance the readability. Section 5.2 defines the sets, indices, parameters, and variables that have been formulated to create the model. The full mathematical model formulation is presented in Section 5.3.

5.1 Modelling choices and model assumptions

This section outlines the modelling choices and the underlying assumptions creating the foundation for the NESL model. The section first describes the overall assumptions that apply to the model, and continues for each specific system component.

5.1.1 Overall assumptions

The NESL is intended to be designed for a 30-year lifetime, thus will the time horizon for this model be 30 years. To reduce the computational time, the model will only run for 12 months, and the variable costs will be scaled up by multiplying with 30 to account for that accordingly. Degradation effects occurring to different components, e.g. solar panels and batteries, is neglected and not implemented in this model. That is because the degradation effects are small. However, it is important to be aware that the system will change over its lifetime.

The model is created to consider hourly effects to increase the precision of the results. This allows for designing the system for hourly peak demands and irradiation, which are varying significantly in Longyearbyen, as seen in Section 2.1.

Uncertainty factors such as the different demands, solar irradiance, and variable costs are assumed constant over the model lifetime, i.e. 30 years. The values will most likely fluctuate, but it is assumed to be a satisfactory approach. Temperature effects are affecting the system, e.g. heat demand, electricity demand, and storage losses, and are integrated into the applicable input data. It is, thus, not implemented as a factor in itself.

The natural gas will be considered as LNG through the whole model. This is done to avoid an extra transformation term, which does not impact the results.

Operating costs for the LNG storage, LNG power plant and solar park in terms of crew and maintenance are assumed fixed independently of the final NESL design. Variation in operating costs for crew and maintenance are considered to be roughly equal independent of the different solutions and NESL designs, and are therefore not included in the model because it will not affect the optimal system dimensions(Vartdal, 2018).

All input data is given in section 7.2.

5.1.2 Ship supply

The ships supplying Longyearbyen are assumed to depart from Rotterdam, Netherlands, and the sailing route is illustrated in Figure 30. Rotterdam has been chosen because other ports closer does not offer LNG for so small ships applicable to supply Longyearbyen. Associated sailing time and costs for the different ships are considered constant over the time period. No ice has been assumed in cooperation with the industry because the sailing route into Longyearbyen has been ice-free for the last 7 years. Ship deliveries are modelled monthly and will supply at the beginning of each month. Four ships with different loading capacities are used in this model.

LNG is stored under high pressure and cold temperature. For that reason, losses will occur due to regasification during transportation. This has been implemented in the model. Procurement of LNG is outside the scope of the model and is considered not to be of any limitation.

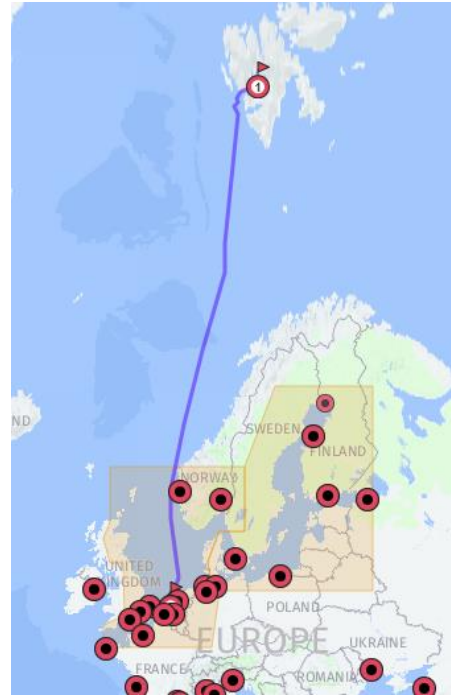


Figure 30 Sailing route from Rotterdam to Longyearbyen(Searoutes.com)

5.1.3 LNG storage

Building costs related to the LNG storage are assumed linear for each cubic meter within the storage dimensions relevant to this system, in accordance with the industry partners(Wallentinsen, 2018). The costs are mainly associated with steel and insulation.

Alike ship transportation, there will be storage losses due to regasification in the storage because the gas is stored liquified. The loss factor is considered constant over the time period and is a certain percentage of the stored volume in the tank, i.e. higher loss when more LNG is stored. Incoming and outgoing LNG from the storage is modelled monthly, and not hourly, to reduce computational time. That is because hourly precision does not affect the LNG storage capacity because the dimensioning storage levels occur at the start of each month, right before and after a possible ship supply.

Trading is not considered in the model. That is because the circulating volumes in Longyearbyen are limited, hence are there not much potential for it as the LNG storage should only satisfy the bunkering demand.

A safety limit corresponding to 30 days of energy production during winter is determined together with Longyearbyen Lokalstyre(Dyrstad, 2018).

5.1.4 LNG power plant

The gas engines in the power plant consist of the same engine type, i.e. same power output and price. The engines are producing equally much heat and electricity when operating, and

they do have an ideal workload interval where they are more efficient. A penalty is added when the engines are operating below ideal workload, and the engines must operate above the minimum workload.

The power production in the gas engines is modelled hourly because peak loads for electricity and heat are the dimensioning factors for the number of required engines.

The price of natural gas related to power production is considered constant, and the conversion from LNG to useful heat and electricity is considered constant. The thermal efficiency is considered constant, except when the engines are operating at unideal workload, then, a penalty is added.

5.1.5 Solar park

The solar panel efficiency is considered constant, i.e. production will only vary with received GHI. Solar radiation and electricity production in the panels are modelled hourly to design for dimensioning loads, i.e. hourly energy demand and GHI variations.

Only one-panel type is used in the model. There are no space limitations for building the solar park. The number of panels includes private solar panels already installed in Longyearbyen.

5.1.6 Battery

Incoming and outgoing electricity flow in the battery is modelled hourly. A loss factor has been implemented for all incoming electricity, and the loss is considered constant over the model run. That is because the battery is assumed to be sufficiently insulated in the GraviFloat so that temperature effects will be negligible.

Overcharging and undercharging the battery will damage the capacity and lifetime. Restrictions to avoid this are, thus, implemented.

5.1.7 Heat pump

The heat pump is modelled with a constant efficiency ratio. That is because the energy source where the pump will bring heat from will be deep down in the ground or sea with constant temperature (NOVAP, 2018).

The capacity of the heat pump has been modelled with respect to the electricity input capacity. That means that the output of the heat from the heat pump will be the input times the efficiency ratio. The heat pump flows are modelled hourly.

5.1.8 Thermal storage

The thermal storage flows are modelled hourly. A loss factor is modelled to account for heat losses in the thermal storage. The factor corresponds to a percentage of the stored heat in the tank and is assumed constant during the model period. It is a simplification as the losses will be greater when the temperature is colder. However, the tank will be insulated and located in the GraviFloat, making the season effects smaller, which made the foundation of the assumption.

There are space limitations associated with the storage. It is intended to be an integrated part of GraviFloat, which determines an upper space restriction. In addition, the input and output values of the storage size are given in cubic meters after a request from the industry partners. That is because cubic meters are more intuitive to understand than KWh. The model will convert the energy storage potential per cubic meter to KWh, and back to cubic meters.

5.1.9 Electricity and heating network

The infrastructure of today's electricity and district heating network handles the current demand. The networks are therefore considered sufficient for the new energy system without any expansions, and is not implemented in the model.

5.1.10 Demand

The ship bunkering demand is modelled monthly, heat and electricity are modelled hourly. That is because of the dimensioning impacts mentioned earlier in this section related to the decision variables.

It has been implemented an upper limit for energy waste to limit the misuse. That has been done due to the environmental focus in Longyearbyen and at Svalbard.

When at least one gas engine is running in the power plant, the electricity demand will increase as the power plant will need more energy. Hence is an additional electricity demand implemented when this happens.

5.2 Definition of sets, indices, parameters, and variables

Table 2: Indices.

Index		
h	-	Hour
m	-	Month
s	-	Ship size

Table 3: Sets.

Set			
H	-	Set of hours	$H : \{1, \dots, H \}$
M	-	Set of months	$M : \{1, \dots, M \}$
S	-	Set of ship sizes	$S : \{1, \dots, S \}$

Table 4: Parameters

Parameter	
$A^{ElectricityDemand}$	- Additional electricity demand if the power plant is producing energy [KWh]
$C^{Battery}$	- Investment costs battery storage per KWh [USD/KWh]
$C^{Engines}$	- Investment cost per gas engine [USD/engine]
$C^{HeatPump}$	- Investment costs heat pump [USD/KW]
$C^{LNGcombustion}$	- Costs of combusted LNG in the power plant [USD/m ³]
$C^{LNGStorage}$	- Building cost per cubic meter of LNG storage [USD/m ³]
$C^{SolarPanel}$	- Investment costs solar panels [USD/panel]
$C_s^{ShipCharter}$	- Cost for chartering ship of size s [USD/ship]
$C^{ThermalStorage}$	- Building cost per KWh of thermal storage capacity [USD/KWh]
$D_{hm}^{Electricity}$	- Electricity demand in hour h in month m [KWh]
D_{hm}^{Heat}	- Heat demand in hour h in month m [KWh]
D_m^{LNG}	- Demand of LNG to ships through month m [m ³]
E_{hm}^{Solar}	- Global Horizontal Irradiance each hour h in month m [kW/m ²]
$F^{HeatPump}$	- Conversion rate electricity to heat [KWh/KWh]
$F^{Powerplant}$	- Conversion rate LNG to electricity/heat [KWh/m ³]
$F^{SolarPanel}$	- Conversion rate solar radiation to electricity [KWh/KWh]
$I^{Battery}$	- Initial battery level [%]
$I^{LNGStorage}$	- Initial LNG storage level [%]
$I^{ThermalStorage}$	- Initial thermal storage level [%]
$L^{Battery}$	- Energy loss in battery [%]
$L^{EnginePenalty}$	- Gas engine penalty for operating below ideal workload [KWh]
$L^{LNGStorage}$	- Energy loss in the LNG storage [%]
$L^{ThermalStorage}$	- Energy loss in thermal storage [%]
$M^{IdealOperation}$	- Big M to linearize the ideal operation constraints [KWh]
$M^{OperatingEngines}$	- Big M to linearize the operating engines constraints [engine]

$O^{LowerIdealOperatingLimit}$	- Engines operating above this limit is operating at ideal workload [%]
$O^{LowerOperatingLimit}$	- Lower operating limit for the engines [%]
$P^{PowerplantMachines}$	- Power output per engine [KWh]
P_s^{Ship}	- Load capacity for ship s [m ³]
R	- Ratio electricity/heat production in gas engines [%]
$S^{MaxBattery}$	- Max battery level to avoid overcharging [%]
$S^{MaxThermalStorage}$	- Upper thermal storage size due to space restrictions [m ³]
$S^{MinBattery}$	- Min battery level to avoid undercharging [%]
$S^{MinLNGStorage}$	- LNG storage safety level [m ³]
$S^{MinThermalStorage}$	- Min capacity thermal storage [KWh]
T	- Time horizon [years]
$W^{MaxElectricity}$	- Max level of electricity waste [KWh]
$W^{MaxHeat}$	- Max level of heat waste [KWh]

Table 5: Variables

Variable

a_{ms}^{Ship}	- LNG loaded on ship s in month m [m ³]
$b^{Battery}$	- Bought battery [KWh]
$b^{HeatPump}$	- Bought heat pump [KW]
b_{hm}^{LNG}	- Bought LNG in hour h in month m [m ³]
$b^{LNGStorage}$	- Bought LNG Storage [m ³]
$b^{Engines}$	- Bought gas engines to power plant [-]
$b^{SolarPanel}$	- Bought solar panels [-]
$b^{ThermalStorage}$	- Bought thermal storage [m ³]
$\delta_{hm}^{Powerplant}$	- Binary variable, takes value 1 if the power plant is operating in hour h in month m, 0 otherwise
δ_{ms}^{Ship}	- Binary variable, takes value 1 if ship s is used in month m, 0 otherwise [-]
$e_{hm}^{BatteryToHeatPump}$	- Electricity from battery to heat pump in hour h in month m [KWh]
$e_{hm}^{BatteryToNetwork}$	- Electricity from battery to electricity network in hour h in month m [KWh]

$e_{hm}^{PlantToBattery}$	- Electricity from power plant to battery in hour h in month m [KWh]
$e_{hm}^{PlantToHeatPump}$	- Electricity from power plant to heat pump in hour h in month m [KWh]
$e_{hm}^{PlantToNetwork}$	- Electricity from power plant to electricity network in hour h in month m [KWh]
$e_{hm}^{SolarParkToBattery}$	- Electricity from solar park to battery in hour h in month m [KWh]
$e_{hm}^{SolarParkToHeatPump}$	- Electricity from solar park to heat pump in hour h in month m [KWh]
$e_{hm}^{SolarParkToNetwork}$	- Electricity from solar park to electricity network in hour h in month m [KWh]
$h_{hm}^{HeatPumpToNetwork}$	- Heat from heat pump to district heating in hour h in month m [KWh]
$h_{hm}^{HeatPumpToStorage}$	- Heat from heat pump to thermal storage in hour h in month m [KWh]
$h_{hm}^{PlantToNetwork}$	- Heat from power plant to district heating in hour h in month m [KWh]
$h_{hm}^{PlantToStorage}$	- Heat from power plant to thermal storage in hour h in month m [KWh]
$h_{hm}^{StorageToNetwork}$	- Heat from thermal storage to district heating in hour h in month m [KWh]
$\mu_{hm}^{Engines}$	- Number of engines operating in hour h in month m [-]
$S_{hm}^{Battery}$	- Existing electricity in battery in hour h in month m [KWh]
$S_m^{LNGStorage}$	- Existing LNG in the storage tank in month m [m ³]
$S_{hm}^{ThermalStorage}$	- Existing heat in thermal storage in hour h in month m [KWh]
$\zeta_{hm}^{Powerplant}$	- Binary variable, takes value 1 if the engines are operating below ideal workload, 0 otherwise

5.3 Mathematical model

5.3.1 Objective function

$$\min z = C^{LNGStorage} * b^{LNGStorage} \quad (5.1a)$$

$$+ \sum_{m \in M} \sum_{s \in S} C_s^{ShipCharter} * \delta_{ms}^{Ship} \quad (5.1b)$$

$$+ \sum_{h \in H} \sum_{m \in M} C^{LNGcombustion} * b_{hm}^{LNG} + C^{Engines} * b^{Engines} \quad (5.1c)$$

$$+ C^{SolarPanel} * b^{SolarPanel} \quad (5.1d)$$

$$+ C^{Battery} * b^{Battery} \quad (5.1e)$$

$$+ C^{HeatPump} * b^{HeatPump} \quad (5.1f)$$

$$+ C^{ThermalStorage} * b^{ThermalStorage} \quad (5.1g)$$

The objective function z minimises the total cost related to the NESL. Part (5.1a) is the investment cost associated with the LNG storage. Part (5.1b) is the total voyage cost for shipping LNG to Longyearbyen. Part (5.1c) contains the LNG consumption and investment costs of the LNG power plant. Part (5.1d)-(5.1g) are the investment costs related to the solar panels, battery, heat pump and thermal storage respectively.

5.3.2 Constraints

LNG supply constraints

$$a_{ms}^{Ship} \leq P_s^{Ship} * \delta_{ms}^{Ship} \quad m \in M, s \in S \quad (5.2)$$

Constraints (5.2) ensure that the transported quantity of LNG is shipped on a ship with sufficient capacity, and that the ship is selected for the charter. The left-hand side is the volume transported on the ship, the right-hand side contains the loading capacity of the ship, and a binary variable telling whether the ship is selected or not.

LNG storage constraints

$$S_m^{LNGStorage} + \sum_{s \in S} a_{ms}^{Ship} \leq b^{LNGStorage} \quad m \in M \quad (5.3)$$

$$\begin{aligned} (S_m^{LNGStorage} + \sum_{s \in S} a_{ms}^{Ship} - D_m^{LNG} - \sum_{h \in H} b_{hm}^{LNG}) * L^{ThermalStorage} \\ = S_{(m+1)}^{LNGStorage} \quad m \in M \end{aligned} \quad (5.4)$$

$$\begin{aligned} (S_m^{LNGStorage} + \sum_{s \in S} a_{ms}^{Ship} - D_m^{LNG} - \sum_{h \in H} b_{hm}^{LNG}) * L^{ThermalStorage} \\ \geq S^{MinLNGStorage} \quad m \in M \end{aligned} \quad (5.5)$$

$$S_1^{LNGStorage} = I^{LNGStorage} * b^{LNGStorage} \quad (5.6)$$

$$S_{|M|+1}^{LNGStorage} = I^{LNGStorage} * b^{LNGStorage} \quad (5.7)$$

Constraints (5.3) ensure the model to never store more LNG in the storage than the capacity. The left-hand side adds the stored LNG and the LNG ship supply, the right-hand side is the bought capacity of the LNG storage. Constraints (5.4) make sure the amount of LNG in the storage for the next month is equivalent to the incoming and outgoing flows of the storage in the current month. A loss term is added to account for regasification of LNG stored to the next month. Constraints (5.5) ensure the amount of LNG in the storage to always be above the safety limit. Constraint (5.6) and (5.7) controls the starting and ending storage levels of the model to take a value equal to the selected initial level. The ending constraint has been selected to avoid unfavourable end-effects, i.e. an empty storage when moving into a new year. The value of the starting and ending level is equal to ensure a system in balance.

LNG power plant constraints

$$\mu_{hm}^{Engines} \leq b^{Engines} \quad h \in H, m \in M \quad (5.8)$$

$$\mu_{hm}^{Engines} \leq D_{hm}^{Heat} \quad h \in H, m \in M \quad (5.9)$$

Constraints (5.8) ensure that the number of gas engines operating for each hour in the power plant does not exceed the total number of bought engines. Constraints (5.9) limit the model to not operate during hours that does not exist in the respective month, i.e. shorter months like February. The demand has been set to zero for those hours as there is no demand, thus will the operating engines be zero.

$$b_{hm}^{LNG} * F^{Powerplant} \leq b^{Engines} * P^{PowerplantMachines} \quad h \in H, m \in M \quad (5.10)$$

$$b_{hm}^{LNG} * F^{Powerplant} \leq \mu_{hm}^{Engines} * P^{PowerplantMachines} \quad h \in H, m \in M \quad (5.11)$$

$$\begin{aligned} b_{hm}^{LNG} * F^{Powerplant} \\ \geq O^{LowerOperatingLimit} * \mu_{hm}^{Engines} \\ * P^{PowerplantMachines} \quad h \in H, m \in M \end{aligned} \quad (5.12)$$

$$\begin{aligned} b_{hm}^{LNG} * F^{Powerplant} \\ \geq O^{LowerIdealOperatingLimit} * \mu_{hm}^{Engines} * P^{PowerplantMachines} \\ - M^{IdealOperation} * \zeta_{hm}^{Powerplant} \quad h \in H, m \in M \end{aligned} \quad (5.13)$$

Constraints (5.10) ensure that the natural gas combusted in the power plant will never exceed the power output of the bought gas engines. Constraints (5.11) control that the natural gas that is converted into electricity and heat does not exceed the power output capacity of the operating engines operating in the power plant for each specific hour. Constraints (5.12) ensure that the energy production in the operating gas engines never drops below their minimum workload. Constraints (5.13) determine if the operating gas engines are running at ideal workload or not. The restrictions utilize the big M method, forcing a binary variable to take value 1 if the power plant is operating below the ideal workload. It is, thus, important that the big M has a value big enough so that the constraint can always be feasible when the binary variable is 1. The unideal interval for the gas engines is between 30-70%, thus has the value of the big M been set to 40% of the theoretical maximum power output from the gas engines in the system. That is determined by the demand that occurs for the most energy demanding hour during the model length.

$$\begin{aligned} b_{hm}^{LNG} * F^{Powerplant} * R - L^{EnginePenalty} * \zeta_{hm}^{Powerplant} \\ = h_{hm}^{PlantToStorage} + h_{hm}^{PlantToNetwork} \quad h \in H, m \in M \end{aligned} \quad (5.14)$$

$$\begin{aligned} b_{hm}^{LNG} * F^{Powerplant} * (1 - R) - L^{EnginePenalty} * \zeta_{hm}^{Powerplant} \\ = e_{hm}^{PlantToNetwork} + e_{hm}^{PlantToBattery} \\ + e_{hm}^{PlantToHeatPump} \quad h \in H, m \in M \end{aligned} \quad (5.15)$$

$$M^{OperatingEngines} * \delta_{hm}^{Powerplant} - \mu_{hm}^{Engines} \geq 0 \quad h \in H, m \in M \quad (5.16)$$

Constraints (5.14) handle the outgoing heat flow from the power plant, and add a production penalty if the gas engines are not operating at ideal workload. The penalty is determined by the binary variable, expressed by the big M method in the previous paragraph. Constraints (5.15) control the electricity flow out of the power plant, with the

penalty term for unideal workload. Constraints (5.16) tell if the power plant is operating or not, applying the big M method. The same approach is used for this big M value as mentioned above, where this M value corresponds to the maximum theoretical number of engines required in the LNG power plant.

Solar park constraints

$$\begin{aligned}
 E_{hm}^{Solar} * F^{SolarPanel} * b^{SolarPanel} & & (5.17) \\
 = e_{hm}^{SolarParkToNetwork} + e_{hm}^{SolarParkToHeatPump} & \\
 + e_{hm}^{SolarParkToBattery} & \quad h \in H, m \in M
 \end{aligned}$$

Constraints (5.17) ensure the produced electricity in the solar park to flow out to the system. The left-hand side gives the production of the solar park, multiplying the solar irradiance with the number of solar panels and their respective efficiency. The right-hand side contains the electricity flows out of the solar park to the different system components.

Battery constraints

$$\begin{aligned}
 e_{hm}^{PlantToBattery} + e_{hm}^{SolarParkToBattery} + S_{hm}^{Battery} & \\
 \leq b^{Battery} * S^{MaxBattery} & \quad h \in H, m \in M \quad (5.18)
 \end{aligned}$$

$$\begin{aligned}
 (e_{hm}^{PlantToBattery} + e_{hm}^{SolarParkToBattery}) * L^{Battery} + S_{hm}^{Battery} & \\
 - e_{hm}^{BatteryToNetwork} - e_{hm}^{BatteryToHeatPump} & \quad (5.19) \\
 = S_{h+1,m}^{Battery} & \quad h \in H, m \in M
 \end{aligned}$$

$$\begin{aligned}
 (e_{hm}^{PlantToBattery} + e_{hm}^{SolarParkToBattery}) * L^{Battery} + S_{hm}^{Battery} & \\
 - e_{hm}^{BatteryToNetwork} - e_{hm}^{BatteryToHeatPump} & \quad (5.20) \\
 \geq b^{Battery} * S^{MinBattery} & \quad h \in H, m \in M
 \end{aligned}$$

Constraints (5.18) make sure there is never more electricity stored in the battery than its capacity. In addition, they ensure the battery to not be overcharged and lose capacity. The left-hand side contains the incoming electricity and the already stored electricity in the battery. Outgoing electricity flows are not included for conservative reasons. The right-hand side accommodate the bought battery capacity, as well as the level of overcharging.

Constraints (5.19) control the electricity flow balance into and out of the battery for the next hour. A loss factor is implemented to account for the losses of using the battery, i.e. for the incoming electricity flow. Constraints (5.20) ensure the storage level in the battery never to drop below the lower limit, to avoid undercharging.

$$S_{1,1}^{Battery} = b^{Battery} * I^{Battery} \quad (5.21)$$

$$S_{1,|M|+1}^{Battery} = S_{|H|+1,m}^{Battery} \quad m \in M \quad (5.22)$$

$$S_{1,|M|+1}^{Battery} = b^{Battery} * I^{Battery} \quad (5.23)$$

Constraint (5.21) initialises the battery level at the beginning of the run. Constraints (5.22) ensure that the storage level from the last hour in the previous month is the starting level for the first hour in the current month. Constraint (5.23) controls the ending battery level to be equal the starting level of the model. That is to avoid undesired end-effects.

Heat pump constraints

$$\begin{aligned} (e_{hm}^{PlantToHeatPump} + e_{hm}^{SolarParkToHeatPump} + e_{hm}^{BatteryToHeatPump}) * F^{HeatPump} \\ = h_{hm}^{HeatPumpToNetwork} + h_{hm}^{HeatPumpToStorage} \quad h \in H, m \in M \end{aligned} \quad (5.24)$$

$$\begin{aligned} e_{hm}^{PlantToHeatPump} + e_{hm}^{SolarParkToHeatPump} + e_{hm}^{BatteryToHeatPump} \\ \leq b^{HeatPump} \quad h \in H, m \in M \end{aligned} \quad (5.25)$$

Constraints (5.24) control the energy conversion in the heat pump. The incoming electricity multiplied by the efficiency factor gives the outgoing heat flows. Constraints (5.25) ensure that the power input to the heat pump never exceeds the bought capacity. The bought capacity corresponds to the maximum electrical input.

Thermal Storage constraints

$$\begin{aligned} h_{hm}^{PlantToStorage} + h_{hm}^{HeatPumpToStorage} + S_{hm}^{ThermalStorage} \\ \leq b^{ThermalStorage} \quad h \in H, m \in M \end{aligned} \quad (5.26)$$

$$\begin{aligned} (h_{hm}^{PlantToStorage} + h_{hm}^{HeatPumpToStorage} + S_{hm}^{ThermalStorage} - h_{hm}^{StorageToNetwork}) \\ * L^{ThermalStorage} = S_{h+1,m}^{ThermalStorage} \quad h \in H, m \in M \end{aligned} \quad (5.27)$$

$$\begin{aligned} (h_{hm}^{PlantToStorage} + h_{hm}^{HeatPumpToStorage} + S_{hm}^{ThermalStorage} - h_{hm}^{StorageToNetwork}) \\ * L^{ThermalStorage} \geq S^{MinThermalStorage} \quad h \in H, m \in M \end{aligned} \quad (5.28)$$

$$b^{ThermalStorage} \leq S^{MaxThermalStorage} \quad h \in H, m \in M \quad (5.29)$$

Constraints (5.26) ensure the stored heat in the thermal storage never to exceed its bought capacity. The left-hand side contains the incoming heat and the already stored heat in the thermal storage. Outgoing heat flows are not included for conservative reasons. Constraints (5.27) control the heat flow balance into and out of the thermal storage from one hour to the next. A loss factor is implemented to account for the losses that occur to the ambient

environment. Constraints (5.28) handle the storage level never to be below the minimum value. Constraint (5.29) ensure that the bought size of the thermal storage does not exceed the space limitations of the GraviFloat.

$$S_{1,1}^{ThermalStorage} = I^{ThermalStorage} * b^{ThermalStorage} \quad (5.30)$$

$$S_{1,m+1}^{ThermalStorage} = S_{|H|+1,m}^{ThermalStorage} \quad m \in M \quad (5.31)$$

$$S_{1,|M|+1}^{ThermalStorage} = I^{ThermalStorage} * b^{ThermalStorage} \quad (5.32)$$

Constraint (5.30) creates the initial conditions for the beginning of the model run. Constraints (5.31) ensure that the storage level at the end of one month, corresponds to the starting hour in the next month. Constraint (5.32) controls the ending conditions of the run to correspond to the initial conditions, to avoid unfavourable end-effects.

District heating constraints

$$h_{hm}^{PlantToNetwork} + h_{hm}^{StorageToNetwork} + h_{hm}^{HeatPumpToNetwork} \geq D_{hm}^{Heat} \quad h \in H, m \in M \quad (5.33)$$

$$h_{hm}^{PlantToNetwork} + h_{hm}^{StorageToNetwork} + h_{hm}^{HeatPumpToNetwork} - D_{hm}^{Heat} \leq W^{MaxHeat} \quad h \in H, m \in M \quad (5.34)$$

Constraints (5.33) ensure the incoming heat flow to the network to always satisfy the heat demand. Constraints (5.34) control the heat waste never to exceed the predetermined limit.

Electricity network constraints

$$e_{hm}^{PlantToNetwork} + e_{hm}^{BatteryToNetwork} + e_{hm}^{SolarParkToNetwork} \geq D_{hm}^{Electricity} + \delta_{hm}^{Powerplant} * A^{ElectricityDemand} \quad h \in H, m \in M \quad (5.35)$$

$$e_{hm}^{PlantToNetwork} + e_{hm}^{BatteryToNetwork} + e_{hm}^{SolarParkToNetwork} - D_{hm}^{Electricity} - \delta_{hm}^{Powerplant} * A^{ElectricityDemand} \leq W^{MaxElectricity} \quad h \in H, m \in M \quad (5.36)$$

Constraints (5.35) ensure the incoming electricity flow to the network to always satisfy the electricity demand. An additional demand is added to the right-hand side if the power plant is operating, thus requiring additional electricity. Constraints (5.36) control the electricity waste never to exceed the predetermined limit.

Non-negativity constraints

$$\begin{aligned}
 \mathbf{a}_{ms}^{Ship} &\geq 0 & m \in M, s \in S & \quad (5.37) \\
 \mathbf{b}^{Battery} &\geq 0 & & \quad (5.38) \\
 \mathbf{b}^{HeatPump} &\geq 0 & & \quad (5.39) \\
 \mathbf{b}_{hm}^{LNG} &\geq 0 & h \in H, m \in M & \quad (5.40) \\
 \mathbf{b}^{LNGStorage} &\geq 0 & & \quad (5.41) \\
 \mathbf{b}^{Engines} &\geq 0 & & \quad (5.42) \\
 \mathbf{b}^{SolarPanel} &\geq 0 & & \quad (5.43) \\
 \mathbf{b}^{ThermalStorage} &\geq 0 & & \quad (5.44) \\
 \delta_{hm}^{Powerplant} &\geq 0 & h \in H, m \in M & \quad (5.45) \\
 \delta_{ms}^{Ship} &\geq 0 & m \in M, s \in S & \quad (5.46) \\
 e_{hm}^{BatteryToHeatPump} &\geq 0 & h \in H, m \in M & \quad (5.47) \\
 e_{hm}^{BatteryToNetwork} &\geq 0 & h \in H, m \in M & \quad (5.48) \\
 e_{hm}^{PlantToBattery} &\geq 0 & h \in H, m \in M & \quad (5.49) \\
 e_{hm}^{PlantToHeatPump} &\geq 0 & h \in H, m \in M & \quad (5.50) \\
 e_{hm}^{PlantToNetwork} &\geq 0 & h \in H, m \in M & \quad (5.51) \\
 e_{hm}^{SolarParkToBattery} &\geq 0 & h \in H, m \in M & \quad (5.52) \\
 e_{hm}^{SolarParkToHeatPump} &\geq 0 & h \in H, m \in M & \quad (5.53) \\
 e_{hm}^{SolarParkToNetwork} &\geq 0 & h \in H, m \in M & \quad (5.54) \\
 h_{hm}^{HeatPumpToNetwork} &\geq 0 & h \in H, m \in M & \quad (5.55) \\
 h_{hm}^{HeatPumpToStorage} &\geq 0 & h \in H, m \in M & \quad (5.56) \\
 h_{hm}^{PlantToNetwork} &\geq 0 & h \in H, m \in M & \quad (5.57) \\
 h_{hm}^{PlantToStorage} &\geq 0 & h \in H, m \in M & \quad (5.58) \\
 h_{hm}^{StorageToNetwork} &\geq 0 & h \in H, m \in M & \quad (5.59) \\
 \mu_{hm}^{Engines} &\geq 0 & h \in H, m \in M & \quad (5.60) \\
 s_{hm}^{Battery} &\geq 0 & h \in H, m \in M & \quad (5.61) \\
 s_m^{LNGStorage} &\geq 0 & m \in M & \quad (5.62) \\
 s_{hm}^{ThermalStorage} &\geq 0 & h \in H, m \in M & \quad (5.63) \\
 \zeta_{hm}^{Powerplant} &\geq 0 & h \in H, m \in M & \quad (5.64)
 \end{aligned}$$

6. Solution method

To run the full size of the problem presented in the previous chapter, i.e. containing 12 months, will not be possible to solve exactly within an applicable time window. This chapter describes the work that has been done to reduce the computational time to an acceptable level. Section 6.1 explains the data pre-processing that has been done to tighten the model formulation, and Section 6.2 describes the RHH method and how it was created to reduce the computational time.

6.1 Data pre-processing

The exact method will solve the model using the B&B method, section 4.3.1. The down-side of the exact method is that it requires a lot a computational effort. By performing data pre-processing, a tighter mathematical formulation has been achieved, which has reduced the required calculations, thus the computational effort, of the model solving. The mathematical formulation presented in the previous chapter contains the tightened formulation, but this section will explain what terms that have been processed, and how it was done.

There is a lot of information connected to the ship deliveries. That is, charter costs, harbour costs, fuel costs, sailing speed, sailing distance and boil-off losses. The interesting information for the model is total transportation costs and total delivery volume. This data have therefore been pre-processed to remove “unnecessary” calculations. See appendix for details related to cost and boil-off, and section 7.2 for final input data.

In addition, the energy production in the gas engines is dependent on both the energy content in the LNG, as well as the thermal efficiency of the engines. This data has been merged as it is constant over the model period.

6.2 Rolling Horizon Heuristic method

Three different types of RHH methods were presented in section 4.3.2, which were the forward, backward and overlapping RHH. The forward RHH has been chosen for this thesis. The decision was made because the forward RHH considers the whole time domain during the calculations, which may be crucial due to the seasonal variations this problem contains in terms of solar irradiance. If running the overlapping RHH, the solar irradiance will not exist during the first periods, which may affect the solution of the problem by not implementing solar panels at all. The forward RHH was preferred above the backward RHH because the management of the energy flows in the system is dependent on the previous conditions. Solving it backwards may be unfortunate for this model.

The mathematical model for the RHH method is the same as for the exact method. The difference is the relaxation of integer variables for future months, and the fixing of variables from previous months, as explained in section 4.3.2. The final RHH algorithm created in this thesis is presented in the pseudocode below.

RHH algorithm

Input: Instance data

For all (m in Months) **do**

If $m > 1$ **then**

 Read solved integer variables from previous months into the model from the external file, and fix them.

End if

 Relax integer variables for future periods to continuous variables

 Solve the mathematical model with integer constraints for the current period m

 Write the solved integer variables to the external file

End-do

7. Computational study

This chapter aims to evaluate the applicability of the NESL problem formulation as a decision support tool through a computational study. The main objectives are to reduce the computational time of the model to an applicable level, determine the validity of the model, and analyse the economic and environmental effects of four different NESL designs.

A description of the software and hardware implementation will be given in Section 7.1. Section 7.2 presents the input data used in the computational study. The technical study is explained in Section 7.3, aiming to reduce computational time and validate the results of the model. Section 7.4 analyses how different factors affect the NESL from an economic perspective in a sensitivity analysis. Further, four different NESL designs will be tested and evaluated for a realistic future scenario, and a final recommendation will be given based on the economic study. Section 7.5 analyses the environmental effects of the four different NESL designs, and evaluates the environmental impacts of an LNG and/or solar energy based NESL compared with today's energy system in Longyearbyen.

7.1 Implementation

The mathematical model has been written in the algebraic modelling language Mosel and run in the program FICO® Xpress Optimisation suite 7.9 using an ASUS S56CB with Intel® Core™ i5-3337U CPU 1.8 GHz and 8 GB RAM. The operating system in use is Windows 10 Home. It has been created two codes in this thesis, one for the exact method and one for the RHH method. The mathematical model is the same for both codes.

The statistical analysis tool used for the sensitivity analysis is MiniTab® 18. MiniTab® 18 is a software designed to auto-calculate the statistical models and provide clear, illustrative figures. The intention is to allow more focus on the data analysis and interpretation of the results.

Microsoft Excel has been used for the pre-processing and post-processing of the results.

7.2 Data provided by the industry

This section describes the selection of all input parameters. The data has been collected by the industry partners and literature searches, and the values of all parameters have been selected to the best of the author's abilities. The problem owner has agreed that the values seem reasonable, and applicable to simulate realistic instances as accurate as possible.

Overall data

The overall input data to the model are listed in Table 6. These values are used if not otherwise is stated. All months contain the same number of hours, i.e. 31 days multiplied with 24 hours, but shorter months, as February, have been taken into account by setting demand and production to zero for the none-existing hours. The product of the model length in years and the time horizon, equals the designed lifetime of the NESL, i.e. 30 years. Variable costs, i.e. the LNG consumption cost and transportation cost, will be scaled up to 30 years by multiplying with the time horizon. That is to obtain a realistic relationship

between investment cost and variable cost. The waste limits were selected in cooperation with the problem owner (Vartdal, 2018).

Table 6: The overall input data in the model (Vartdal, 2018).

Hours per month [hours]	Model length [months]	Time Horizon [years]	Waste limit electricity [KW/hour]	Waste limit heat [KW/hour]
744	12	30	1 000	1 000

LNG ships

The ship supply information consists of many parameters, e.g. charter cost, harbour taxes, fuel costs and voyage distance, which are given in Appendix A. To avoid extra calculations, the data have been pre-processed as explained in Section 6.1. The two important input parameters, i.e. the total transportation cost and delivery volume, are used for the LNG ship input, Table 7.

Table 7: The input data in the model related to the LNG ships (Vartdal, 2018).

Total transport cost [USD]	Delivery volume [m ³]
369 417	4 958
319 285	7 439
440 938	9 919
531 909	15 888

LNG Storage

The loss factor in the LNG storage is a result of boil-off, and the percentage corresponds to the loss in modern LNG ships. The safety level corresponds to running the gas engines in the power plant for one month during the winter season. Initial storage level is selected to have a starting condition for the model, and is a percentage of the full capacity. The initial level is also the ending level. Table 8 shows the input data connected to the LNG storage.

Table 8: The input data in the model related to the LNG storage (Vartdal, 2018).

Investment cost [USD/m ³]	Loss [%/month]	Safety level [m ³]	Initial storage level [%]
3 050	4.5	1047	50

LNG power plant

The power plant is thought to be outfitted with only one type of gas engines for reliability and maintenance reasons. An additional electricity demand will be present when the gas engines in the power plant are operating because the engines require additional electricity. Note that the energy content of LNG and the ideal engine efficiency have been pre-

processed and added together to reduce model input, see section 6.1. The gas engines produce equally much heat and electricity. Table 9 shows the input data for the power plant.

Table 9: The input data in the model related to the LNG power plant(Vartdal, 2018).

Power output per gas engine [KWh]	3 500
Investment costs per gas engine [USD]	3 100 000
Cost LNG consumption for power production [USD/m³]	430
Energy content LNG [KWh/m³]	6 250
Ideal engine thermal efficiency [%]	88
Pre-processed energy content and engine thermal efficiency [KWh/m³]	5 500
Heat and electricity ratio [%]	50-50
Ideal workload interval [%]	70-100
Minimum workload [%]	30
Additional electricity consumption when the power plant is operating [KW]	100
Production penalty for operating at unideal workload [KW/engine]	123

Solar park

The solar park in the model has been based on 72 cell solar panels with watt class 300 W. That means that with a solar irradiance of 1000 W/m², the panel will produce 300 W at a temperature of 25°C. This is called Standard Test Conditions(Melaa, 2018). Table 10 shows the input data for the solar park.

Table 10: Input data in the model related to the solar park(Melaa, 2018).

Investment cost [USD/panel]	Watt class [W]
300	300

Battery

The initial battery level is selected to have a starting point for the model, and the level will also be the ending level. Minimum and maximum capacities are implemented to avoid over and undercharging, Table 11 shows the input data for the battery. The loss factor applies to incoming electricity.

Table 11: Input data in the model related to the battery. Data has been collected by Melaa(2018) and Vartdal (2018).

Investment cost[USD/KWh]	Maximum capacity [%]	Min Capacity [%]	Loss factor [%]	Initial battery level [%]
600	80	20	4	50

Heat pump

The heat pump is a very efficient way to convert electricity into heat. The following specifications for this heat pump are given in Table 12. Notice that investment costs are for each KW electricity into the heat pump.

Table 12: Input data in the model related to the heat pump(Vartdal, 2018).

Investment cost [USD/KW]	Efficiency [-]
375	3.5

Thermal Storage

Table 13 shows the input data for the thermal storage. An upper storage size has been selected due to space restrictions at the Gravifloat. The initial level is the same as for the other storages.

Table 13: Input data in the model related to the thermal storage(Dahlberg, 2018).

Investment cost [USD/KWh]	Loss factor of stored energy [%/hour]	Lower Storage size [m ³]	Upper storage size [m ³]	Initial storage level [%]
5.35	0.2	0	2 000	50

Notice that the upper storage level is given in cubic meters, while the investment cost is given in KWh. That is because the model converts the cubic meter limit into KWh by a factor of 0.0257143 m³/KWh. The output of the model is then converted back to cubic meters. This has been done on request from the industry partners.

The solar irradiance and the energy demands

The solar irradiance and the energy demands are the data that build the foundation of this system. This data is uncertain as it is based on future predictions, and changes in the data will highly affect the solution of the model. A sensitivity analysis of this data will be performed in section 7.4.

The data that will be used in the technical study is the same as presented in section 2.1 for the ship bunkering demand, electricity demand and solar irradiance. As the LNG ship bunkering demand is not existing today, it has been assumed for this study to be equal to the MGO demand today. For the heat demand, there are some shortcomings in the data set. That is, the monitored period does only correspond to about six months, and there are some missing data in the dataset, see Figure 7 in sub-section 2.1.1. As the heating demand is highly dependent on the temperature, a linear regression model was created to complete the data set and predict the missing months. Figure 31 shows the heat demand that has been used in the technical study.

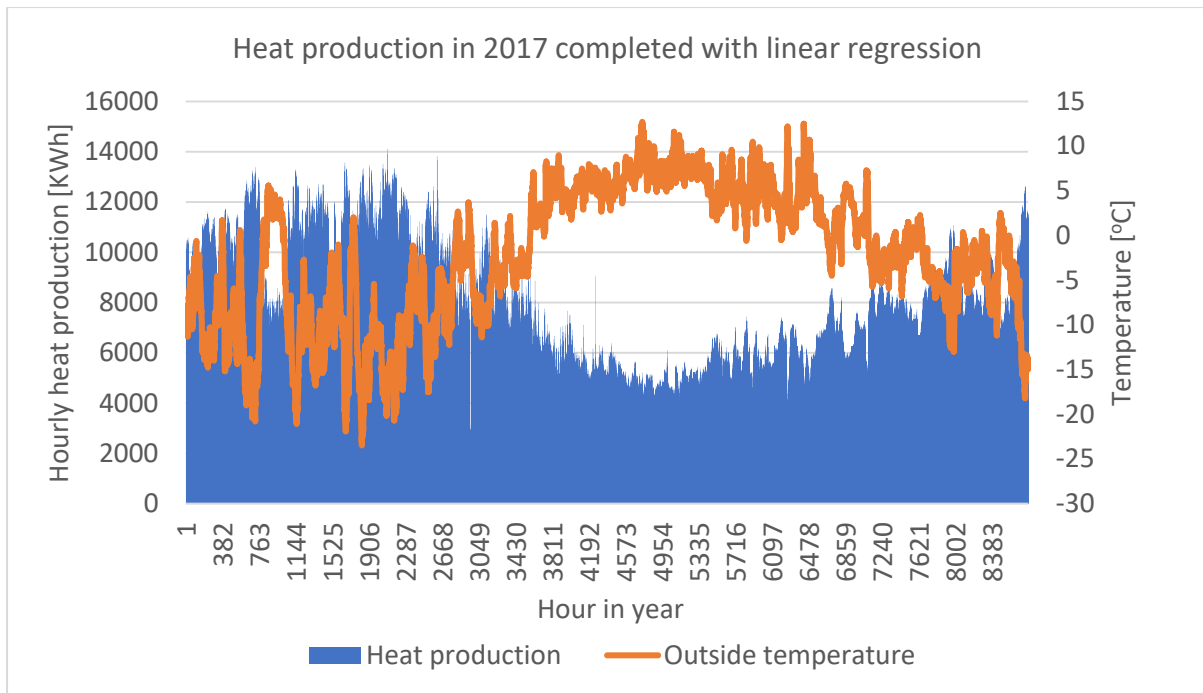


Figure 31: Hourly heat production in Longyearbyen 2017 completed by linear regression. The obtained heat production data contained missing data. Linear regression based on temperature has been used to estimate the missing values.

7.3 Technical study

The technical study aims to reduce the computational time and validate the results of the model, and is, thus, one of the main objectives of this thesis. It has been crucial to reduce the computational time of the model for two reasons. That is because it is important to simulate the problem for all seasons and conditions as the seasonal variations are big, e.g. solar irradiance. And because it will improve the applicability of the model as a decision-making tool as it is more time-efficient. The validation of the model provides reliability in the model results.

The analyses performed in this section are:

- Computational time reduction.
 - o Verification of the RHH method compared with the exact method.
 - o Stopping criteria analysis using the RHH method.
 - o Analysis of the starting and ending storage conditions using the RHH method.
 - o Analysis of the model starting month using the RHH method.
 - o Analysis of the model simulation length using the RHH method.
- Validation of the model using the RHH method.

The data input for the analyses in this section is the same as given in the previous section 7.2, unless otherwise is stated. The energy demands and the solar irradiance are at the same levels as presented in section 7.2

The total cost, also called objective value, related to the system for an operational time of 30 years, has been used as the verification parameter for all the technical analyses in this

section. This value contains information about all the decision variables, and makes the verification process more convenient by only comparing one superior variable.

7.3.1 Verification of the Rolling Horizon Heuristic

Running the exact method will provide the minimum cost solution of the model. However, the computational time of the model will be several days, thus, not applicable to run many different scenarios and analyses. Both the exact method and the RHH method has been run for different problem sizes, i.e. different number of months. The intention has been to be able to verify whether the RHH works as intended, i.e. by giving results close to the exact method, with much less computational effort. As the computational time propagates with the size of the problem, the comparison of the exact and RHH method has only been run for a problem size corresponding to 5 months. That is because the problem sizes of four and five months proved to be very time consuming for the exact method, and it was not able to find the optimal model solution within a time limit of 40 000 seconds. 40 000 seconds have been determined to be the upper acceptable computational time limit to be able to run through all analyses in this thesis. The stopping criterion for this analysis was set to 0% for both the exact method and the RHH method. That means that the model will not abort the simulation before the solution is ensured to be the optimal solution for the method. When the maximum time limit is reached, the simulation will stop, and the current best solution found will be the best result. The optimality gap will occur for these simulations, which will be the difference between the best solution found and the best possible solution the model can find which may not be feasible. For the RHH method, the best solution found is the best possible, thus, there are no optimality gaps. The results from the runs are given in Table 14 below.

Table 14: Result of the computational time and minimum total cost found for the exact method and the RHH method. Optimality gap is the difference between the best solution found and the best possible solution that still can be found for the exact method.

Number of months	Exact method			RHH method	
	Minimum total cost found for 30 years operation [USD]	Optimality gap [%]	Computational time [s]	Minimum total cost found for 30 years operation [USD]	Computational time [s]
1	63 669 500	0	13.8	63 669 500	13.7
2	89 582 000	0	103.8	89 577 100	45.7
3	119 247 000	0	209.8	124 237 000	59.2
4	147 030 000	1.96	Stopped at 40000	144 884 000	116.9
5	165 033 000	0.20	stopped at 40000	165 737 000	380.3

Table 15 below shows the computational time difference between the exact method and the RHH method, as well as the belonging total cost deviation. Note that for the problem size of one month, the exact and RHH methods are identical because there are no frozen or future periods, section 6.2, thus are the computational time and objective value equal. The computational time propagates with the problem size. For the problems with a size of four and five months, the computational time would have been even bigger if the model had run to optimality. The deviations, Table 15 below, remains inside a level of 5%, which is assumed sufficient considering the computational time reduction. If the deviation is negative, it means that the total cost of the RHH method was lower than the exact method. That happens because the exact method has an optimality gap larger than the deviation, and has not yet succeeded in finding the same, or a better solution.

Table 15: Computational time difference and total cost deviation between exact method and RHH method.

Number of months	Computational time difference [s]	Deviation total cost 30 years operation [%]
1	0.1	0.0
2	58.2	0.0
3	150.6	4.2
4	39883.1	-1.5
5	39619.7	0.4

Data in Table 15 shows that using the RHH method significantly reduces the computational time and provides a solution near optimality. The RHH method will, therefore, be applied for the rest of the analysis, with a model length of 12 months.

7.3.2 Stopping criteria analysis using the RHH method

This analysis looks at how an implementation of a stopping criteria limit to the RHH method can reduce the computational time further, and how the solution will deviate from the RHH solution with a stopping criterion of 0%. The stopping criterion means that the model will abort the simulation when the best-found solution deviates within a certain percentage of the best possible solution. For the RHH method, the stopping condition will occur to each individual month in the for-loop in the RHH method, see section 6.2, when the optimality gap drops below a certain percentage. That means that the model will proceed to the next month quicker, and it will reduce the total computational time. Table 16 shows the final results, where the deviation represents the deviation from 0% stopping criteria. Figure 32 gives a graphical presentation of the deviation and time reduction associated with different stopping criteria limits.

Table 16: Resulting computational time and minimum total cost deviation with different stopping criterion percentage. The stopping criterion is a value that determines when the found solution is assumed accurate enough, and the calculations can proceed. The deviation is against the total cost found for the model run with 0% stopping criteria.

Stopping criteria [%]	Computational time [s]	Minimum total cost found [USD]	Deviation [%]
0	1788.0	291 162 000	0.00
0.1	1408.7	291 338 000	0.06
0.25	1363.0	291 357 000	0.07
0.5	1333.9	291 357 000	0.07
0.75	854.4	296 668 000	1.89
1	842.7	296 668 000	1.89
2	815.7	296 668 000	1.89
5	677.9	336 840 000	15.69
10	476.9	424 657 000	45.85

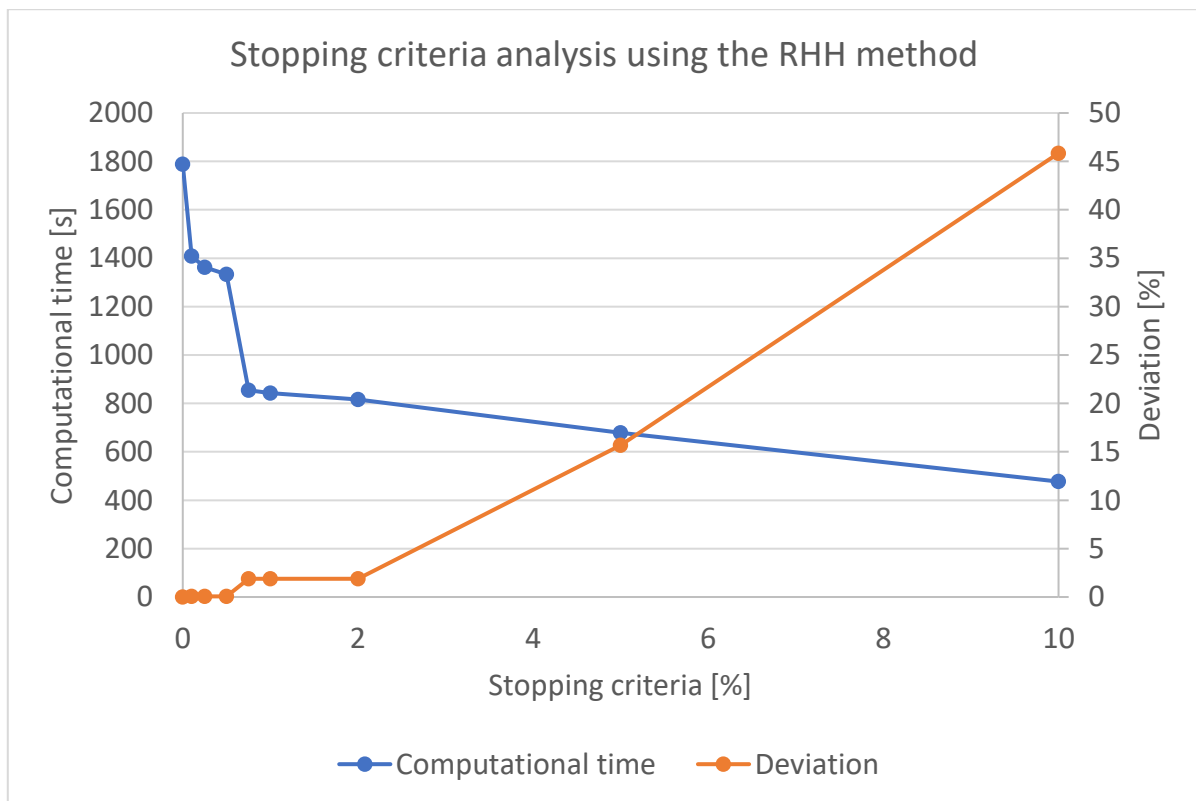


Figure 32: A graphical presentation of how the stopping criterion affects the computational time and total cost deviation from 0% stopping criteria using the RHH method.

The results show that the total computational time drops significantly with higher stopping criteria percentage, and so does the quality of the best solution found as well. However, when reaching a stopping level of 0.5%, the deviation has dropped to a negligible level and the computational time has been reduced by about 25% compared to a stopping criterion of

0%. It has, therefore, been concluded that the ideal stopping criterion for further analysis is 0.5%.

7.3.3 Analysis of the starting and ending storage conditions using the RHH method

The initial and ending storage levels have for the previous runs been 50%, see section 7.2. This analysis investigates if the quality of the solution and the computational time of the model is affected by the initial and ending storage levels selected. The storages in the model are the LNG storage, battery, and thermal storage. It is assumed that the starting and ending levels should be the same, to ensure an energy balance in the system. The different levels are determined to be above 20% and below 80% because that is the upper and lower limit for ideal battery operation. The stopping criterion is set to 0.5% in this analysis. Figure 33 presents the solution time and total costs corresponding to the different starting and ending storage levels.

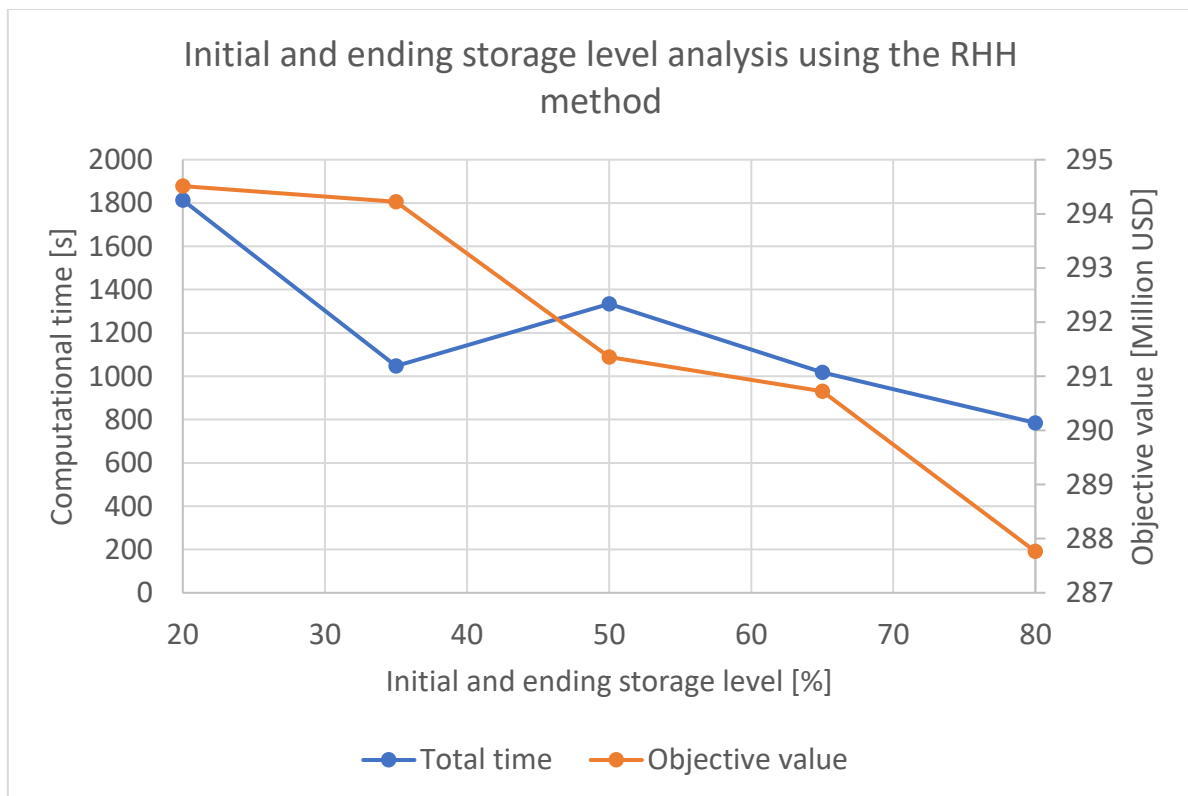


Figure 33: A graphical presentation of how the computational time and total cost is affected by different starting and endings storage levels using the RHH method.

The graph shows that the model finds a better solution with lower total cost when the initial and ending storage level is higher. It is believed to be the case because the model is then more flexible to balance the storage levels, i.e. it has more time to find a better ship supply option. Notice that the total cost savings corresponds to around 1% comparing the storage level of 80% with 50%, and is, thus, not significantly big. The most important finding is that the computational time dropped significantly with higher storage levels, potentially reducing the computational time with 40% for a storage level of 80%, compared with 50%. For the following analysis, the initial and ending storage levels are set to 80% of its capacity.

7.3.4 Analysis of the model starting month using the RHH method

For all the previous runs, the starting month has been January. This analysis investigates whether it will be advantageous to simulate with another starting month with respect to total cost or computational time. To reduce the number of model runs, four months were chosen, namely January, April, July, and October. It is assumed that the step-length is short enough to discover a possible ideal starting month. The results from the simulations are shown in Figure 34.

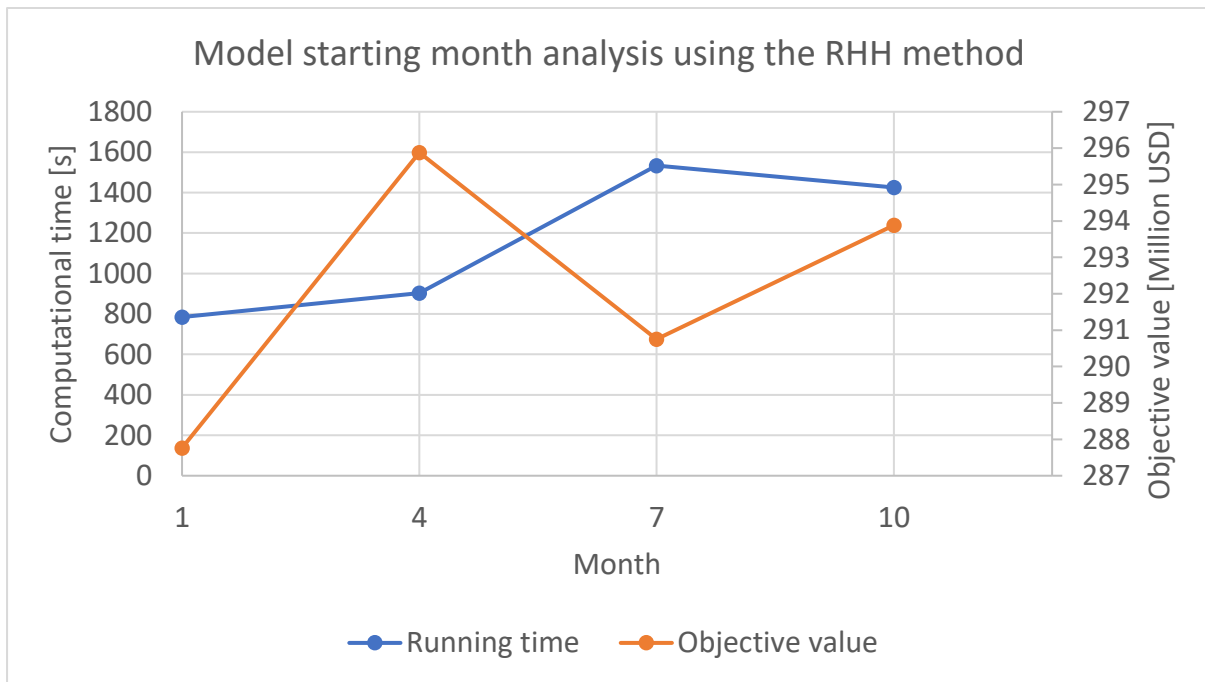


Figure 34: A graphical presentation of how the computational time and total cost is affected by different model starting months using the RHH method. The four starting months are January, April, July, and October.

The figure shows that the best solution to the problem was found when the starting month was January. In addition, January was the starting month of the problem that was quickest to solve. The oscillations of the found total cost from the model results are believed to happen because the model starts within different solar irradiance seasons, which may affect the results as the RHH method solves one month at a time. Notice that the total cost differences are only deviating with around 2%, while the computational time deviates with more than 50% between January and July as the starting months.

January will, thus, be used as the starting month for the following analyses because it provides the shortest computational time.

7.3.5 Analysis of the model simulation length

The analysis in section 7.3.1 showed that the RHH worked as intended to provide good results with less computational effort compared with the exact method. This section will analyse how the model responds to an increased model length, i.e. running for two or three years, equal 24 and 36 months respectively. This will allow for scheduling of LNG transportation that can be planned over a longer time horizon, potentially being

advantageous. Table 17 below shows the total cost and deviations for three different model lengths, and Figure 35 shows the computational time.

Table 17: Total cost of the system and deviation when running the model with different model lengths. A longer model length means that the time horizon is adjusted, so that the operational time is 30 years for all model lengths.

Model length [years]	Adjusted scaling for time horizon [-]	Total cost for an operational time of 30 years [USD]	Deviation from the minimum total cost [%]
1	30	287 763 000	0,00
2	15	288 644 000	0,31
3	10	287 770 000	0,00

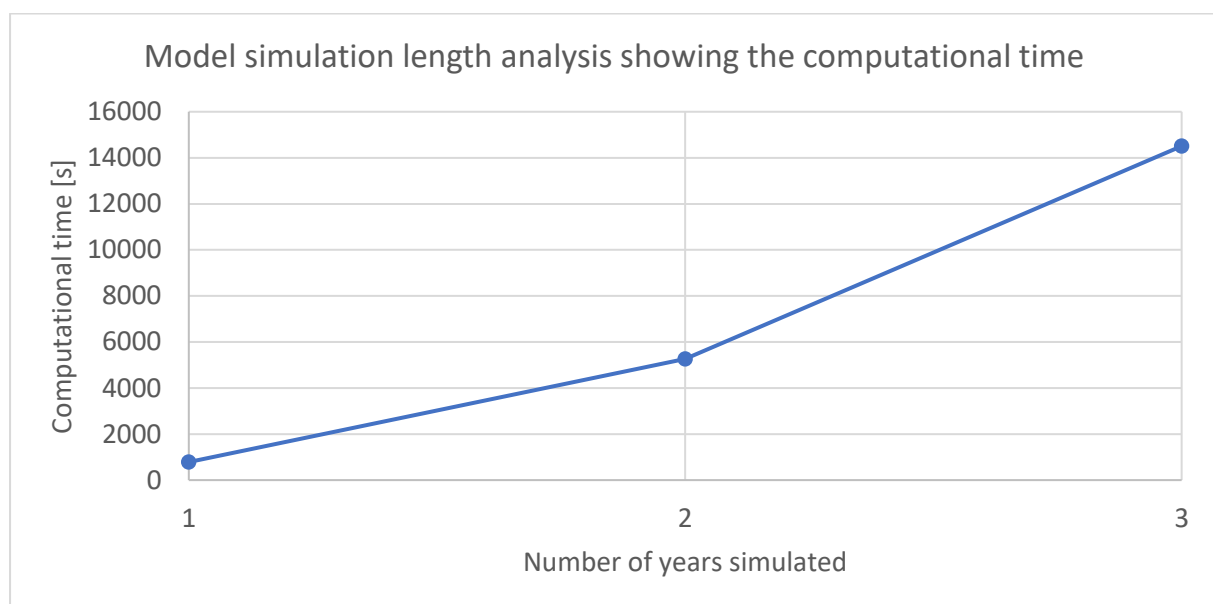


Figure 35: A graphical presentation of how the computational time is affected by the model length simulated.

The table shows that the model length does not affect the total cost considerably, thus are the effects of the LNG transportation costs negligible. In addition, the graph shows that the computational time increases exponentially with the model length.

A model length corresponding to one year has been selected for further analysis because it provides good results within the shortest computational time.

7.3.6 Quantitative validation

This section aims to evaluate the model results to confirm that they are logical and in accordance with the industry partners experience. This is one of the main objectives of this thesis, to evaluate that the formulated mathematical model is valid and can be used as a decision-support tool for the NESL. There are no existing data that can be comparable for this system, which makes the industry partners experience an important validation source. To reduce the total computational time without jeopardizing the accuracy of the model, the following has been selected from the previous analyses in this section:

- The solution method is set to RHH
- Stopping criterion is set to 0.5%
- Initial and ending storage level is set to 80%
- The model starting month is set to January
- Model simulation length is set to 1 year (12 months).

Figure 36 below shows the monthly LNG consumption obtained from the model. It seems logical because the power plant consumption decreases during the summer months. That happens because the heat and electricity demands drop, and the solar park starts to produce solar electricity. The ship bunkering demand is present during the cruise season, as expected. The results have been presented to the industry partners, and they agree that the magnitude and variations of the LNG consumption look logical.

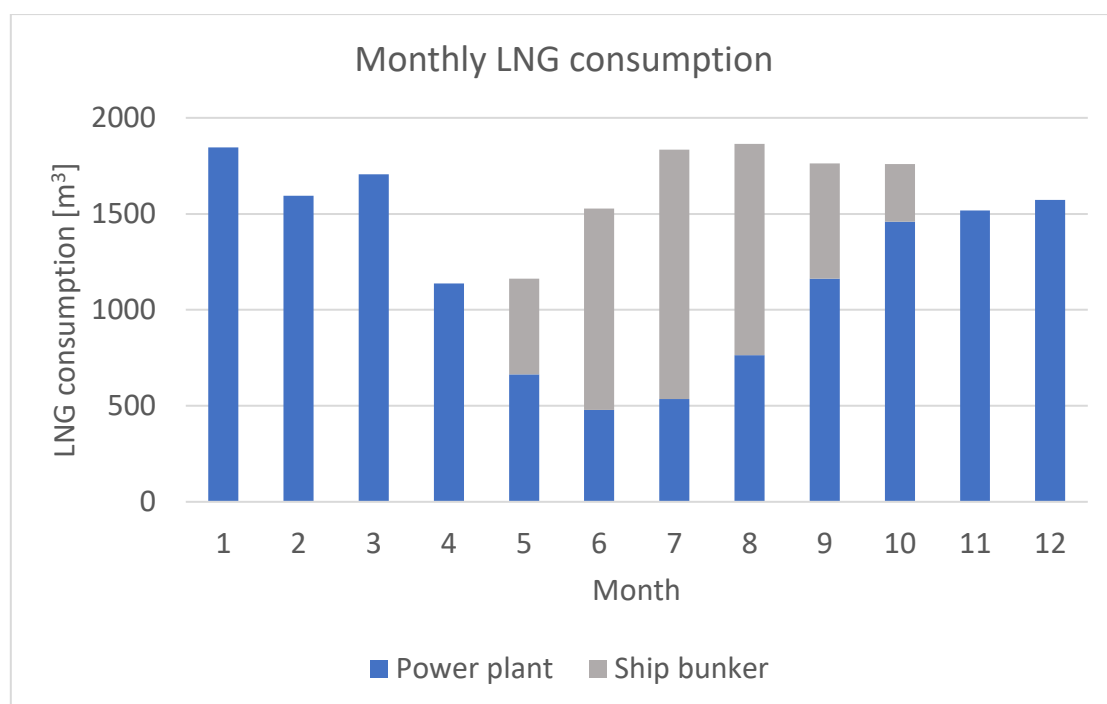


Figure 36: A graphical presentation of the monthly LNG consumption for the studied NESL in this section.

Figure 37 shows the ratio of electricity that is produced by the power plant or by the solar park. The first solar irradiance starts to occur in March, and ends in October. The graph shows that the solar production is present for these months, but that the production is much bigger during the remaining months with midnight sun and stronger irradiance, in accordance with the GHI graph in Figure 11, sub-section 2.1.3. The magnitude of the monthly production seems logical for the industry partners. Notice that the sum of the yearly electricity production corresponds to 10 GWh more than the yearly electricity demand in Longyearbyen, but that this additional electricity will mainly be converted to heat in the heat pump. A minor amount of the additional electricity is waste.

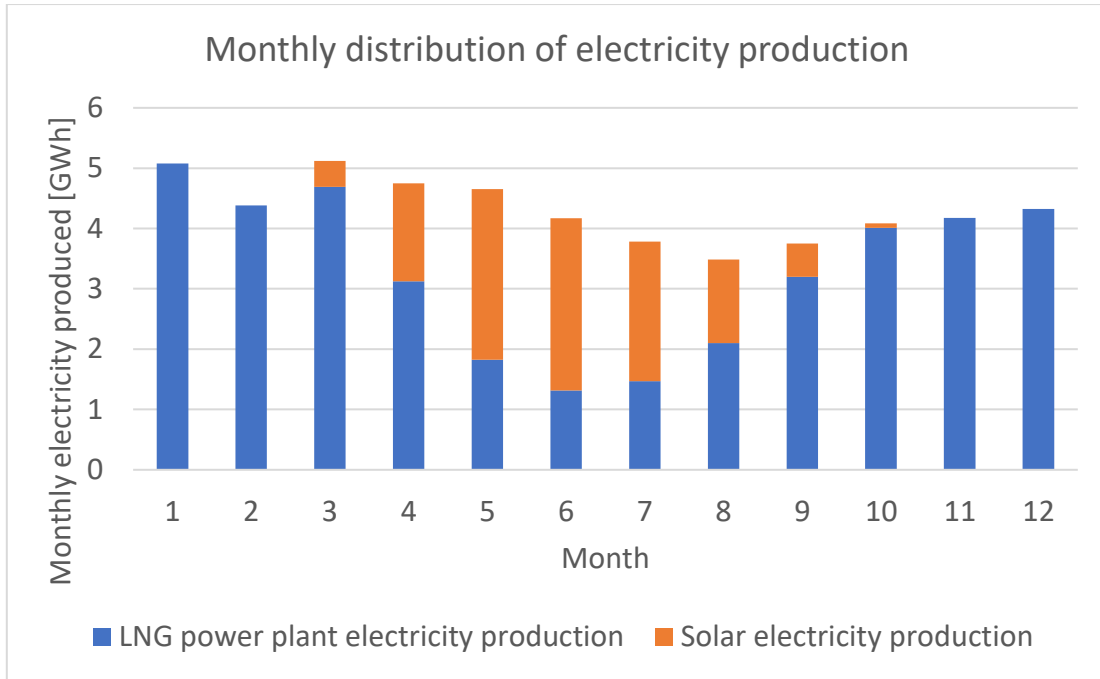


Figure 37: A graphical presentation of the monthly distribution of produced electricity for the NESL.

Figure 38 below shows the heat production distribution. As mentioned above, the main part of the additional 10 GWh produced electricity in the figure above, is converted into heat in the heat pump. The electricity to the heat pump is converted to around 30 GWh heat annually, due to the high efficiency of the heat pump of 3.5. As the heat and electricity demand ratios during the year vary significantly with the months, this graph indicates the importance of the heat pump to balance the energy production. That is both during winter, where the excess electricity can be converted to heat, and during summer, when solar electricity can be converted, reducing the operational hours of the LNG power plant.

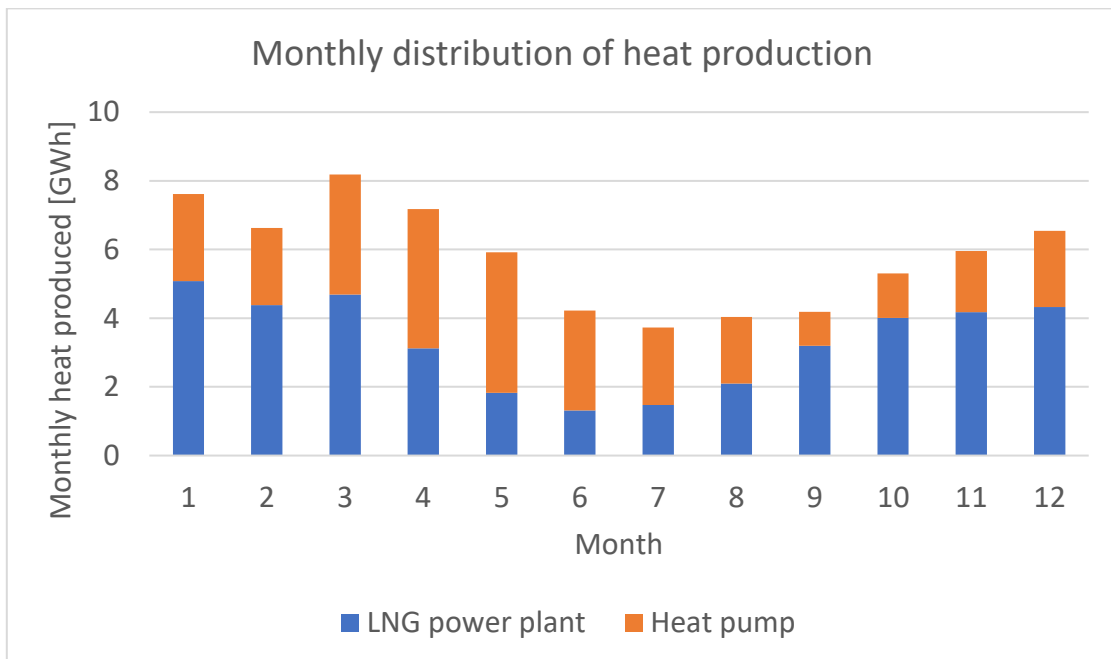


Figure 38: A graphical presentation of the monthly heat distribution from the LNG power plant and from the heat pump.

Figure 39 shows the LNG storage level for each month. Notice that the storage volume decreases until a new ship supply arrives. The graph shows that the level never drops below the safety limit, and never above the LNG storage capacity. This storage profile is as expected by the industry partners. However, the utilization of the capacity is not exactly as expected, as it should ideally, based on experience, be maximized for each ship supply. This happens because of the model length, section 7.3.5, that does not allow for better transportation logistic. The cost effects of that, are, as concluded earlier, very small. Also, note that the ending level of the last month corresponds to the ending conditions of 80% of the storage capacity.

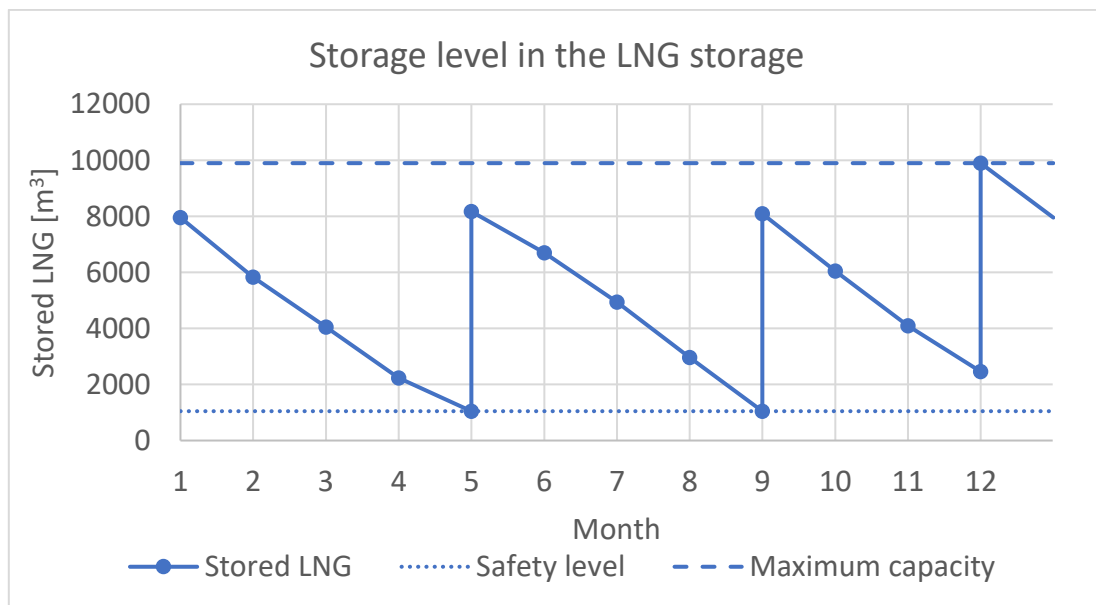


Figure 39: A graphical presentation of the monthly storage level in the LNG storage.

Table 18 below shows the resulting decision variable dimensions for the validation study. These dimensions are confirmed by the industry partners to be logical for the energy demands used in the model.

Table 18: The decision variables obtained from the validation run.

	Decision variables
Yearly ship arrivals	3 ships with capacity 7 500 m ³ Close to fully loaded
LNG storage [m³]	9 937
Gas engines à 3500 KW [-]	5
Yearly LNG consumption in the power plant [m³]	14 435
Thermal storage [m³]	2 000
Battery [KWh]	246
Heat pump electricity input [KW]	4 926
Solar park including private panels [solar panels à 300 W]	63 131

To summarize, the results of the model validation study indicates that the model can realistically reflect the behaviour of the NESL system. In addition, the optimised decision variables appear to be realistic based on the experience of the industry partners.

7.4 Economic study

The economic study is conducted for three purposes. It aims (1) to obtain a better understanding of how the NESL responds to different scenarios and uncertainty, and (2) to discover some design conditions that can obtain a better final solution. The main purpose is (3) to see the cost effects of four different NESL designs, which is one of the main objectives of this thesis. Different designs of the NESL will be compared, to see the economic advantages and disadvantages of the designs, followed by a recommended NESL design.

The simulations in this study have been run with the settings found in the previous Section, 7.3. They are listed here for your convenience:

- RHH method
- Stopping criteria 0.5%
- Initial and ending storage level 80%
- Starting month January
- Model length 1 year, time horizon 30 years

Section 7.4.1 describes the likely events that may affect the energy demands and solar irradiance in Longyearbyen in the future, and how that made the foundation for the full factorial design. The results of the sensitivity analysis are presented in Section 7.4.2. In Section 7.4.3, further studies have been executed on how an upper LNG storage limit will affect the results of what is thought to be the most likely scenario. This scenario, called scenario 15, will be used for the remaining studies in this chapter. The effects of changing the safety level for the LNG storage is analysed in Section 7.4.4. Section 7.4.5 looks at how allowing waste will change the model results, and in Section 7.4.6, a comparison of four different NESL designs is executed. A recommendation of the final NESL design is given in Section 7.4.7.

7.4.1 Future scenarios and full factorial design

In order to understand how different factors affect each other in the model, a full factorial design of numerical simulations, consisting of different scenarios, has been executed in order to perform a sensitivity analysis. The different scenarios have been created to reflect some of the likely events that may happen in Longyearbyen based on the experts and industry partners thoughts. Table 19 below shows the different events that have been used for the full factorial design, based on the information presented in Section 2.1. The sensitivity analysis is performed in the next sub-section.

Table 19: The factors and events that have been used to create the full factorial design.

Factor	Level 1	Level 2	Level 3
Electricity demand	Today's level without Energiverket and mining	Level 1 with shore power	30% increase of level 1 with shore power
Heat demand	Today's level	40% reduction	
LNG ship bunkering demand	50% of today's MGO demand	80% of today's MGO demand	
Solar irradiance	Today's level	15% reduction	

All of the electricity events that have been determined reflects today's demand without the consumption related to the coal electricity production, i.e. mining and the coal power plant. Level 1 scenario for electricity will, therefore, be the switch from the coal power plant to an LNG power plant and a solar park, decreasing the electricity demand by approximately 25%. Level 2 will in addition to level 1 include a shore power demand that is likely to arise due to the environmental focus at Svalbard. This demand will be present during the cruise season which goes from May to August, see section 2.1.2, and correspond to around 250 KW per hour. Level 3 corresponds to a population increase of twice the size today, with shore power of 250 KW per hour.

The future heat demand in Longyearbyen is uncertain and has been categorised into two scenarios. Level 1 corresponds to today's heat demand, which represents a population increase in Longyearbyen with the energy efficiency actions mentioned in Section 2.3.10. New houses, better standards, and a new energy-saving policy are likely to occur, which will maintain today's level rather than increase the demand if a population increase happens. Level 2 will represent a population stagnation, but with the energy efficiency actions. It has been assumed to correspond to a heat demand reduction of 40%.

The LNG ship bunkering demand in Longyearbyen today is not existing. However, more and more ships are designed and built to sail on LNG, and with the environmental focus at Svalbard, it is likely that LNG will be the most common marine fuel in the future. However, the transition is a long-lasting process. It has been determined that the level 1 scenario will contain an LNG demand corresponding to 50% of today's MGO bunkering consumption, and level 2 will contain 80%.

The solar irradiance scenarios consist of two levels. Level 1 is today's level of irradiance, as indicated in Figure 11. Level 2 represents a 15% reduction in the radiation as global climate change is affecting Svalbard, see section 2.1.3. A consequence of global warming is an increasing cloud layer above Svalbard, resulting in less solar irradiance(Endsjø, 2018).

That makes a total of 24 different scenarios, and the full factorial design means that a model run for each scenario will be executed and analysed.

7.4.2 Sensitivity analysis

A sensitivity analysis has been executed to obtain a better understanding of the NESL model and how it will respond to likely events. The aim is to be able to design a more robust energy system by having a better knowledge of it.

This analysis is executed with the input parameters given in Section 7.2, and with the full factorial design for the energy demands and solar irradiance in the previous section. The variables that have been selected for the sensitivity analysis are the decision variables of the NESL, as well as the total lifetime cost of the NESL, i.e. the objective value. They are listed for your convenience:

- Annual supply rate and volume of LNG transported by ships
- Capacity of the LNG-Storage
- Number of gas engines à 3500 KW in the power plant
- Number of solar panels in the solar park
- Capacity of the battery package
- Capacity of the heat pump
- Capacity of the thermal storage tanks
- Objective value corresponding to the total cost of the system

The results obtained from the simulations are presented in a table in Appendix B. This table has made the foundation for the sensitivity analysis. Note that the results obtained from this analysis are only valid within the range of the considered scenarios, mentioned in 7.4.1.

To analyse the NESL sensitivity, the statistical software MiniTab 18 has been used. The graphs that will be presented in this analysis are histograms, pareto charts, main effects plots and interaction plots.

The pareto chart shows the magnitude and effect each factor will have on the decision variable. If the effect is greater than the red line, the factor is statistically affecting the decision variable design with a significance level of 5%. The main effects plot shows how the factors do affect the decision variables, and the interaction plots show how the interactions between different factors are affecting the decision variables.

Ship arrivals

Table 20 below shows the three different supply schedules that have been obtained from the model runs for all the scenarios.

Table 20: The schedule routines that are present in the model results in the sensitivity analysis.

Schedule type	Ship supply schedule
1	2 ships supplies with capacity 7500 m ³ annually
2	2 ships supplies with capacity 7500 m ³ , and 1 ship supply with capacity 5000 m ³ , arrives annually
3	3 ships supplies with capacity 7500 m ³ annually

Figure 40 below shows the pareto chart of the ship supply. The ship supply schedules are statistically dependent on the ship bunkering demand, electricity demand and heat demand. That is because the factors are greater than the vertical red line, thus are the factors statistically significant at a 5% level.

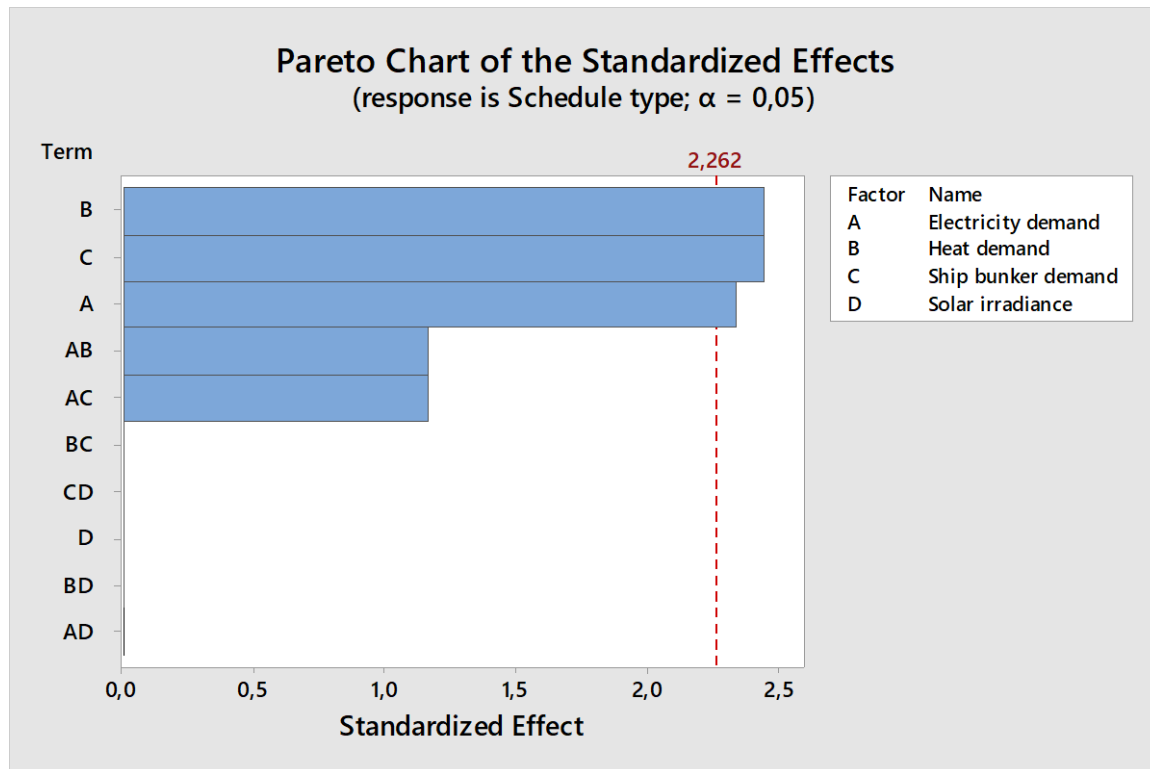


Figure 40: Pareto chart of the ship schedules indicating what factors are significantly affecting the ship scheduling.

The histogram, Figure 41, shows how often each schedule occurs. As seen, the trend is to follow schedule type 2. When that does not happen, that is because the LNG consumption is at a level so low, that there is no need for an additional LNG supply with the 5000 m³ ship. The other case is that the LNG consumption is so high, that it requires more LNG than the 5000 m³ ship can supply. That means that for all the scenarios, two ship supplies of 7500 m³ are always present. The supplying ships do not necessarily have to be fully loaded.

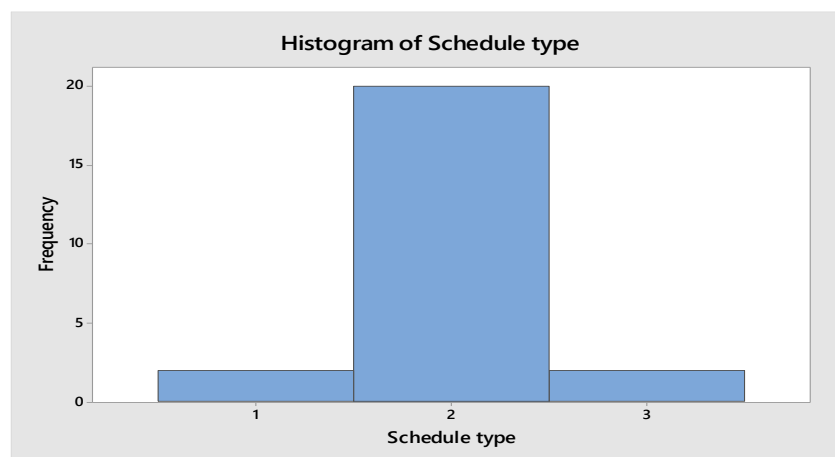


Figure 41: Histogram showing the frequency of the occurring schedule types in the sensitivity analysis.

LNG Storage

Figure 42 below, shows that the size of the LNG storage is statistically affected by the electricity and heat demand. Other main effects and interactions are non-significant. The magnitude of the electricity demand is almost twice the size of the heat demand, meaning it is influencing the LNG storage design twice as much. Note that the ship bunkering demand is not affecting the LNG storage design. That is probably because the ship bunkering demand and the LNG power plant demand are in antiphase. The power plant's LNG consumption is reduced during summer due to the solar park, and the ship bunkering demand is, thus, not big enough to affect the LNG storage capacity for these months. Resultantly, the storage levels will not be any bigger during summer than the rest of the year as the monthly consumption is even, see Figure 36, Section 7.3.6, for illustration.

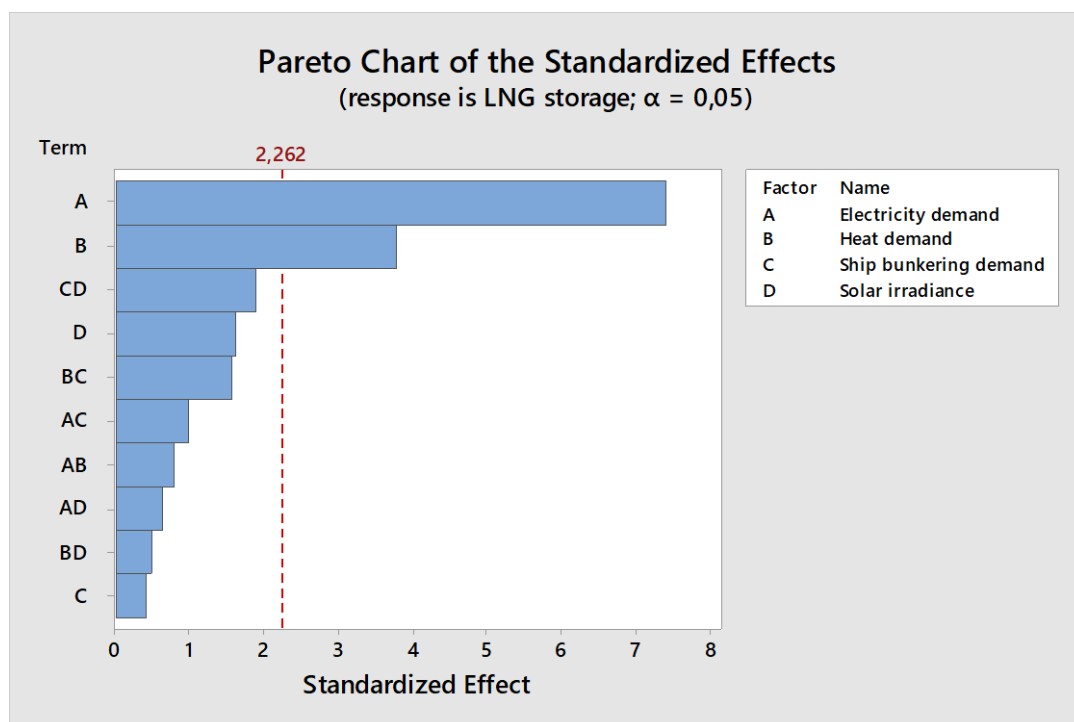


Figure 42: Pareto chart of the LNG storage showing what factors are significantly affecting the capacity of the LNG storage.

The main effects plot of the LNG storage, Figure 43, shows how the factors are influencing the size of the LNG storage. The impact of electricity and heat are much bigger than the other factors, pursuant to the pareto chart. Electricity increase and heat reduction are highly affecting the size, and a change to level 3 electricity demand is affecting the LNG storage the most. The electricity demand is believed to have a higher impact on the LNG storage capacity than the heat demand, because the magnitude of the electricity demand is lower than the heat, meaning that a change results in bigger repercussions. In addition, heat can be produced by excess electricity in the heat pump with a very good efficiency of 3.5, and not opposite. Note that there seems to be a small reduction in the storage volume between level 1 and 2 for the electricity demand. This deviation between the scenarios is very small as the slope is gentler than for the solar irradiance, which is statistically insignificant. It is therefore not a trend, but a result deviation.

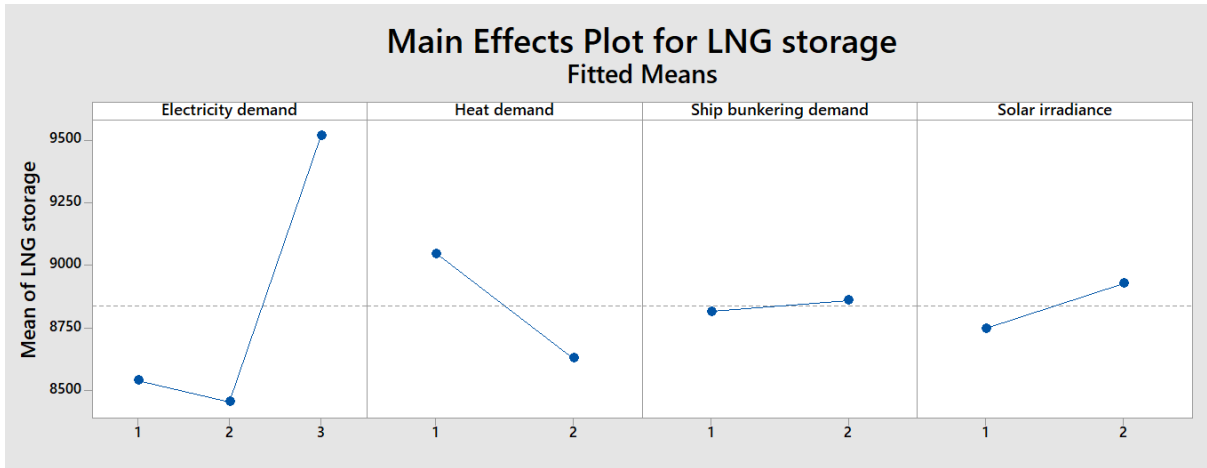


Figure 43: Main effects plot of the LNG storage showing how the levels of the factors are affecting the capacity of the LNG storage.

Gas engines

The number of gas engines obtained for the different scenarios was strictly following a constant trend without any deviation, and it was therefore not possible to create a pareto chart. The main effects plot, Figure 44, shows how the number of required gas engines are affected by the different scenarios. Note that it is the electricity and heat demand that affects the number of engines. There is no difference in the number of gas engines for electricity demand level 1 and 2, because the increased electricity demand of level 2, the shore power, occurs during the summer months which will be handled by the solar park and not the gas engines.

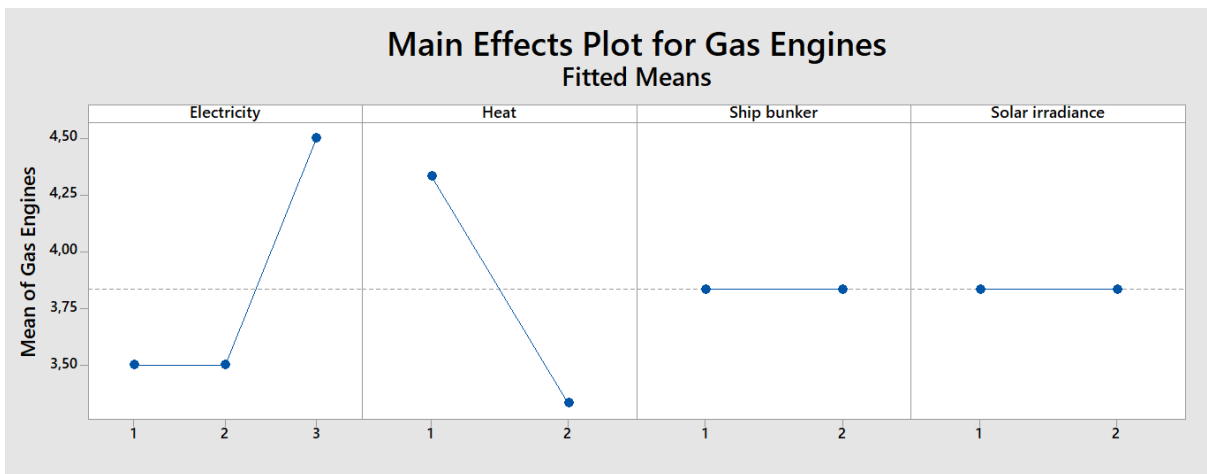


Figure 44: Main effects plot of the gas engines showing how the levels of the factors are affecting the number of gas engines in the LNG power plant.

Solar park

The pareto chart of the solar panels, Figure 45, shows the significant main effects and that there is a significant interaction effect. Note the magnitude of the effect each factor has, and that the interaction effect is very much smaller than the other main effects.

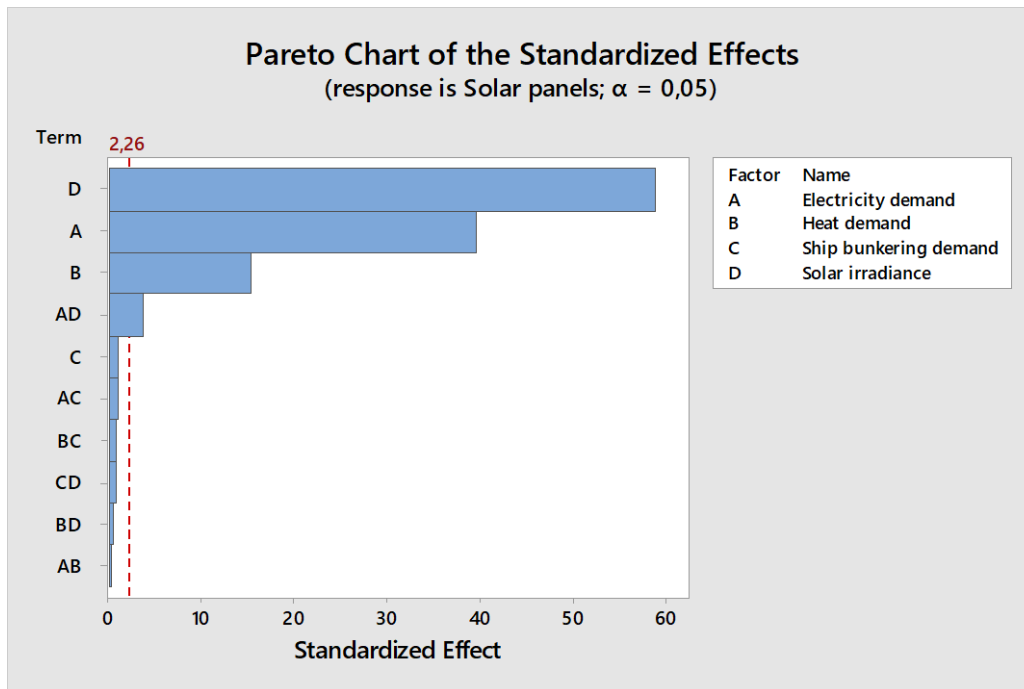


Figure 45: Pareto chart of the number of solar panels in the solar park showing what factors are significantly affecting the number of solar panels.

The number of solar panels is increasing with increased electricity demand, Figure 46. As mentioned above, the electricity demand level 2 will affect the size of the solar park, which is why it does not affect the gas engines. The solar irradiance reduction of 15% shows to affect the solar park size the most, increasing the number of panels with around 15%. That means that solar panels are very cost-efficient for power production in Longyearbyen, as the model expands the solar park equal to the solar irradiance reduction.

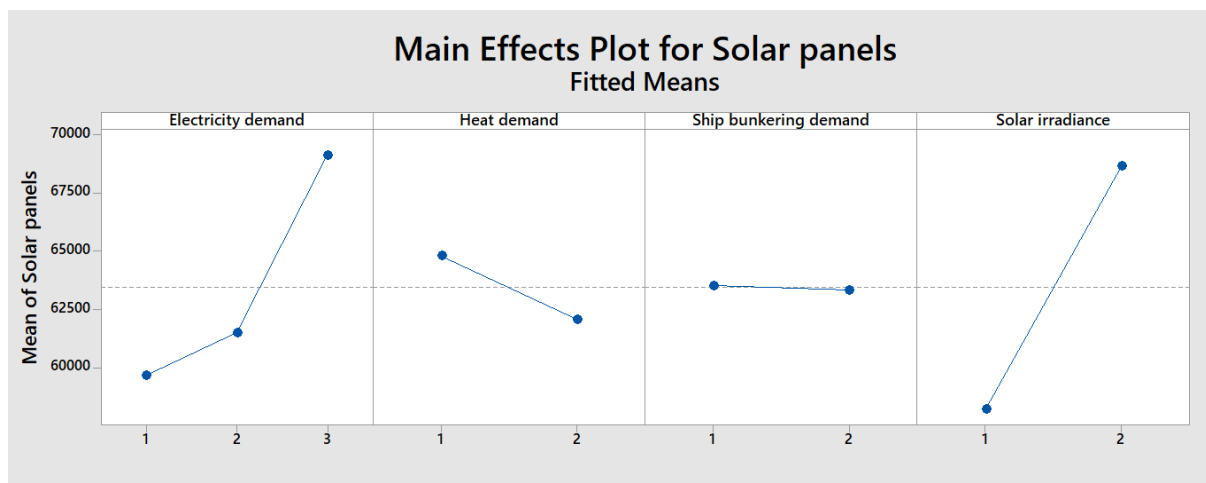


Figure 46: Main effects plot of the solar panels showing how the levels of the factors are affecting the number of solar panels in the solar park.

The interaction plot for the solar panels is given in Figure 47 below. The significant interaction is the one at the bottom left corner. It is believed that the interaction occurs because of the nonlinear relation for the solar irradiance. Level 2 corresponds to 85% of level 1, and the resulting number of panels will thus not be parallel for each electricity level,

which causes the significant effect. However, as seen, the interaction is not very big as the plots are close to parallel.

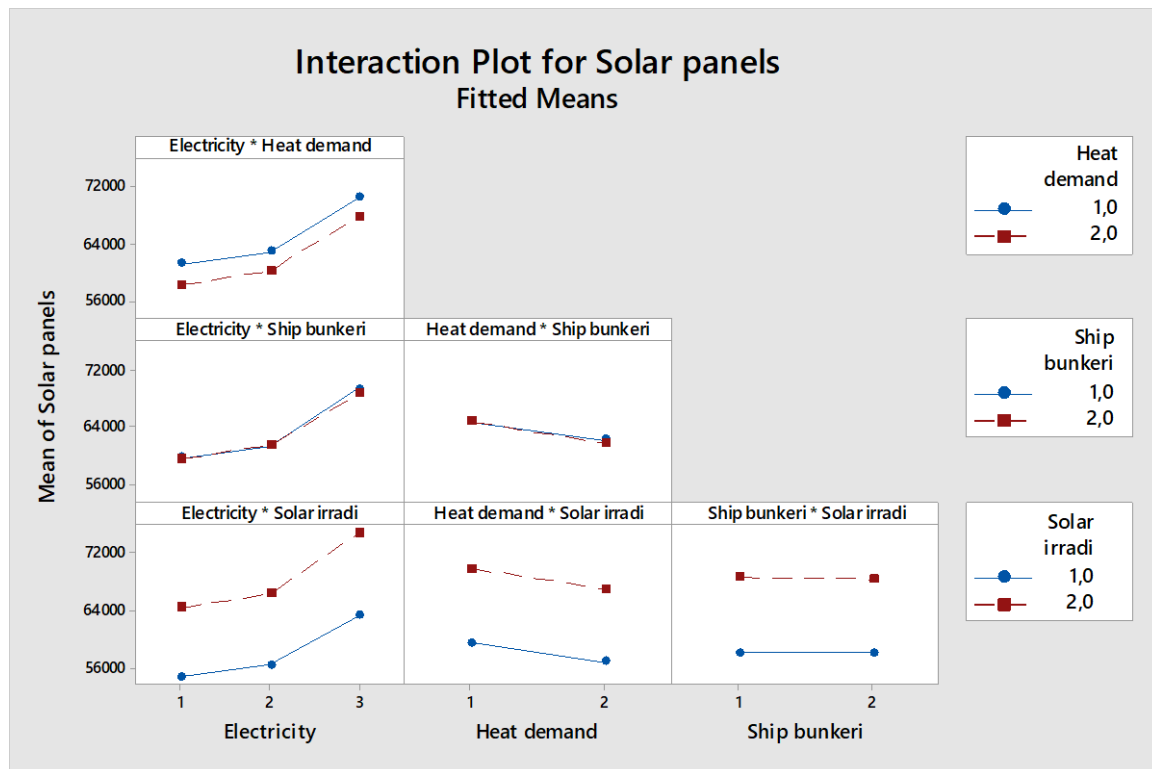


Figure 47: Interaction plot of the number of solar panels showing how different levels of two factors are affecting the number of solar panels. It is the interaction plot at the bottom left corner that has a significant effect on the solar park size.

Battery

The pareto chart of the battery capacity, Figure 48, shows that the only statistical factor affecting the battery capacity is the heat demand. Notice that the effect of the electricity demand is insignificant in affecting the battery size.

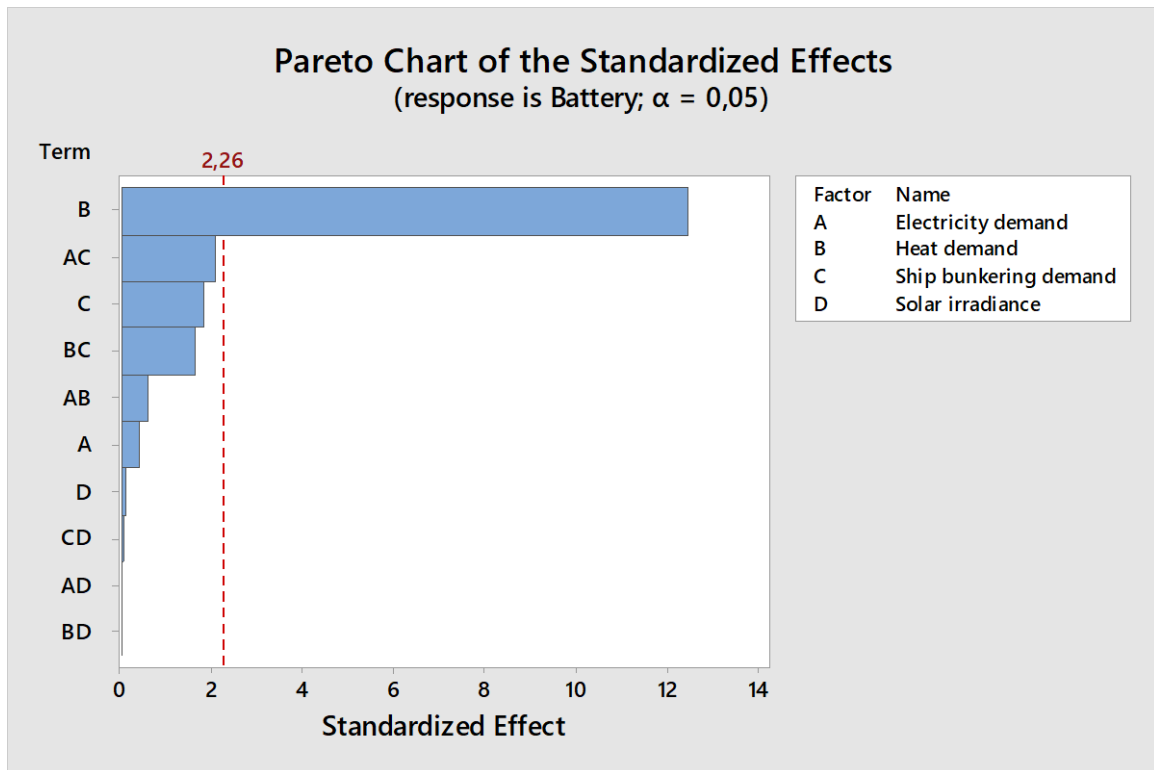


Figure 48: Pareto chart of the battery showing what factors are significantly affecting the capacity of the battery.

Figure 49 shows how the heat demand affects the battery capacity. The system today has a bigger heat demand compared with electricity for every month and every hour. That means that overproduction of electricity is very efficient to store as heat as it is much cheaper and will be consumed sooner or later. When the heat demand drops to a level where the electricity demand is higher than the heat demand for some months and hours, i.e. level 2 heat demand, storing electricity becomes much more attractive. That is because the electricity demand will be the dimensioning factor for these months, making it valuable to store overproduced electricity rather than converting it to heat or waste it.

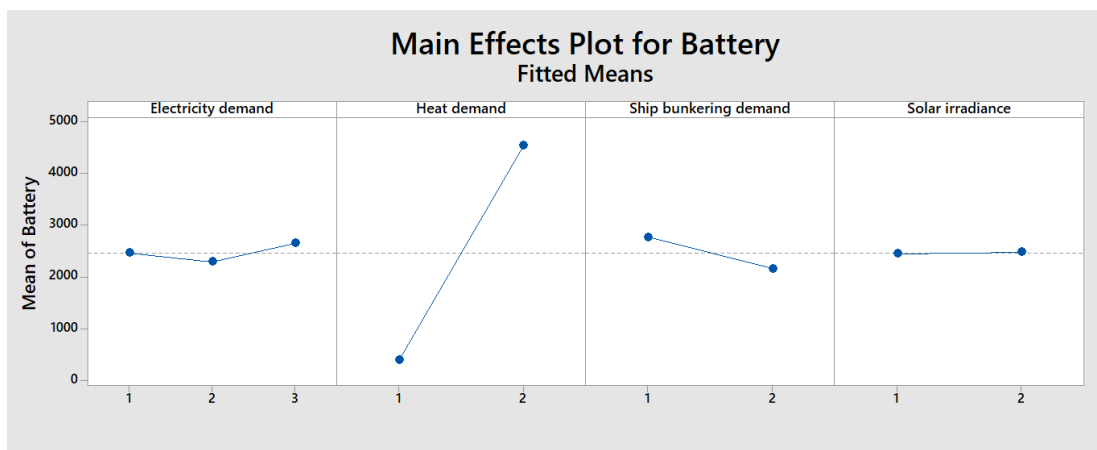


Figure 49: Main effects plot of the battery showing how the levels of the factors are affecting the battery capacity.

Heat pump

The capacity of the heat pump is significantly affected by the heat demand, Figure 50 below. Figure 51 shows how the capacity decreases with reduced heat demand. When the heat demand is reduced, the difference between the electricity and heat demand is more balanced, thus is the need to convert electricity into heat, less. For the summer season, when energy is produced mainly by solar power, resulting in only electrical energy, the heat pump will be crucial to deliver a satisfactory level of heat. When the heat demand is reduced, the output requirement of the heat pump is significantly reduced as well.

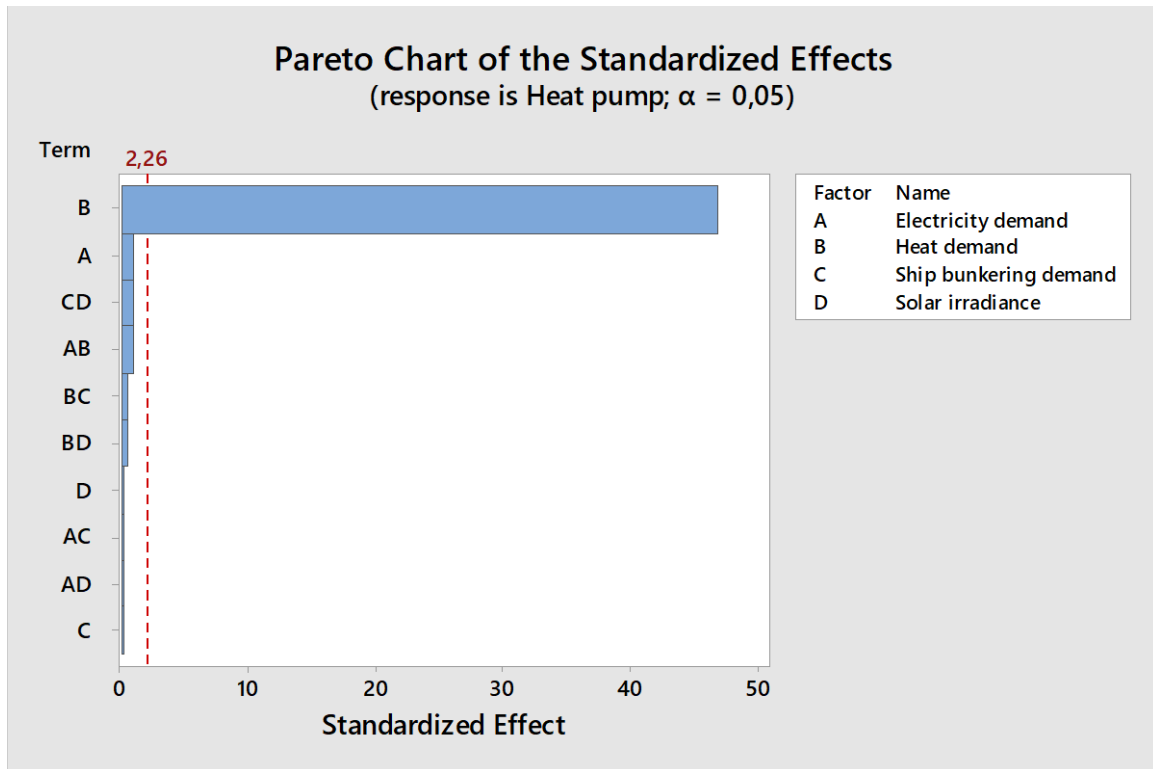


Figure 50: Pareto chart of the heat pump showing what factors are significantly affecting the capacity of the heat pump.

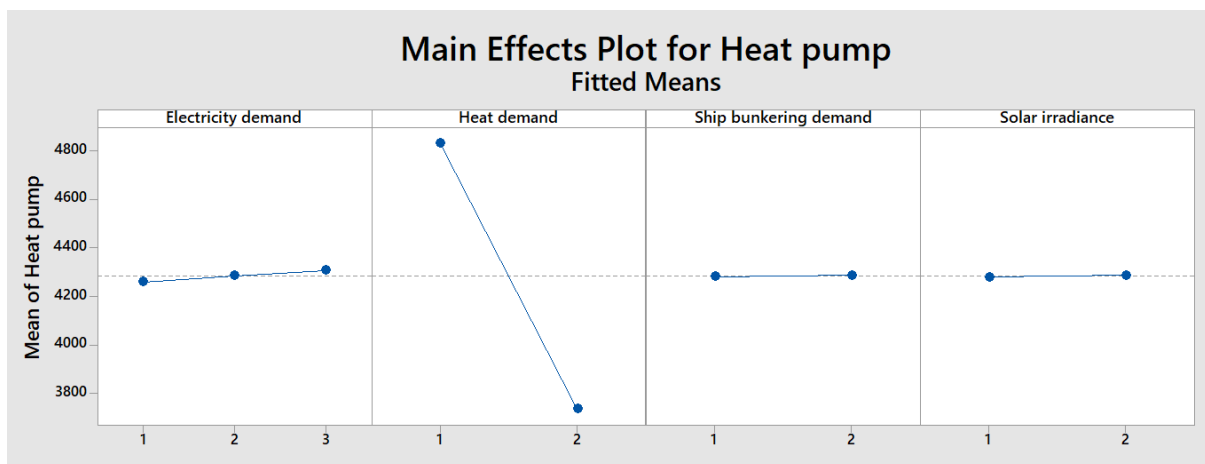


Figure 51: Main effects plot of the heat pump showing how the levels of the factors are affecting the battery capacity.

Thermal storage

The thermal storage has for all the different scenarios been dimensioned to its upper limit of 2000 m³. The thermal storage is a cheap storage, and within the scenario range, it is most economical to maximise its space capacity. That is probably because the heat demand during winter is for all scenarios much higher than the electricity demand. Storing heat will thus lead to peak shaving during the most energy demanding season, and can potentially reduce the number of required gas engines.

Objective value

The objective value, i.e. the total cost of the energy system over a 30-year lifetime, is statistically dependent on the electricity and heat demand, as well as the solar irradiance, Figure 52. The electricity and heat demand affects the total cost the most. That is because those effects are affecting the dimensions of most of the decision variables and respective cost magnitude, which again gives the cost dependency for the objective value. Notice that the ship bunkering demand does not affect the objective value significantly.

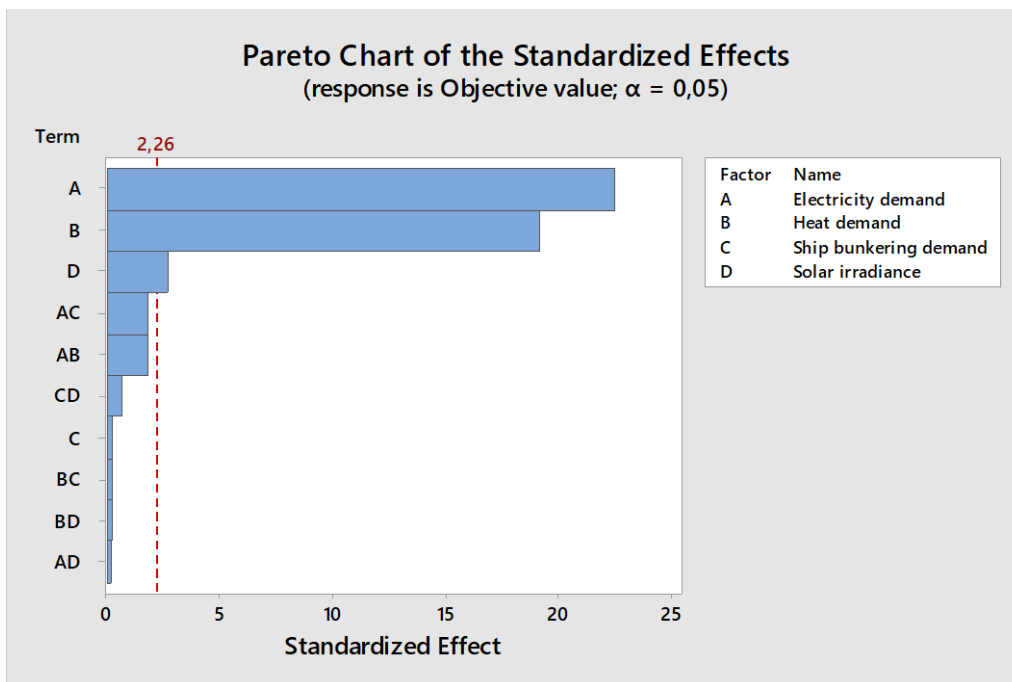


Figure 52: Pareto chart of the objective value showing what factors are significantly affecting the objective value, i.e. total cost of the NESL when operating in 30 years.

The main effects plot for the objective value is shown in Figure 53. The cost trends are a result of all the decision variable sensitivities seen above. Notice that the electricity demand is affecting the total cost of the system more than the heat demand. That is in spite of the heat demand has been present for all the different components. This happens because the magnitude of the electricity factor has been greater for the most expensive components, thus affecting the objective value the most.

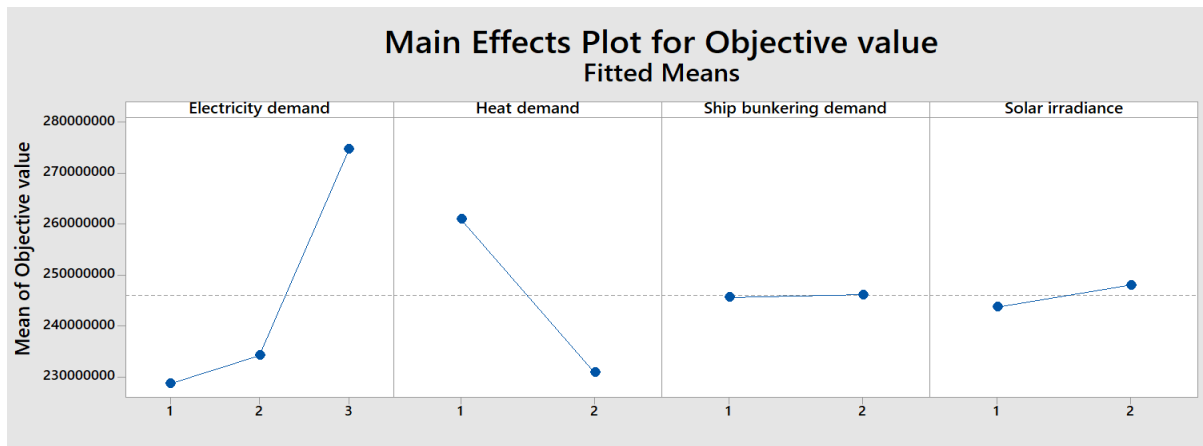


Figure 53: Main effects plot of the objective value showing how the levels of the factors are affecting the objective value, i.e. total cost of the NESL, when operating for 30 years.

Sensitivity analysis summary

The results obtained in this section have been summarised for your convenience. Below are the statistically significant dependencies listed for each decision variable and the objective value.

- | | |
|-----------------|-----------------------------------------------------------------------------------------------------------------------------------------------------|
| Ship arrivals | - Dominating factors are the electricity demand, heat demand, and ship bunkering demand |
| LNG storage | - Dominating factors are the electricity and heat demand |
| Gas engines | - Dominating factors are the electricity and heat demand |
| Solar park | - Dominating factors are the electricity demand, heat demand, solar irradiance, and the interaction between electricity demand and solar irradiance |
| Battery | - Dominating factor is the heat demand |
| Heat pump | - Dominating factor is the heat demand |
| Thermal storage | - Capacity maximised to the upper limit for all scenarios |
| Objective value | - Dominating factors are the electricity demand, heat demand, and solar irradiance |

Notice that the heat demand is significantly affecting the capacity of all the decision variables. However, it is the electricity demand that is affecting the total cost, i.e. objective value, of the NESL the most, and is thus the most important parameter to minimize the cost. The reason why electricity is affecting the costs more than heat, which are dominating all variables, is because the magnitude of the electricity factor has been greater for the most expensive components, thus affecting the objective value the most. Note that the solar irradiance level has a significant effect on the total cost. The factor is only dominating the number of panels in the solar park, which indicates that the costs related to the solar park are significantly affecting the total cost of the NESL.

These results are only valid within the range of the tested factors. Future events are hard to predict, and this sensitivity analysis has considered big changes in the different demand and solar irradiance levels. For instance, if no energy efficiency actions are made in Longyearbyen, the heat demand will probably increase with increased population, making this sensitivity analysis invalid. However, there are indications that actions will be made to reduce the heat demand as there is a lot of waste associated with it today (Ellingsen, 2017).

Scenario 15 in Section 7.4.1, with the related results in Appendix B, has been selected for further analyses. The scenario contains the electricity demand with shore power (level 2), a heat reduction of 40% (level 2), the ship bunkering demand corresponding to 80% of today's demand (level 2) and a solar irradiance level equal to today's level (level 1). The author and the industry partners have agreed that this scenario is believed to be the most realistic future scenario for the energy demands in Longyearbyen. This scenario has, thus, been assumed to be the most applicable and relevant option for more thorough studies.

7.4.3 Space limitations LNG storage

This analysis aims to discover how the investment cost and total lifetime cost are affected by different LNG storage volumes. The intention of the model is to minimize the total cost of the NESL over the lifetime of 30 years. In addition, it is from an economic point of view, advantageous to reduce the investment costs as much as possible, because it will require less equity. The analysis has been run for scenario 15, which is considered the most realistic future scenario, see the previous paragraph.

This analysis was performed by selecting several upper size restrictions for the LNG storage. Table 21 shows the storage limits, and the resulting optimal storage level solution. The NESL can be thought of as a divided system, one containing the LNG ship arrival, LNG storage and LNG supply to the rest of the system, and the other system concerning about the power production. The power production part of the system has in general not been affected by the LNG storage restrictions. Note that further relaxation of the LNG storage does not affect the optimised LNG storage level, and it is, thus, not added any upper restrictions above 10 000 m³.

Table 21: Maximum LNG storage capacity restriction implemented in the model and resulting optimal LNG storage capacity for the respective restriction.

Maximum LNG storage capacity [m³]	Optimal LNG storage capacity [m³]
3000	3000
4000	3977
5000	4784
6000	5488
7000	5488
8000	7172
9000	8570
10000	8570

Figure 54 below shows how the total and investment costs are changing with the maximum LNG storage levels. As shown, the stricter the constraint is, i.e. smaller LNG storage capacity allowed, the higher the total cost becomes. That is a consequence of more frequent ship calls, and that the supplying ships are loaded with less LNG. The transportation costs are therefore greatly increasing compared to the investment cost savings, which result in an increased total cost.

The investment cost decreases with smaller LNG storage. However, when the storage is limited to 3000 m³, the associated costs increases. That is a result of the storage being too small, not providing the power production system with sufficient LNG. Consequently, a bigger battery package and solar park are bought to reduce the LNG consumption in the power plant. For all the other storage level limits, the power production system dimensions are not affected because sufficient LNG supply is present, thus is the investment decrease only related to the storage reduction.

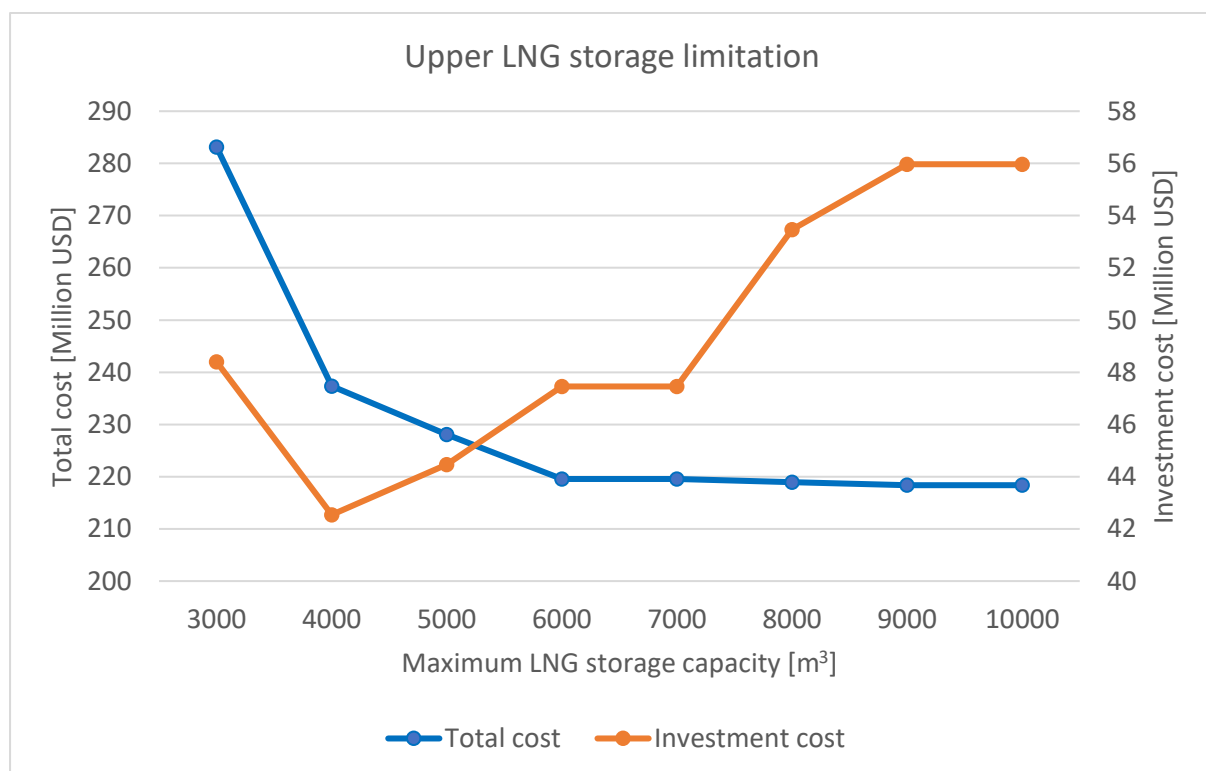


Figure 54: A graphical presentation of how the total cost and the investment cost are affected by upper LNG storage capacity restrictions. Further relaxation of the maximum LNG storage capacity will result in the same numbers as are present for the upper two LNG storage capacity restrictions in the figure because that provides the minimum total cost of the model.

The ideal storage level will be where the total cost has converged, and the investment costs are at the lowest. A restriction corresponding to 6000 m³ shows to remain the total cost at the minimum level, while the investment cost has been reduced by around 8 million USD compared with the solution with a free LNG storage capacity. It has therefore been concluded that an upper LNG storage restriction of 6000 m³ is the best, and has been used for further analysis.

7.4.4 Changing safety level for different seasons

A safety storage is important to secure that if something unforeseen happens to the LNG supply to Longyearbyen, the consequences will not be fatal. From an economic perspective, however, it is a dead investment. This analysis aims to see how the NESL will respond when the safety level is changing dependent on the different seasons. The analysis has been run for scenario 15 with an upper LNG storage limit of 6000 m³ based on the results from the previous studies.

During winter, the LNG power plant will operate consistently, and consume a lot of LNG. During the summer, on the other hand side, the solar park will produce most of the required energy, and the safety level can be reduced by still meeting the 30 days safety requirement. Table 22 below shows the limits for the old and new LNG safety limits. Note that the old limit has been used until now. The numbers for the new safety limit is based on the roughly average monthly LNG consumption in the power plant during the respective seasons for the model run in the previous section.

Table 22: The new and old safety limits for stored LNG in the storage. The new limit is based on actual monthly LNG consumption in the power plant for the respective season.

	Polar night season	Transition season (April and September)	Midnight sun season
Old safety limit [m³]	1047	1047	1047
New safety limit [m³]	1047	700	400

Figure 55 shows the storage levels in the LNG storage for each month. The storage level when using the new safety limit drops below the old safety limit when it can, and is nearly consequently lower for every month. That means that the resulting LNG storage capacity can be reduced by around 350 m³ if having a dynamic safety limit dependent on the seasons, which again reduces the investment cost.

Note that the model maximises the LNG storage capacity when resupplying. The supplying ships have a capacity of 5000 m³, and are not fully loaded. Also, note that the storage level in month 12 corresponds to the ending condition. One of the ship calls is loaded much less than the other arrivals. That is due to the model length of one year and the ending condition. If running the model for two years, the model would not have needed to achieve a storage level of 80% in month 12, but in month 24 instead, which potentially could have resulted in a better transportation logistic. For the total cost of model results, this has proved not to affect the results significantly, section 7.3.5. However, for practical application, this is important to be aware of it.

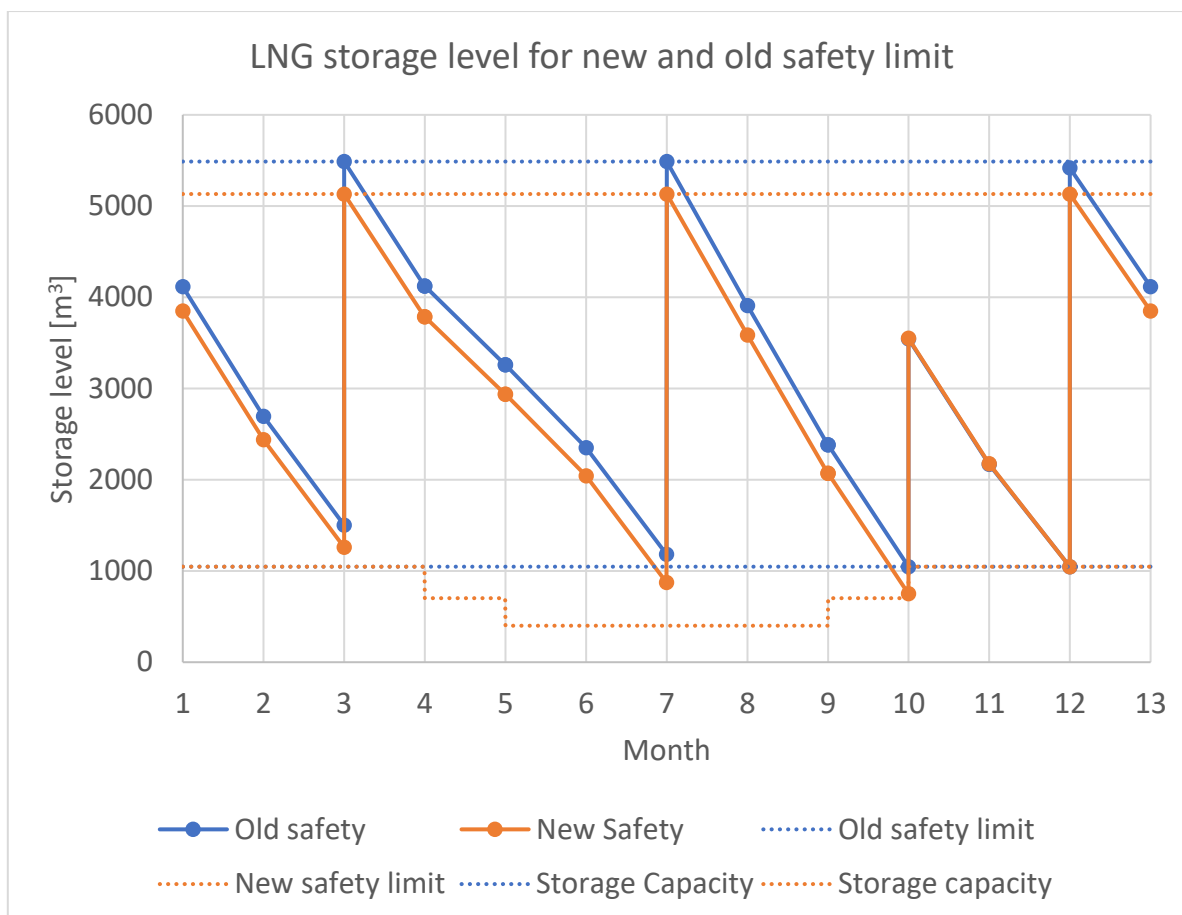


Figure 55: A graphical presentation of the monthly LNG storage levels when having the new and old safety limits.

The following, Table 23, shows that it is only the LNG storage capacity that has been affected significantly by the new safety limit. That is logical, as the new limit only influence the stored volume and results in less dead capital. The power production system is nearly not affected.

Table 23: Resulting decision variables associated with the new and old safety limits from the model results.

	Old safety limit	New safety limit
Yearly ship arrivals	4 ships à 5 000 m ³	4 ships à 5 000 m ³
LNG storage capacity [m³]	5 488	5 132
Gas engines à 3500 KW[-]	3	3
Yearly LNG consumption in the power plant [m³]	9 874	9 873
Thermal storage [m³]	2 000	2 000
Battery [KWh]	5 486	5 549
Heat pump electricity input [KW]	3 666	3 663
Solar park [solar panels à 300 W]	55 805	55 833

As the safety level is only affecting the LNG storage capacity, nothing of the remaining system, it is only the investment costs, resultantly the total cost, that is affected by adjusting

the safety limit. Table 24 below shows the resulting costs. The investment saving potential by adjusting the safety limit depending on the season can be around 1.9 million USD, which are only related to the LNG storage capacity reduction.

Table 24: Cost associated with the new and old safety limits.

	Old safety limit	New safety limit
Total cost [USD]	219 573 000	217 682 225
Investment cost [USD]	47 456 950	45 566 175
LNG consumption cost [USD]	127 786 010	127 786 010
Transportation cost [USD]	44 330 040	44 330 040

The new safety limit will be used for further analysis.

7.4.5 Waste limit analysis

This analysis studies if it can be more cost-efficient to increase the number of panels in the solar park. This will allow for more solar energy during hours where the solar irradiance is weaker, reducing the LNG consumption in the power plant. However, it will also result in overproduction and waste of solar energy when the irradiance is strong. An optimal energy system is often defined as a system where energy waste is as low as possible because there is a variable cost associated with the production, i.e. fuel. Solar panels, however, does not have this variable cost when producing. In the initial model, an upper acceptable limit for hourly energy waste was determined. The waste constraints have, thus, been removed for this analysis. Notice that the waste is related to renewable energy only. The analysis has been run for scenario 15, with the upper LNG storage capacity of 6000 m³ and the new, dynamic safety limit based on the previous results.

Figure 56 shows how the electricity production in the LNG power plant is reduced when the energy waste limit is removed, thus allowing waste. As can be seen, the electricity production in the LNG power plant drops significantly, which again means that the LNG consumption is reduced. This is a consequence of the solar park producing a bigger share of the demanded energy, Figure 57. Energy production above the waste line is waste of renewable energy, while production below the waste line is used by the system. The solar park greatly overproduces electricity during the midnight season compared with the no waste model. However, during the transition months, when the solar irradiance is less, the larger solar park will produce more energy without wasting it. That also occurs on an hourly basis during the midnight season when the solar irradiance is weaker, typically when it is cloudy or during the night.

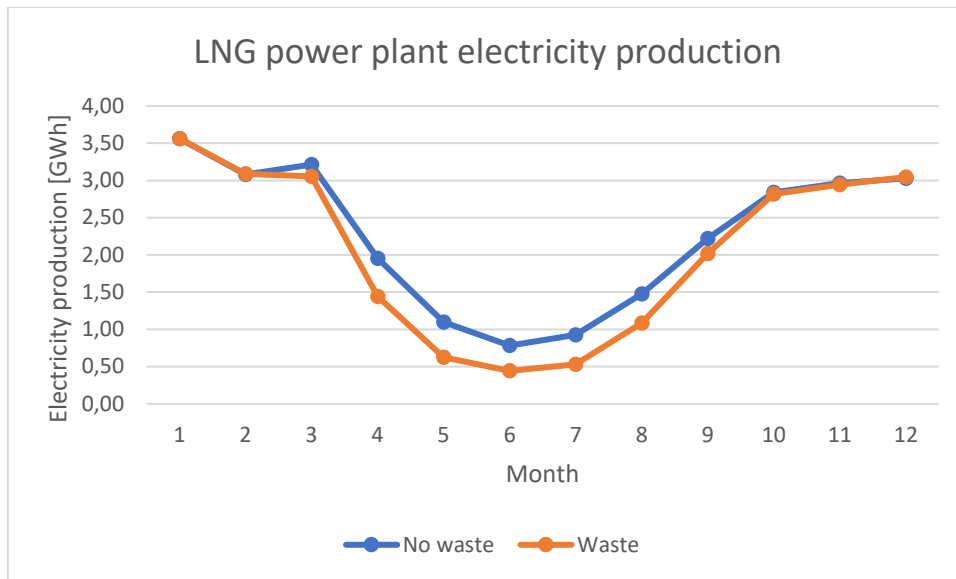


Figure 56: A graphical presentation of the monthly electricity production in the power plant with and without waste of renewable energy.

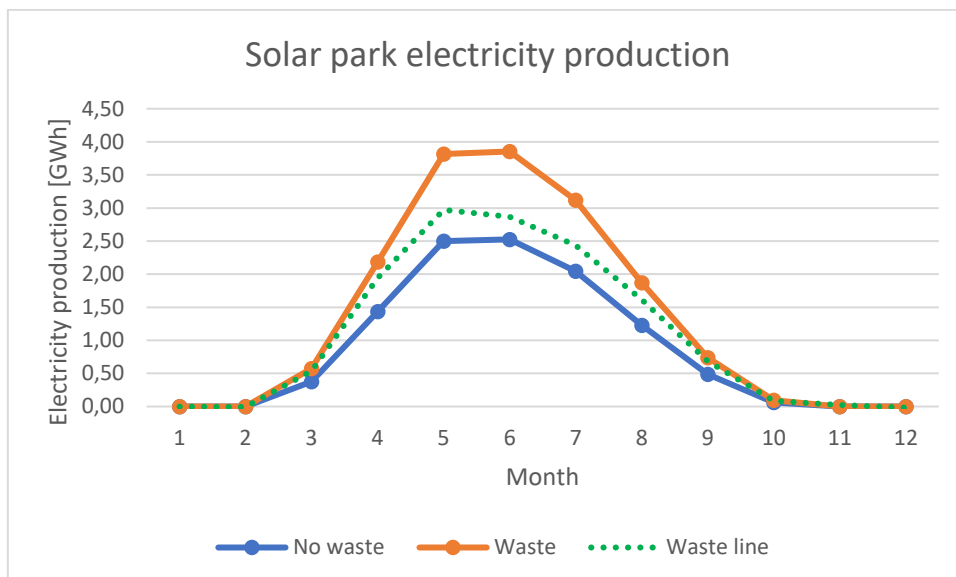


Figure 57: A graphical presentation of the monthly electricity production in the solar park with and without waste of renewable energy. The electricity production that lies above the waste line indicates wasted solar energy due to overproduction.

Table 25 shows the resulting dimensions for the two waste conditions. The model increases the number of panels in the solar park when waste of renewable energy is allowed. Notice that the battery capacity has been reduced, which is probably because the need for peak shaving and storing is less as the solar park can produce a sufficient amount of electricity with less irradiance. The heat pump capacity has been reduced as well, because it is not as important to fully utilise the heat pump during hours with high solar irradiance to store heat later in the thermal storage, because the hourly solar energy production is higher. Notice that the heat pump capacity is in terms of electricity input and that it has an efficiency of 3.5 times the input. That means that it is still able to produce a sufficient amount of heat hourly to satisfy the heat demand during the summer.

Table 25: Resulting decision variables associated with and without the waste from the model results.

	Without waste	With waste
Yearly ship arrivals	4 ships à 5 000 m ³	4 ships à 5 000 m ³
LNG storage capacity [m³]	5 132	5 486
Gas engines à 3500 KW[-]	3	3
Yearly LNG consumption in the power plant [m³]	9 913	8 975
Thermal storage [m³]	2 000	2 000
Battery [KWh]	5 549	4 490
Heat pump electricity input [KW]	3 663	2 830
Solar park [solar panels à 300 W]	55 833	85 194

Figure 58 shows the resulting costs when allowing for renewable energy waste. The total cost of the NESL over its lifetime can be reduced by around 0,7%, Table 26, when allowing for waste. In addition, by having a bigger solar park, the NESL will be more robust to population increase in Longyearbyen. However, the investment costs will greatly increase by almost 18%. That means that this design requires a lot more equity, which makes the option less attractive when the lifetime reward is small. It has therefore been concluded, together with the industry partners, that the best option is to continue with the waste restrictions to avoid the investment cost.

Table 26: The cost deviations between the result with and without the waste- Negative deviation means that the result with waste is more expensive.

Cost type	Deviation [%]
Total cost	0,7
Investment cost	-17,7
LNG consumption cost	9,7
Transportation cost	0,00

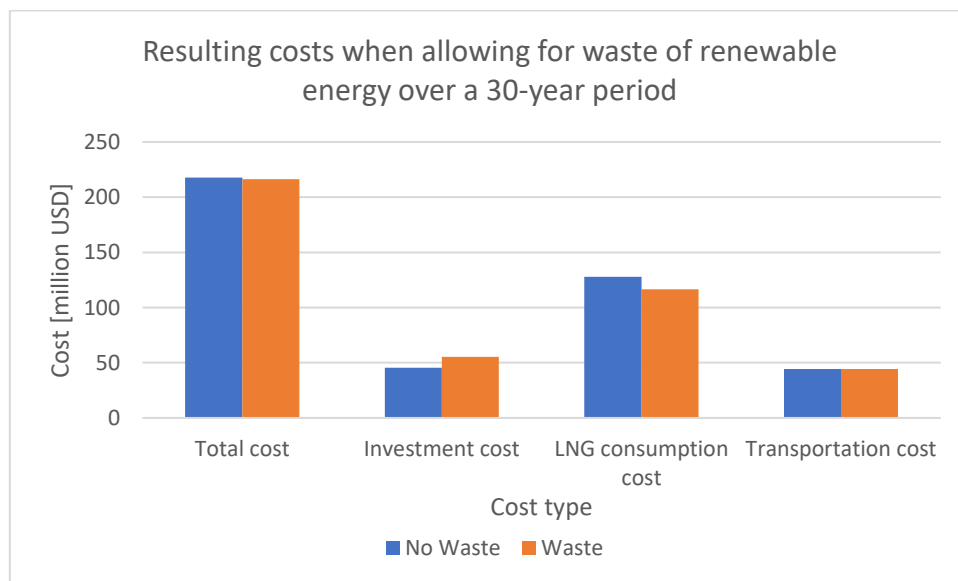


Figure 58: The resulting costs associated with and without the waste obtained from the model results.

7.4.6 Comparison of different NESL designs

One of the main objectives of this thesis is to see the economic effects of different NESL designs. This section will study how the costs and decision variables are affected by comparing different complexities of the NESL design. The different system designs that have been investigated are all related to the NESL design presented earlier in Section 3.1, and are:

- A NESL with a LNG storage and LNG power plant
- A NESL with a LNG storage, LNG power plant, battery, thermal storage and heat pump
- A NESL with a LNG storage, LNG power plant, battery, thermal storage, heat pump and solar park
- A NESL with a LNG storage, LNG power plant, battery capacity of 50 MWh, thermal storage, heat pump and solar park

The battery capacity has been selected to be 50 MWh because this is a battery size that is available on the market, and will provide a big electricity storage based on the existing energy demands in Longyearbyen. Bigger battery capacities are also available, but it has been considered sufficient with 50 MWh due to the high costs(Melaa, 2018).

Table 27 shows the dimensions of the model runs for each of the NESL designs.

Table 27: Resulting decision variables associated with the different NESL designs.

	With LNG storage and LNG power plant	With LNG storage LNG power plant, battery, thermal storage and heat pump	With LNG storage, LNG power plant, battery, thermal storage, heat pump and solar park	With LNG storage, LNG power plant, 50 MWh battery, thermal storage, heat pump and solar park
Yearly ship arrivals	5 ships à 5 000 m ³	4 ships à 5 000 m ³	4 ships à 5 000 m ³	4 ships à 5 000 m ³
LNG storage [m³]	5 840	5 887	5 132	5 037
Gas engines à 3500 KW [-]	5	4	3	3
Yearly LNG consumption in the power plant [m³]	15 604	12 870	9 913	9 286
Thermal storage [m³]	0	507	2 000	2 000
Battery [KWh]	0	606	5 549	50 000
Heat pump electricity input[KW]	0	726	3 663	2 094
Solar park [panels]	0	0	55 833	66 327

Looking at the two designs to the left in Table 27, the effects of implementing small energy storages and a heat pump can reduce the number of gas engines by one and reduce the yearly LNG consumption in the power plant considerably. These results show the effects of having energy storages for peak shaving, and how valuable a heat pump can be when the heat demand is significantly higher than the electricity demand for some periods during the year. These results are, thus, backing up *Bjørn Thorud's (2018)* information in Section 2.3, which gave the inspiration for the design of the NESL in this thesis.

The impact of the NESL design when implementing a solar park to the system is shown in the middle, two columns in Table 27. The energy storages have been increased to allow for more renewable, i.e. cheap energy, to be used. In addition, the heat pump capacity has been increased to be able to operate mainly on solar energy during summer, by converting necessary electricity into heat. With these dimensions for the battery, thermal storage, and heat pump, the NESL can reduce the number of gas engines in the power plant with one engine. Note that it is also possible to have only three gas engines without the solar park, but that the total cost of that solution will be more expensive than the optimal solution found with four gas engines.

Lastly, the two columns to the right show the effect of implementing a battery of 50 MWh. By having a big battery capacity, the heat pump capacity can be reduced significantly. That happens as the need for converting electricity to heat during strong irradiance hours are not as big, because excess electricity can be stored in the battery, and converted later. In addition, the number of panels in the solar park has been increased as more electricity can be stored in the battery without wasting energy. The battery results in more solar energy produced and used in the system, hence has the yearly LNG consumption been reduced.

Figure 59 shows the resulting costs for the different NESL designs. The main advantage with a more complex NESL design is that they allow for better energy efficiency, consuming less LNG. LNG expenses is the single biggest cost associated with the 30-year lifetime of the NESL, affecting the total cost the most.

Notice that the transportation costs are the same for the three NESL designs to the right. That is because the supplying ships have not been fully loaded, so that the designs consuming more LNG can use the same ships and supply rate, just loading the ships more. For the NESL design to the left, the consumption has increased to a level that requires an additional supply.

The investment cost increases with increased system complexity. However, notice that the NESL design to the left is costlier than the system with the energy storages and heat pump. That happens because the energy storages and heat pump make it possible to reduce the number of gas engines in the power plant, which is less costly. The investment cost increase for the NESL designs to the right is due to the solar park and battery.

It is, thus, concluded that to minimize the total lifetime costs of this system, a more complex design containing energy storages, heat pump and solar panels is the best solution because it reduces the LNG costs significantly. However, it requires more equity as the investment cost becomes higher.

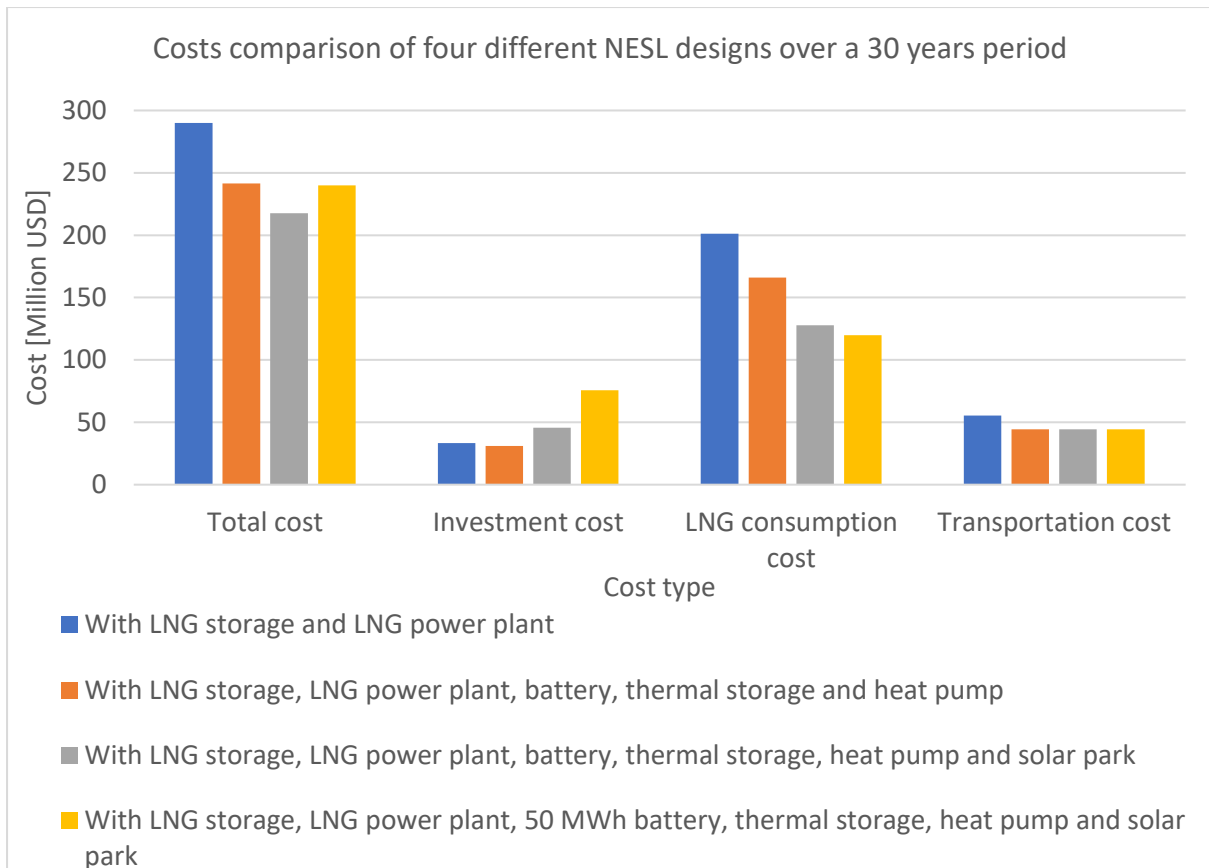


Figure 59: The resulting costs associated with the four different NESL designs investigated.

7.4.7 Summary and final cost recommendation of the NESL based on LNG and/or solar energy

This section gives the final recommendation of what NESL design that is the most cost-effective to implement in Longyearbyen based on the assumptions made for the optimisation model. This is one of the main objectives of this thesis. The recommendation depends on that the future energy demand predictions the model has assumed are correct, which has been called scenario 15 previously.

A short recap of scenario 15. Scenario 15 assumes that the electricity demand in Longyearbyen will be reduced by 25% due to the removal of Energiverket and mining in Gruve 7. In addition, shore power will be installed, requiring additional electricity during the cruise season. Further, the scenario assumes a 40% reduction of the heat demand in Longyearbyen due to energy efficiency actions. The LNG bunkering demand for ships is assumed to be equal to 80% of today's MGO demand, and the solar irradiance is assumed to remain at today's level.

In the design of the NESL is it recommended to:

- Analyse the relation between the total lifetime cost and the investment cost of having an upper LNG storage restriction. In this study, an LNG storage capacity between 5000 and 6000 m³ is recommended. That is because it ensures the total lifetime costs of the NESL to remain at the minimum level, while the investment cost related to the LNG storage has been reduced by about 8 million USD compared with the initial solution without an upper LNG storage restriction.
- Use a dynamic safety limit for stored LNG in the LNG storage, corresponding to 30 days of full power production in the respective season. The LNG storage capacity was reduced by 350 m³ using a new dynamic limit in this model, saving around 1.9 million USD in investment cost.
- Design the solar park in such a way that overproduction and waste are limited. This will help to keep the total cost of the NESL lifetime to a minimum while reducing the investment cost, thus the need for equity, with approximately 18%.
- Build the NESL with a solar park, battery, thermal storage and heat pump, in addition to an LNG power, because the total lifetime cost saving of doing that is around 72 million USD based on the model results. Table 28 presents the optimal NESL dimensions that are recommended for scenario 15 based on the model results in this thesis.

Table 28: The recommended decision variables for the NESL to achieve the minimum total cost for scenario 15.

Yearly ship arrivals	4 ships à 5 000 m ³
LNG storage [m³]	5 132
Gas engines à 3500 KW [-]	3
Yearly LNG consumption in the power plant [m³]	9 913
Thermal storage [m³]	2 000
Battery [KWh]	5 549
Heat pump electricity input[KW]	3 663
Solar park [solar panels à 300 W]	55 833

Note that the ship arrivals are not fully loaded.

The annual costs of the NESL over a 30-year period is presented in Table 29. The LNG consumption cost will be the main expense of the yearly costs.

Table 29: Yearly costs associated with the recommended NESL design for scenario 15.

Cost type associated with the NESL based on scenario 15	Yearly cost [USD]
Investment cost	1 518 873
LNG consumption cost	4 259 534
Transportation cost	1 477 668
Total cost	7 256 074

7.5 Environmental study

The environmental aspects are important for Longyearbyen, and an environmentally friendly energy production will be important for the conservation of the vulnerable nature. This section aims to see how much the LNG consumption, thus the CO₂ emissions, can be reduced by different system designs. This is one of the main objectives of this thesis. The four NESL-designs that will be studied in this section are the same as mentioned earlier, and are based on the optimal economic results:

- NESL containing a LNG storage and LNG power plant
- NESL containing a LNG storage, LNG power plant, battery, thermal storage and heat pump
- NESL containing a LNG storage, LNG power plant, battery, thermal storage, heat pump and solar park
- NESL containing a LNG storage, LNG power plant, a battery capacity of 50MWh, thermal storage, heat pump and solar park

Figure 60 shows the monthly LNG consumption of the NESL with only a LNG storage and a LNG power plant. The LNG consumption in the power plant drops during the summer months as the electricity and heat demand is lower. Due to the ship bunkering consumption, the monthly LNG consumption profile is even and not characterised by clear peaks, which it would have been if the consumption was only consisting of the power plant.

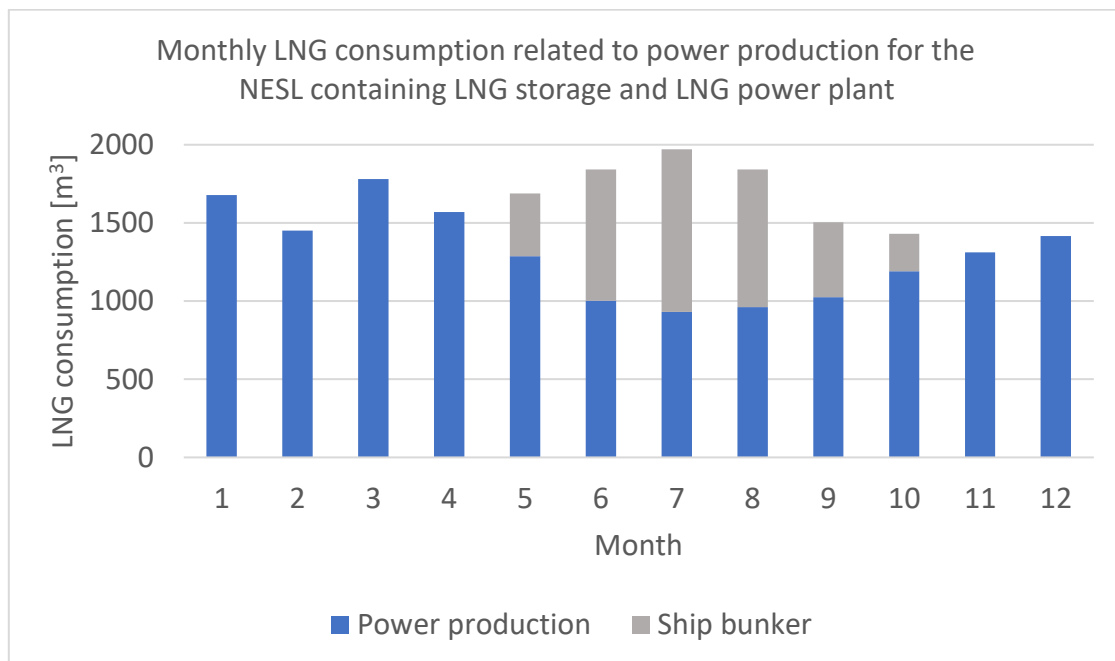


Figure 60: Monthly LNG consumption of the NESL containing a LNG storage and LNG power plant.

Figure 61 below shows the saving potential of LNG when installing the battery, thermal storage and heat pump to the NESL. The LNG consumption in the power plant will decrease significantly during the winter season, mainly because the energy storages and heat pump increase the efficiency when the heat demand is much bigger than the electricity demand.

During summer, when the electricity demand and heat demand are roughly equal, this saving is less. This LNG consumption profile of this NESL design is season dependent, peaking during the summer.

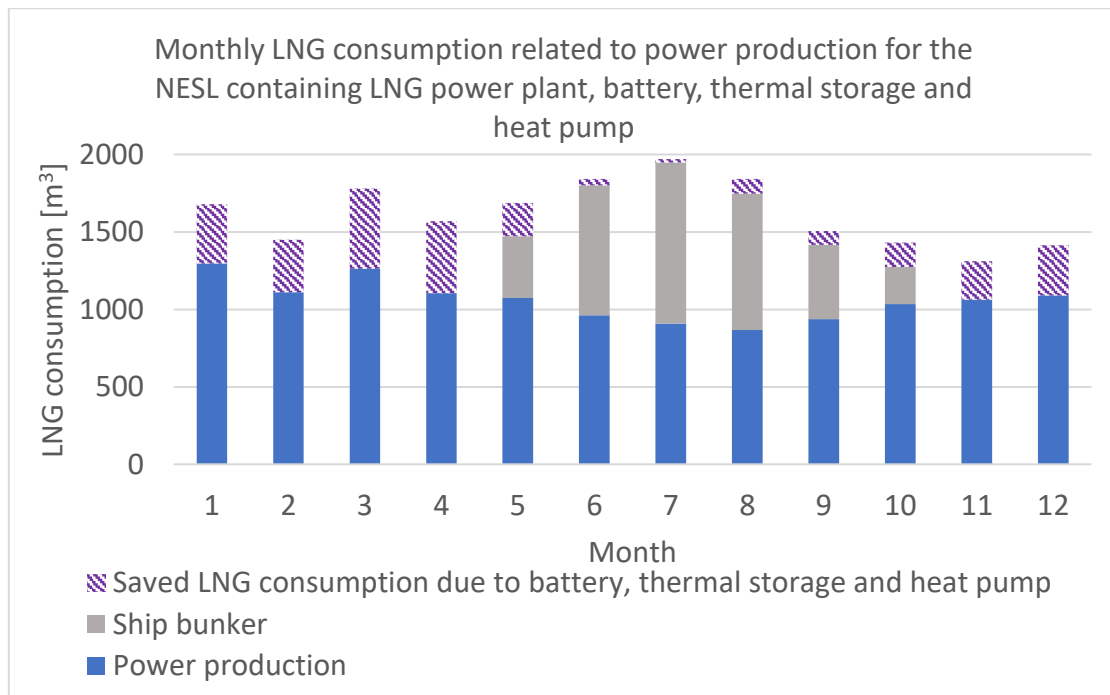


Figure 61: Monthly LNG consumption of the NESL containing an LNG storage, LNG power plant, battery, thermal storage and heat pump. The LNG saving potential due to the battery, thermal storage, and heat pump is indicated versus the previous design.

Figure 62 shows the LNG saving potential when installing a solar park to the NESL presented in Figure 61. The savings are considerable during the daylight season and will reduce the operating hours, thus the emissions, of the power plant significantly. Notice that the solar park will shave the consumption peaks during summer, resulting in a more even consumption profile during the year. That is advantageous because peaks are the dimensioning factors for a system, and avoiding significant peaks can reduce the system capacity, thus, the investment costs.

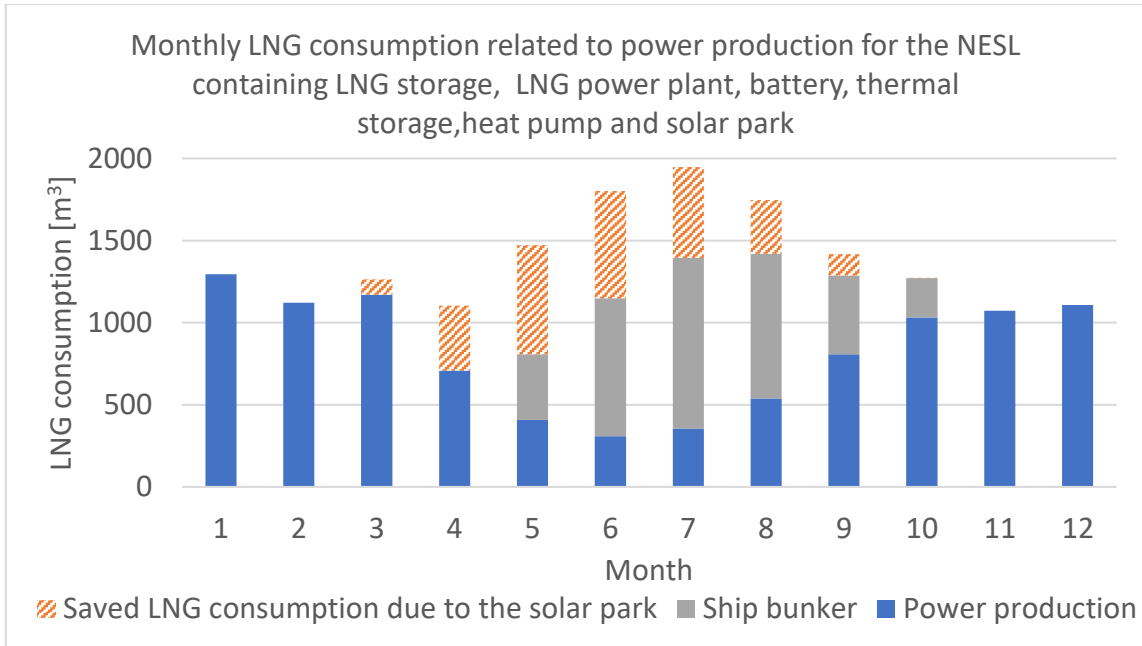


Figure 62: Monthly LNG consumption of the NESL containing an LNG storage, LNG power plant, battery, thermal storage, heat pump and solar park. The LNG saving potential due to the solar park is indicated versus the previous design without the solar park.

Figure 63 below shows the LNG consumption effects of implementing a 50 MWh battery to the NESL presented above. The battery does not have any significant effect on the LNG consumption saving during the polar night season, indicating that the already existing energy storages and heat pump were sufficient for handling this season ideally. However, during the summer, the LNG savings can be considerable. That is because the battery allows the NESL to store and consume more solar energy, thus, reduce the operational time and LNG consumption in the LNG power plant.

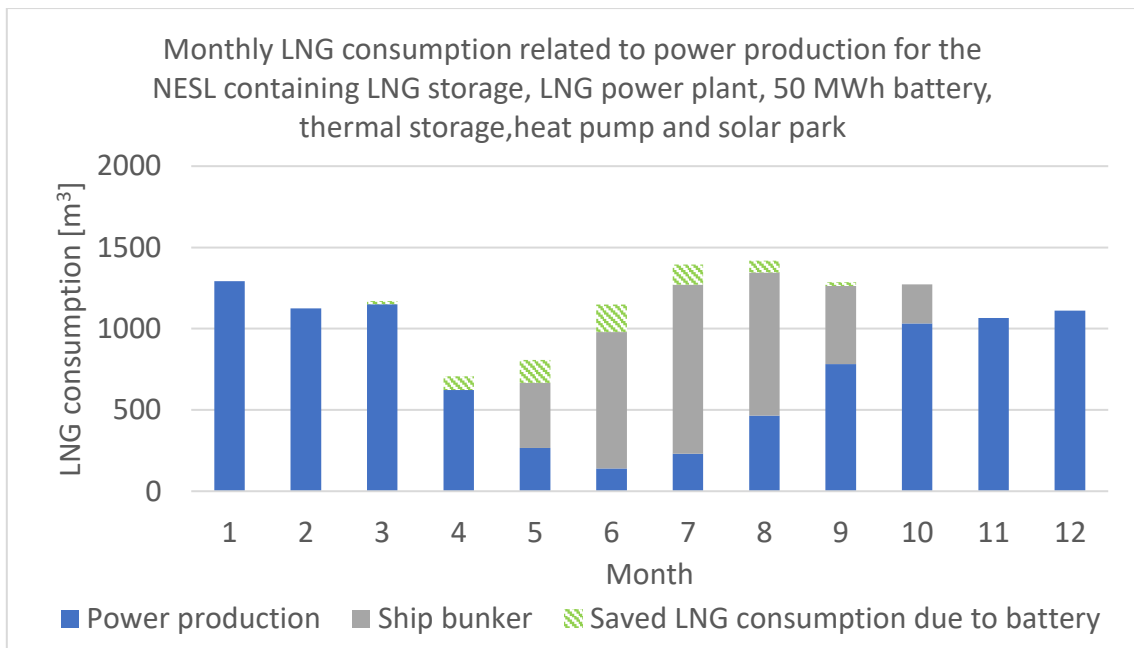


Figure 63: Monthly LNG consumption of the NESL containing an LNG storage, LNG power plant, 50 MWh battery, thermal storage, heat pump and solar park. The LNG saving potential due to the battery is indicated versus the previous design.

Figure 64 shows the total CO₂ emissions related to power production of the four NESL designs and today's energy system in Longyearbyen. The emission factor used for LNG is 0.0566 kg CO₂/MJ(Zijlema, 2018) and a higher heating value of 49 MJ/kg(World Nuclear Association, 2016). The LNG density is 456 kg/m³(U.S. Department of Energy, 2005). For the coal, an emission factor of 0.0898 kg CO₂/MJ(Zijlema, 2018) is used, and a higher heating value 23000 MJ/ton(World Nuclear Association, 2016). An emission factor of 0.0725 kg CO₂/MJ(Zijlema, 2018), and a heating value of 39000 MJ/m³ (World Nuclear Association, 2016), is used for diesel.

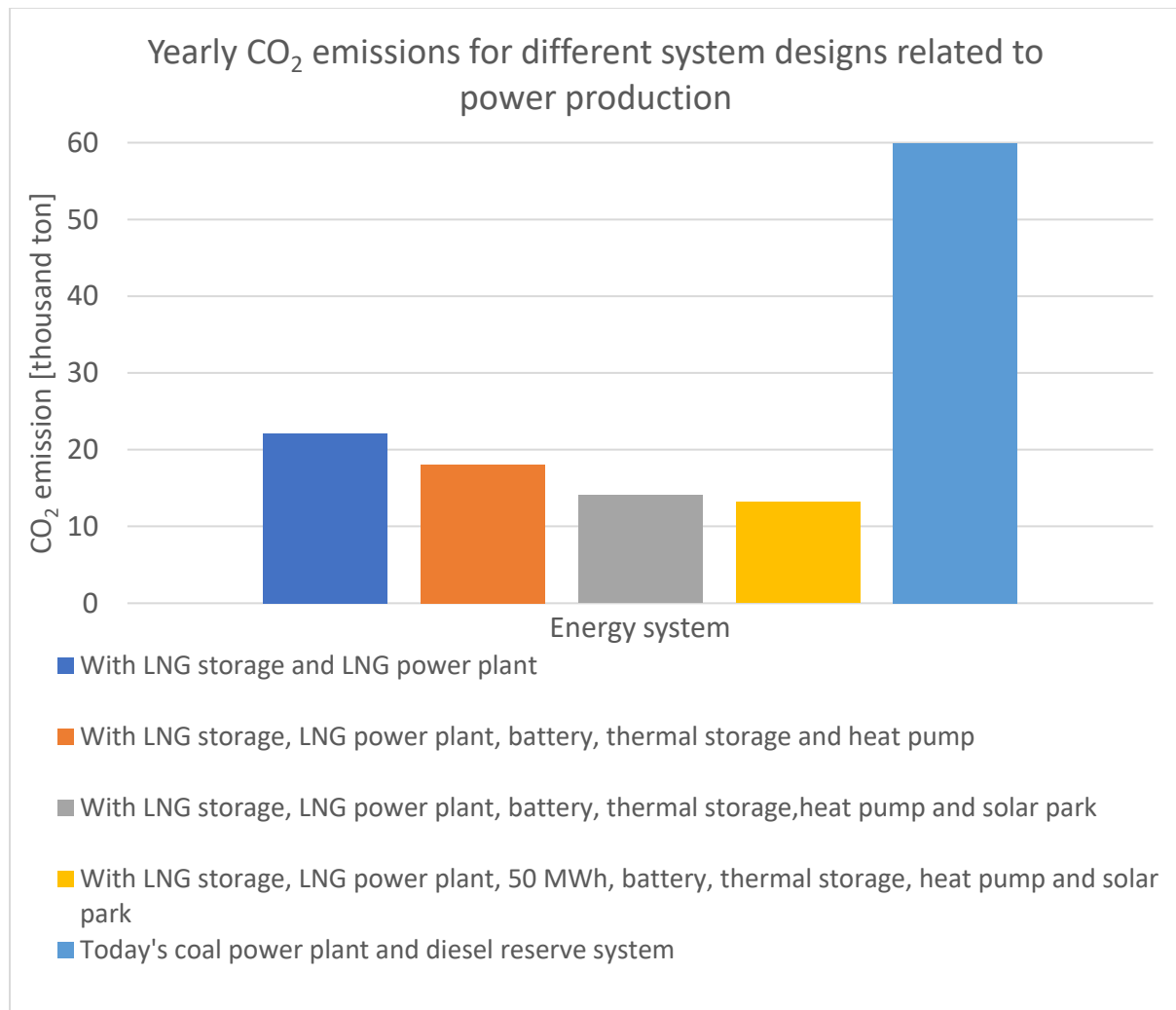


Figure 64: Yearly CO₂ emissions for the different NESL designs related to power production, and today's coal power plant.

Figure 64 shows that no matter which of the NESL designs above that is selected, each of them will reduce the CO₂ emissions by more than 60% compared with today's emission level. Remember that the NESL designs are simulated with a reduced heat demand of 40%, but it gives an indication of the emission reduction potential that can be achieved with LNG, and the effects of how energy efficiency actions in Longyearbyen can save the environment. The implementation of battery, thermal storage, and heat pump reduces the emissions by around 18%, which indicates the reward of storing overproduced energy and avoid waste. In addition, an implementing of a solar park will reduce the emissions further, with around

36% compared with the LNG power plant alone. That happens because less LNG is combusted in the power plant because the solar park produces energy. Lastly, having a big battery of 50 MWh means that more solar energy can be stored and used, reducing the emission by another 6%. However, the battery is expensive, and is, thus, not the most cost-effective solution. Notice that these calculations are based on the CO₂ emissions only. To evaluate the total emissions of the system, it will be important to include emissions related to the manufacturing of the solar panels and battery, and recycling, as well as other emissions such as SO_x and NO_x.

Another important aspect, connecting emissions and costs, is carbon pricing. That is a charge that must be paid for every ton CO₂ that is emitted into the atmosphere. The price today is around 17 USD per ton, but it is not unlikely that the European Union may increase the priced and push them up to 60 EUR per ton. Norway is in the European Economic Area, but Svalbard is not. However, it is likely that Svalbard, thus Longyearbyen, will follow the carbon price charges due to the environmental focus(Endsjø, 2018). The economic effects of designing a system with less emission will, therefore, be even more economical. Table 30 below shows the yearly emission cost difference between the most cost-effective NESL design, with the LNG storage, LNG power plant, battery, thermal storage, heat pump and solar park, and today’s coal power plant. As seen, the cost effects of a significant increase in the carbon price will make the NESL even more attractive from an economic perspective. The carbon price will also affect the solution quality of the different NESL designs, which has not been implemented in the model.

Table 30: The emission difference between the NESL with LNG storage, LNG power plant, battery, thermal storage, heat pump and solar park and today’s coal power plant, and yearly emission costs related to different carbon prices.

Difference between the NESL with LNG storage, LNG power plant, battery, thermal storage, heat pump and solar park and today’s coal power plant	
Yearly CO₂ emissions	45 862 ton
Yearly emission cost with a price of 17 USD/ton	779 654 USD
Yearly emission cost with a price of 60 USD/ton	2 751 720 USD

Figure 65 shows the yearly impact of changing the ship bunkering fuel from MGO to LNG, where the CO₂ emissions can be reduced by nearly 50%. In addition, switching the marine fuel type to LNG will have a considerable effect of the total emissions of the cost-optimal NESL, where the savings alone will correspond to about 30% of the emissions from the power production. The CO₂ emission savings of using LNG as ship fuel is therefore considerable for the whole system.

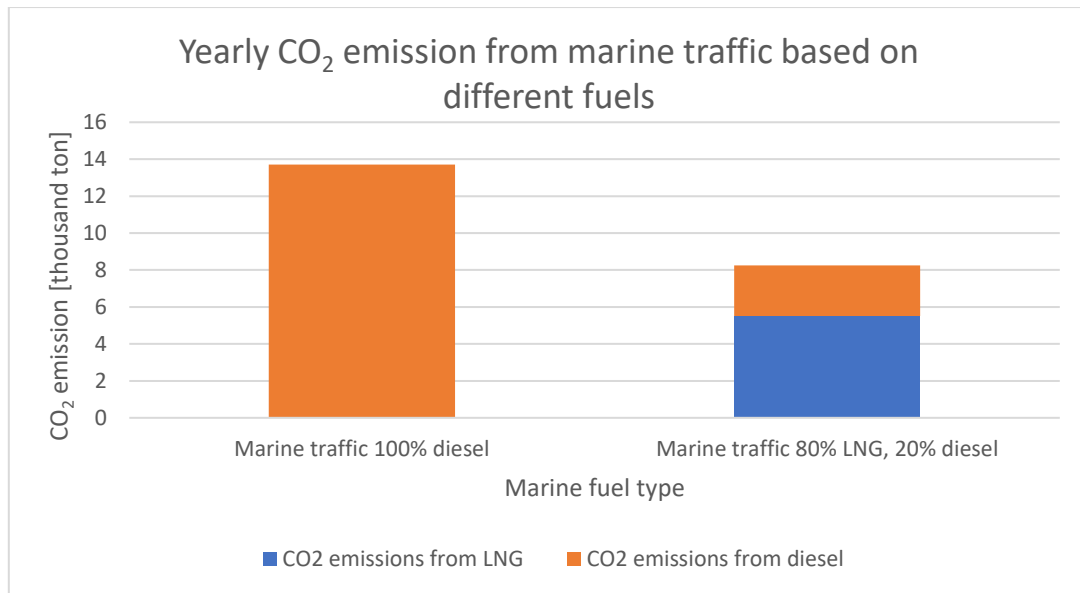


Figure 65: Yearly CO₂ emissions from marine traffic comparing today's level with a fuel type change from MGO to LNG.

To sum up this section, installing a NESL based on LNG will reduce the CO₂ emissions by around 60% compared with today's emissions, given that energy efficiency actions are done. The effects of implementing energy storages, heat pump and solar park to the NESL will reduce the LNG consumption, thus the CO₂ emissions, with around 36% compared with an LNG power plant alone. If implementing a bigger battery package, the emissions can be reduced further by around 6%. The emission saving will be present during the summer if implementing a big battery.

Carbon pricing is an important aspect in terms of emissions and costs, and makes today's energy system, with high emission, economically unfavourable compared with new energy systems with less emissions. A rapid increase in the carbon price will make energy systems with low emission even more cost competitive.

Changing the ship fuel type from MGO to LNG will reduce the CO₂ emission by nearly 50%. The marine emissions savings of switching to LNG will have a considerable effect on the total emissions of the NESL.

7.6 Validity of the results

This section aims to discuss the validity of the results obtained from the model. Models are simplifications of the real world. Sometimes these simplifications are not affecting the accuracy of the results, sometimes they do. The result accuracy is mainly dependent on the model quality and the input data quality, which will be discussed in this section.

7.6.1 Model quality

The model behaviour was concluded to be logical in the quantitative validation, section 7.3.6. However, the model has been established based on different modelling choices and assumptions, section 5.1. This sub-section will discuss whether some of the assumptions made can reduce the quality of the model, or if some extensions will improve the quality.

One of the assumptions made previously was that degradation effects were so small that they could be neglected. However, with the lifetime of 30 years, such small effects will propagate. This degradation effect is especially related to the solar panels and the battery of the NESL. For instance, the degradation effect of the solar panels is around 0.4% yearly (Melaa, 2018). Over a 30-year period, that will result in over 12% degradation, which will affect the energy production capacity in the solar park considerably. The model will, however, give a good indication for the current and short-term future design dimensions requirements of the NESL, and installing additional solar panels or battery capacity at a later stage is possible. It will be important to be aware of the degradation effects in the final decision.

It has been assumed that the supplying ships are not subject to heavy ice conditions during winter. If this happens, the ships will need ice-class which is more expensive, thus will the transportation costs increase. If this had been implemented in the model, the optimal supply schedule may have looked different as the LNG storage would have been full before the ice-season started to avoid ship supplies with ice-class. However, assuming no ice gives much more flexibility to the transportation schedule. Heavy ice conditions are not probable as there has not been ice for seven seasons, and will probably not affect the optimal design much.

The economic consideration done in this thesis in terms of investment cost is only related to the price of the different system components. Thus are, for instance, depreciation and interest rates not considered. This can potentially change the optimal solution and should be implemented at a later stage.

The losses in the LNG storage are modelled monthly. In reality, the losses happen continuously, and it will, thus, be higher LNG losses than what is modelled. These losses are, however, negligible in the overall picture, because they will at most correspond to 4.5% of the monthly consumption.

Carbon pricing was mentioned in the environmental study and showed that sensitivity in the carbon price can highly affect the optimal design. This has not been implemented in the model, and should be an implemented extension to increase the quality of the model because it will give a more accurate cost picture.

The last point worth to mention is the RHH method. This method has the advantage that it discovers a good solution quickly, and much quicker than the exact method. The downside is that it cannot guarantee that the solution is optimal. Section 7.3.1 did, however, show that the method worked as intended, and it has therefore been assumed that the RHH is not affecting the model quality significantly within a 5% significance level.

To summarize, most of the assumptions made have a small effect on the model solution. However, implementing carbon pricing, depreciation and interest rates to the model will increase the detail level and most likely improve the quality, thus validity, of the result.

7.6.2 Input data quality

The quality of the input data is the other major factor determining the quality of the results. The input data was provided in section 7.2, and the data was selected to the best of the author's abilities, with assistance from the industry partners. Factors affecting the data will be discussed.

There may be errors or inaccuracies in the cost data associated with the different system components. This can be due to changing market prices and outdated information. If some of this data deviates a lot from the actual data, this may affect the system design dimensions significantly. The accuracy of this data is, therefore, of high importance.

Another factor affecting the input data is the energy demands. The information used in this thesis are directly based on historical monitored data. However, most of the analyses have been based on future predictions of this historical data. There is a lot of uncertainty connected with the future, and inaccuracy and wrong predictions in this data will lead to lower quality of the final NESL design.

8. Concluding remarks

In this thesis, today's energy system in Longyearbyen, as well as four different future energy systems in Longyearbyen based on LNG and/or Solar energy, have been presented. The aim of the thesis has been to create an optimisation model that can minimize the total lifetime costs of a new energy system in Longyearbyen over a 30-year period. The model of the new energy system in Longyearbyen has been formulated by applying Mixed Integer Linear Programming.

The objectives of the study have been:

- To formulate a valid and time-efficient optimisation model that can be used as a decision support tool for designing and analysing the effects of a new energy system in Longyearbyen based on LNG and/or solar energy.
- To evaluate the economic effects of four different new energy system designs in Longyearbyen, and recommend the most cost-effective design.
- To evaluate the environmental effects of the same four new energy system designs in Longyearbyen in terms of CO₂ emissions, and compare the emissions with today's energy system in Longyearbyen.

A technical study was performed to reduce the computational time of the model to an applicable level, and validate that the model worked as intended.

The applicability of the model was dependent on reducing the computational time to be able to run through more scenarios and, thus, achieve a more comprehensive study. The computational time was reduced by implementing a Rolling Horizon Heuristic method, where the method divided the overall problem into sub-problems. Each sub-problem was then solved individually. This was done because the exact method was not able to solve the overall problem within an applicable time. A comparison of the Rolling Horizon Heuristic and the exact method were executed for smaller problem sizes, showing that the result deviations were within a significance level of 5% between the two methods. By using the exact solving method for the model, the computational time for a problem size of 5 months, which is less than half the problem, was more than 11 hours, and the optimal solution was not found. Note that the computational time increased exponentially with problem size. Using the Rolling Horizon Heuristic method, the computational time was less than 7 minutes for the problem size of 5 months. For the full problem size of 12 months, the Rolling Horizon Heuristic method solved the model within 15 minutes.

The model has been successfully validated, with assistance from the industry partners. The flows and responses of the model results were logical, and the final dimensions were in the area of what to expect. A discussion of the validity of the results was presented, emphasizes the importance of good input data quality for achieving valid model results. The quality of the model was concluded to be good, but further implementation of, for instance, carbon

pricing, depreciation and interest rates, is thought to improve the validity of the model and results even more.

The model was used to evaluate the economic and environmental aspects of four different NESL designs, which were:

- With LNG storage and LNG power plant
- With LNG storage, LNG power plant, battery, thermal storage and heat pump
- With LNG storage, LNG power plant, battery, thermal storage, heat pump and solar park
- With LNG storage, LNG power plant, 50 MWh battery, thermal storage, heat pump and solar park

The economic study showed that it is possible to reduce the total lifetime costs of a new energy system in Longyearbyen with almost 50 million USD if installing a battery, thermal storage and a heat pump in addition to the LNG power plant, which are the upper two system designs above. The saving was mainly related to a big reduction in the power plants LNG consumptions costs due to better system efficiency and less energy waste. In addition, the investment costs were reduced as the battery, thermal storage and heat pump made it possible to reduce the number of gas engines by one engine in the LNG power plant.

If installing a solar park in addition to the battery, thermal storage, and heat pump, which are the middle two designs above, it was possible to reduce the total lifetime costs of the system with more than 24 million USD. The saving was related to LNG consumption savings during the daylight season, because the solar park would produce most of the required energy. This option would, however, require almost 15 million USD more in investment costs, but the LNG consumption costs in the LNG power plant would be reduced with nearly 40 million USD over the 30-year lifetime.

Finally, installation of a battery of 50 MWh would have reduced the LNG lifetime consumption costs in the power plant with around 8 million USD, as it would allow for more storage and usage of solar energy. However, the investment costs for a battery are currently big, meaning that the total lifetime costs of implementing a big battery of 50 MWh were 23 million USD costlier than the previous design.

The recommended design of the new energy system in Longyearbyen is presented in Table 31, and is the 3rd design listed above. It was the design that provided the lowest total lifetime costs considering the investment, LNG consumption and transportation costs. Note that the supplying ships are not fully loaded because it is more economical to have a more frequent supply rate instead of an increased LNG storage capacity.

Table 31: The final system dimensions for the recommended design of the new energy system in Longyearbyen.

Yearly ship arrivals	4 ships à 5 000 m ³
LNG storage [m³]	5 132
Gas engines à 3500 KW [-]	3
Yearly LNG consumption in the power plant [m³]	9 913
Thermal storage [m³]	2 000
Battery [KWh]	5 549
Heat pump electricity input [KW]	3 663
Heat pump heat output [KW]	12 820
Solar park [solar panels à 300 W]	55 833

The environmental study showed that the effects of replacing the power production in Longyearbyen from coal to LNG, and the marine fuel from MGO to LNG, would reduce the CO₂ emission with at least 60% independent of the NESL designs investigated in this study. Notice that these results were assuming a reduction in Longyearbyen's heat demand of 40% due to energy efficiency actions.

If installing a battery, thermal storage, heat pump and a solar park in addition to the LNG power plant, the relative CO₂ emissions for the new energy system could be reduced by around 36% compared with an LNG power plant alone. Further, installing a battery with a capacity of 50 MWh in addition to the energy system with the LNG power plant, battery, thermal storage, heat pump and solar park, the emission could be reduced with another 6%. Compared with the coal power plant today, the emission reduction of the NESL with the 50 KWh battery would have been around 78%.

The impact of a transition of marine fuel from 100% MGO, which it is today, and to 80% of LNG and 20% MGO in the future, will almost reduce the marine CO₂ emission with 50%. Switching the marine fuel type to LNG will have a considerable effect of the total emissions of the new energy system in Longyearbyen, where the savings will correspond to about 30% of the emissions from the power production.

To sum up, the conclusion of this thesis is that a mathematical optimisation model was successfully created to analyse different aspects of a new energy system in Longyearbyen based on LNG and/or solar energy. Further, installation of solar panels, energy storages and heat pump to increase the production efficiency and reduce the LNG consumption had the best impact in terms of total lifetime cost savings for a new energy system design. In addition, an implementation of an LNG and solar energy based energy system will greatly reduce the CO₂ emissions in Longyearbyen emitted by power production and marine traffic.

9. Further work

This thesis formulates an extensive model for the New Energy System in Longyearbyen (NESL) problem. The formulation includes simplifying assumptions and modelling choices, to make the problem manageable. In addition, with gained knowledge during the thesis work, there are aspects that could help in constructing a more realistic and applicable model. This chapter will present thoughts on possible future improvements and reasons that can strengthen the model formulation.

It could be a valuable extension of the mode to include depreciation and interest rates. The formulated model in this thesis has only considered the prices of the different system components capacities, and no further consideration. Including depreciation and interest rates will better reflect the impact of the investment costs of the NESL for the buyer, and, thus, give a more accurate result with respect to the total lifetime costs.

Carbon pricing, i.e. the costs of emitting CO₂, will benefit the more environmental solutions. This has not been implemented in the model, but it is recommended to do so for further study. That is because the yearly costs associated with the carbon price can potentially affect the total yearly costs of the new energy system significantly, meaning that other design solution may be desirable. The extension will, thus, provide a more realistic cost picture.

The model analyses in this thesis have been assuming constant energy demands and solar irradiance over 30 years. It could be of big interest to see how the model results are affected by an increased model length, where the input variables are stochastically changing for each year. This will require more computational effort and time, but can be applicable in a later, more detailed design phase of the NESL.

References

- Ani, V. A. (2016). Design of a Reliable Hybrid(PV/Diesel) Power System with Energy Storage in Batteries for Remote Residential Home. (University of Nigeria).
- Bøckman, R. (2017, 13.10.2017) *Energy situation Longyearbyen/Interviewer: P. Hovden.*
- Clausen, J. (1999). Branch and Bound Algorithms - Principles and Examples. (University of Copenhagen).
- Dahlberg, A. (2018, 20.02.2018) *Thermal storage solution/Interviewer: P. Hovden.*
- Dimitriadis et al., A. D. (1997). RTN-Based Rolling Horizon Algorithms for Medium Term Scheduling of Multipurpose Plants. (Imperial College of Science, Technology and Medicine, London).
- Dyrstad, M. (2018, 13.03.2018) *Meeting Longyearbyen Lokalstyre/Interviewer: P. Hovden & H. Vartdal.*
- Ellingsen, H. (2017, 11.10.2017) *Energy Consumers in Longyearbyen/Interviewer: P. Hovden.*
- Endsjø, P.-C. (2018, 22.05.2018) *GraviFloat and Svalbard/Interviewer: P. Hovden.*
- EPA. (2018). What is CHP. Retrieved from <https://www.epa.gov/chp/what-chp>
- Google sites. (2018). Europe: Sør-Spitsbergen National park, Svalbard, Norway. Retrieved from <https://sites.google.com/a/miamioh.edu/geo121f15/home/soer-spitsbergen-np-svalbard-norway-12>
- Gopalakrishnan, H. (2014). Operational planning in combined heat and power systems. (University of Massachusetts).
- Grinold, R. (1983). *Model Building Techniques for the Correction of End Effects in Multistage Convex Programs* (3 ed. Vol. 31).
- Hegle, M. (2018, 17.10.2017) *Electricity and district heating production in Longyearbyen/Interviewer: P. Hovden.*
- Hillier, F. S., & Lieberman, G. J. (2015). *Introduction to Operations Research* (10th ed.).
- Hovden, P. (2017). Optimisation of the fuel storage capacity in Longyearbyen. (Norwegian University of Science and Technology).
- Ingero, R. O. (2017, 13.10.2017) *Ship Traffic in Longyearbyen/Interviewer: P. Hovden.*

- Jakobsen, F. (2017, 16.10.2017) *Fuel Distribution Longyearbyen/Interviewer: P. Hovden.*
- Kaufmann, A., & Henry-Labordère, A. (1977). *Integer and Mixed Programming: Theory and Applications* (1 ed. Vol. 137).
- Kornfeldt, E.-B. (2017, 13.10.2017) *Cruise traffic Longyearbyen/Interviewer: P. Hovden.*
- Kystverket. (2016). *Ny havnestruktur i Longyearbyen.* Retrieved from <http://www.kystverket.no/globalassets/rapporter-og-brosjyrer/kvu-longyearbyen-hovedrapport-v2.pdf>
- Land, A. H., & Doig, A. G. (1960). An automatic method of solving discrete programming problems. (*Econometrica*).
- Lenstra, J. K., & Rinnooy Kan, A. H. G. (1979). *Computational Complexity of Discrete Optimization Problems.* (Erasmus University, Rotterdam).
- Linderoth, J. T., & Savelsbergh, M. W. P. (1999). *A Computational Study of Search Strategies for Mixed Integer Programming.* (Georgia Institute of Technology, Atlanta).
- Lu et al., C. (2014). *Optimal Sizing and Control of Battery Energy Storage System for Peak Load Shaving.* (Tsinghua University, Beijing).
- Marquant et al., J. F. (2015). *Reducing Computational Time with a Rolling Horizon Approach Applied to a MILP Formulation of Multiple Urban Energy Hub System.* (Swiss Federal Institute of Technology, Zurich).
- Melaa, T. (2018, 29.01.2018) *Solar energy production at Svalbard/Interviewer: P. Hovden, H. Vartdal, & P.-C. Endsjø.*
- MiniTab. (2018). *Factorial and fractional factorial designs.* Retrieved from <https://support.minitab.com/en-us/minitab/18/help-and-how-to/modeling-statistics/doe/supporting-topics/factorial-and-screening-designs/factorial-and-fractional-factorial-designs/>
- National Snow & Ice Data Center. (2017). *Ice Concentration.* Retrieved from https://nsidc.org/data/seaice_index/archives/image_select
- NOVAP. (2018). *Ulike varmpumper.* Retrieved from https://www.novap.no/ulike_varmpumper
- Omu et al., A. (2013). *Distributed energy resource system optimisation using mixed integer linear programming.* (University of Cambridge, Cambridge).

- Pazouki, S. (2014). Impact of Energy Storage Technologies on Multi Carrier Energy Networks. (Islamic Azad University, South Tehran).
- Pearl, J. (1984). Heuristics - Intelligent Search Strategies for Computer Problem Solving. (University of California, Los Angeles).
- Pérez et al., J. (2004). Comparison and Selection of Exact and Heuristics Algorithms. (National Center for Research and Technology Development, Acapantzingo).
- Rakke et al., J. G. (2010). A rolling horizon heuristic for creating a liquified natural gas annual delivery program. (Norwegian University of Science and Technology, Trondheim).
- Rothlauf, F. (2011). *Design of Modern Heuristics* (1 ed.).
- Rønning, O. (2017, 17.10.2017) *SNSK's situation/Interviewer: P. Hovden.*
- Sahai, H., & Ageel, M. I. (2000). *The Analysis of Variance: Fixed, Random and Mixed Models* (1 ed.).
- Schreck, S. (2016). Implementation and Analysis of a Rolling Horizon Approach for the Energy System Model REMix. (University of Stuttgart, Stuttgart).
- Searoutes.com. Searoute Rotterdam-Longyearbyen. Retrieved from <https://www.searoutes.com/portdistance?fromName=Longyearbyen&fromLocode=NOLYR&toName=Rotterdam&toLocode=NLRTM>
- Sethi, S., & Sorger, G. (1991). A Theory of Rolling Horizon Decision Making. (University of Toronto, Toronto).
- Syssemmannen. (2018). Climate and Light in Longyearbyen. Retrieved from <https://www.syssemmannen.no/en/Toppmeny/About-Svalbard/Climate-and-light/>
- Thie, P. R., & Keough, G. E. (2008). *An introduction to linear programming and game theory* (3rd ed.).
- Thorud, B. (2018, 29.01.2018) *Possible energy systems/Interviewer: P. Hovden, H. Vartdal, & P.-C. Endsjø.*
- U.S. Department of Energy. (2005). Liquified Natural Gas: Understanding the Basic Facts. (U.S. Department of Energy,).
- Vartdal, H. (2018, 22.05.2018) *LMG Marin's visions/Interviewer: P. Hovden.*

Visit Svalbard. (2018). Longyearbyen. Retrieved from <https://en.visitsvalbard.com/visitor-information/destinations/longyearbyen>

Wallentinsen, Å. (2018, 13.03.2018) *GraviFloat/Interviewer: P. Hovden.*

World Nuclear Association. (2016). Heat values of Various Fuels. Retrieved from <http://www.world-nuclear.org/information-library/facts-and-figures/heat-values-of-various-fuels.aspx>

WPCI. (2018). Benefits of LNG. Retrieved from <http://www.lngbunkering.org/lng/environment/benefits-of-LNG>

Zijlema, P. J. (2018). The Netherlands: list of fuels and standard CO₂ emission factors version of January 2018. (Netherlands Enterprise Agency).

Appendix

A. Table containing all the information about the ship supply

Tank capacity [m ³]	Time charter cost [USD/day]	Fuel consumption [MT/day]	Starting port	Fuel type	Distance Rotterdam-Longyearbyen-Rotterdam [nautical miles]	Speed [knots]	Unloading. manoeuvring etc [days]	Voyage duration [days]	Total harbour cost [dollar]	Boil-off [%/day]
5000	28000	10.40	Rotterdam	MGO	3296	13.30	0.5	10.8	10000	0.15
7500	30000	12.20	Rotterdam	MGO	3296	14.00	0.5	10.3	10000	0.15
10000	35000	13.60	Rotterdam	MGO	3296	14.00	0.5	10.3	10000	0.15
16000	45000	26.50	Rotterdam	MGO	3296	16.40	0.5	8.9	15000	0.15

B. Results obtained from the sensitivity analysis

Nr.	Scenarios					Decision variables									
	Electricity demand	Heat demand	Ship bunkering demand	Solar irradiance	Engines à 3500 KW [-]	LNG storage [m³]	Battery [KW/h]	Thermal Storage [m³]	Heat pump [KW]	Solar park [panels à 300W]	Objective value [USD]	5000 m³ ship call	7500 m³ ship call		
1	1	1	1	1	4	8557	609	2000	4821	56170	244538000	1	2		
2	1	1	1	2	4	8917	842	2000	4832	66207	248806000	1	2		
3	1	1	2	1	4	8557	608	2000	4804	56173	244551000	1	2		
4	1	1	2	2	4	8558	425	2000	4817	65969	247539000	1	2		
5	1	2	1	1	3	8343	4380	2000	3693	53540	203861000	0	2		
6	1	2	1	2	3	8361	4167	2000	3703	62867	206918000	0	2		
7	1	2	2	1	3	8535	4167	2000	3706	53448	215607000	1	2		
8	1	2	2	2	3	8502	4533	2000	3701	63053	218291000	1	2		
9	2	1	1	1	4	8537	236	2000	4848	57724	246346000	1	2		
10	2	1	1	2	4	9115	231	2000	4842	67900	251162000	1	2		
11	2	1	2	1	4	8719	236	2000	4848	57724	246901000	1	2		
12	2	1	2	2	4	8537	230	2000	4842	67899	251154000	1	2		
13	2	2	1	1	3	7281	4236	2000	3734	55250	217809000	1	2		
14	2	2	1	2	3	8345	4220	2000	3733	64986	222065000	1	2		
15	2	2	2	1	3	8570	4236	2000	3735	55257	218366000	1	2		
16	2	2	2	2	3	8549	4704	2000	3701	65232	220785000	1	2		
17	3	1	1	1	5	9770	320	2000	4842	64718	285874000	1	2		
18	3	1	1	2	5	9770	354	2000	4826	76150	289311000	1	2		
19	3	1	2	1	5	9768	354	2000	4835	64735	286241000	0	3		

20	3	1	2	2	2	5	9767	413	2000	4812	76186	289682000	0	3
21	3	2	1	1	4	4	9238	6809	2000	3798	62034	260062000	1	2
22	3	2	1	2	4	4	9555	6865	2000	3704	74732	271908000	1	2
23	3	2	2	1	4	4	9106	3253	2000	3702	61876	255783000	1	2
24	3	2	2	2	4	4	8986	7141	2000	3706	74888	260591000	1	2

Three-factor Analysis of Variance Model

$$SS_T = SS_A + SS_B + SS_C + SS_{AB} + SS_{AC} + SS_{BC} + SS_E$$

$$SS_T = \sum_{i=1}^a \sum_{j=1}^b \sum_{k=1}^c \sum_{l=1}^n y_{ijkl}^2 - \frac{y_{\dots}^2}{abcn} \quad \left| \quad SS_{AB} = \frac{1}{cn} \sum_{i=1}^a \sum_{j=1}^b y_{ij..}^2 - \frac{y_{\dots}^2}{abcn} - SS_A - SS_B$$

$$SS_A = \frac{1}{bcn} \sum_{i=1}^a y_{i\dots}^2 - \frac{y_{\dots}^2}{abcn} \quad \left| \quad SS_{AC} = \frac{1}{bn} \sum_{i=1}^a \sum_{k=1}^c y_{i.k.}^2 - \frac{y_{\dots}^2}{abcn} - SS_A - SS_C$$

$$SS_B = \frac{1}{acn} \sum_{j=1}^b y_{.j..}^2 - \frac{y_{\dots}^2}{abcn} \quad \left| \quad SS_{BC} = \frac{1}{an} \sum_{j=1}^b \sum_{k=1}^c y_{.jk.}^2 - \frac{y_{\dots}^2}{abcn} - SS_B - SS_C$$

$$SS_C = \frac{1}{abn} \sum_{k=1}^c y_{..k.}^2 - \frac{y_{\dots}^2}{abcn}$$

ANOVA Table for Three-Factor Model

Source of Variation	Sum of Squares	Degrees of Freedom	Mean Square	Expected Mean Square	F_0
<i>A</i>	SS_A	$a - 1$	MS_A	$\sigma^2 + \frac{bcn \sum \tau_i^2}{a - 1}$	$F_0 = \frac{MS_A}{MS_E}$
<i>B</i>	SS_B	$b - 1$	MS_B	$\sigma^2 + \frac{acn \sum \beta_j^2}{b - 1}$	$F_0 = \frac{MS_B}{MS_E}$
<i>C</i>	SS_C	$c - 1$	MS_C	$\sigma^2 + \frac{abn \sum \gamma_k^2}{c - 1}$	$F_0 = \frac{MS_C}{MS_E}$
<i>AB</i>	SS_{AB}	$(a - 1)(b - 1)$	MS_{AB}	$\sigma^2 + \frac{cn \sum \sum (\tau\beta)_{ij}^2}{(a - 1)(b - 1)}$	$F_0 = \frac{MS_{AB}}{MS_E}$
<i>AC</i>	SS_{AC}	$(a - 1)(c - 1)$	MS_{AC}	$\sigma^2 + \frac{bn \sum \sum (\tau\gamma)_{ik}^2}{(a - 1)(c - 1)}$	$F_0 = \frac{MS_{AC}}{MS_E}$
<i>BC</i>	SS_{BC}	$(b - 1)(c - 1)$	MS_{BC}	$\sigma^2 + \frac{an \sum \sum (\beta\gamma)_{jk}^2}{(b - 1)(c - 1)}$	$F_0 = \frac{MS_{BC}}{MS_E}$
<i>ABC</i>	SS_{ABC}	$(a - 1)(b - 1)(c - 1)$	MS_{ABC}	$\sigma^2 + \frac{n \sum \sum \sum (\tau\beta\gamma)_{ijk}^2}{(a - 1)(b - 1)(c - 1)}$	$F_0 = \frac{MS_{ABC}}{MS_E}$
Error	SS_E	$abc(n - 1)$	MS_E	σ^2	
Total	SS_T	$abcn - 1$			